

THESIS

2

2001

LIBRARY
Michigan State
University

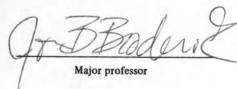
This is to certify that the
thesis entitled
INTERACTION OF S-ADENOSYLMETHIONINE WITH
THE IRON-SULFUR CLUSTER OF
PYRUVATE FORMATE-LYASE ACTIVATING ENZYME

presented by

Wei Hong

has been accepted towards fulfillment
of the requirements for

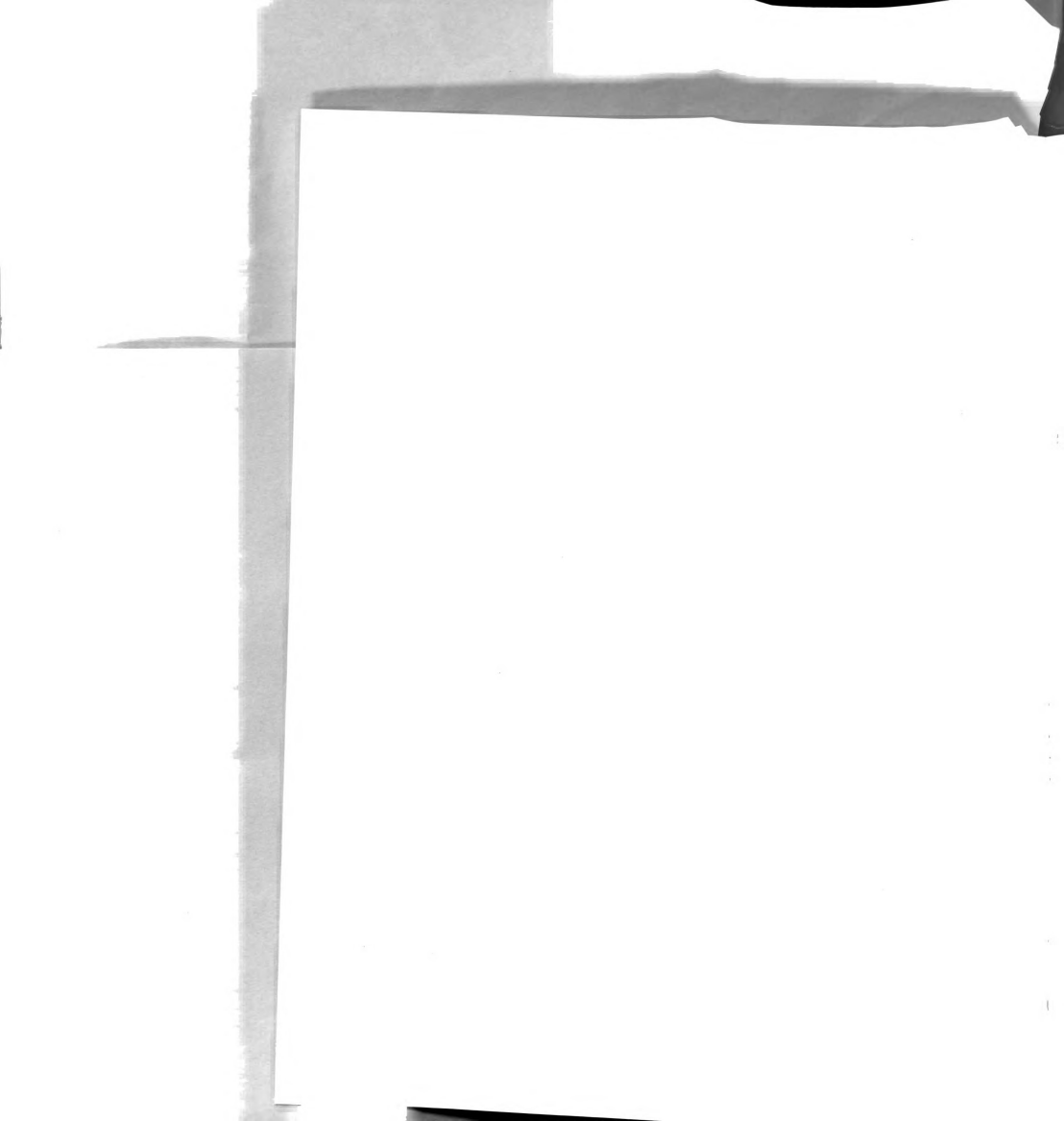
M.S. degree in Chemistry


Major professor

Date 8/23/01

PLACE IN RETURN BOX to remove this checkout from your record.
TO AVOID FINES return on or before date due.
MAY BE RECALLED with earlier due date if requested.

DATE DUE	DATE DUE	DATE DUE
122002		





INTERACTION OF S-ADENOSYLMETHIONINE WITH
THE IRON-SULFUR CLUSTER OF
PYRUVATE FORMATE-LYASE ACTIVATING ENZYME

By

Wei Hong

A THESIS

Submitted to
Michigan State University
in partial fulfillment of the requirements
for the degree of

MASTER OF SCIENCE

Department of Chemistry

2001

**INTERACTION OF *S*-ADENOSYLMETHIONINE WITH
THE IRON-SULFUR CLUSTER OF
PYRUVATE FORMATE-LYASE ACTIVATING ENZYME**

**By
Wei Hong**

AN ABSTRACT OF A THESIS

**Submitted to
Michigan State University
in partial fulfillment of the requirements
for the degree of**

MASTER OF SCIENCE

Department of Chemistry

2001

Professor Joan B. Broderick

ABSTRACT

INTERACTION OF *S*-ADENOSYLMETHIONINE WITH THE IRON-SULFUR CLUSTER OF PYRUVATE FORMATE-LYASE ACTIVATING ENZYME

By

Wei Hong

Pyruvate formate-lyase activating enzyme (PFL-AE) is a member of a growing family of enzymes that utilize [4Fe-4S] clusters and *S*-adenosylmethionine (AdoMet) to generate catalytically essential radicals. PFL-AE generates a glycy radical on pyruvate formate-lyase (PFL), and converts AdoMet stoichiometrically to methionine and 5'-deoxyadenosine. An AdoMet-derived adenosyl radical has been implicated as the intermediate responsible for abstraction of the pro-S hydrogen atom of PFL Gly734. In order to probe the mechanism by which the Fe-S cluster interacts with AdoMet to generate the adenosyl radical intermediate, the methyl group of AdoMet was labeled with ^2H and ^{13}C , and the sulfonium sulfur was replaced by selenium. Investigations of the interaction between AdoMet and the Fe-S cluster of PFL-AE were carried out with the isotopically labeled AdoMet and Se-AdoMet, using a variety of spectroscopic methods. A close association of the PFL-AE [4Fe-4S] cluster with AdoMet has been demonstrated for the first time by using ^2H and ^{13}C ENDOR spectroscopy. Our results suggest that the Fe-S cluster of PFL-AE is directly involved in generating the putative adenosyl radical from AdoMet.





ACKNOWLEDGEMENTS

First of all, I would like to thank my advisor, Prof. Joan B. Broderick for guiding me through my graduate study. She has shown a great deal of support, encouragement, understanding and patience for the past two years that I worked in the lab. I am grateful to Dr. William E. Broderick, who has put so many great ideas in my work, and provided suggestions in my thesis writing.

I want to thank Jennifer and Tim for being so helpful all the time. I gained so much knowledge, as well as hands-on experience in our group's research from them. Also, Jennifer ran all the EPR samples for me. Mbako, Danilo, Silvana, and all the people who used to be in this group, have been great friends to me. I have enjoyed being a part of this group.

I appreciate the tremendous contributions that Dr. Charles Walsby, Prof. Brian Hoffman, and all the collaborators have given to the work I did in the lab and to our research as a whole.

Lastly, I am truly indebted to my parents' endless love and support, and all the things they have done for me during the month they spent with me here.



TABLE OF CONTENTS

LIST OF SCHEMES	vi
LIST OF TABLES	vii
LIST OF FIGURES.....	viii
LIST OF ABBREVIATIONS.....	x

CHAPTER I

INTRODUCTION	1
I.1 Pyruvate formate-lyase	1
I.2 Pyruvate formate-lyase activating enzyme	3
I.3 Adenosylmethionine-dependent iron-sulfur enzymes	6
I.4 <i>S</i> -adenosylmethionine and the Fe-S cluster of PFL-AE in radical generation	10

CHAPTER II

OVEREXPRESSION AND CHARACTERIZATION OF PYRUVATE FORMATE-LYASE AND PYRUVATE FORMATE-LYASE ACTIVATING ENZYME	14
II.1 Introduction.....	14
II.2 Experimental methods	17
II.3 Results and Discussion	24





CHAPTER III

SYNTHESES AND CHARACTERIZATION OF ISOTOPICALLY LABELED S-ADENOSYL-L-METHIONINES AND Se-ADENOSYL-L-SELENOMETHIONINE33

III.1	Introduction	33
III.2	Experimental methods	37
III.3	Results and Discussion	41

CHAPTER IV

INVESTIGATING THE INTERACTION OF ADOMET WITH PFL-AE USING EPR AND ENDOR SPECTROSCOPY51

IV.1	Introduction	51
IV.2	Experimental methods	55
IV.3	Results and Discussion	58

CHAPTER V

Se-ADENOSYL-L-SELENOMETHIONINE AND ITS INTERACTION WITH PYRUVATE FORMATE-LYASE ACTIVATING ENZYME75

V.1	Introduction	75
V.2	Experimental methods	81
V.3	Results and Discussion	84

CHAPTER VI

CONCLUSIONS94

REFERENCES96

CHAPTER III

SYNTHESIS AND CHEMICAL FORM OF ISOTOPICALLY LABELED 2-ADENOSYL-5'-UTRIPHOSPHATE

33

33

33

41

CHAPTER IV

INVESTIGATION OF THE INTERACTION OF ADENET WITH PHASE USING THE ADENET SPECIFICITY

51

51

52

52

CHAPTER V

2-ADENOSYL-5'-UTRIPHOSPHATE AND ITS INTERACTION WITH PYRIDATE FORMYL-5'-UTRIPHOSPHATE

53

53

81

84

CHAPTER VI

CONCLUSIONS

94

REFERENCES

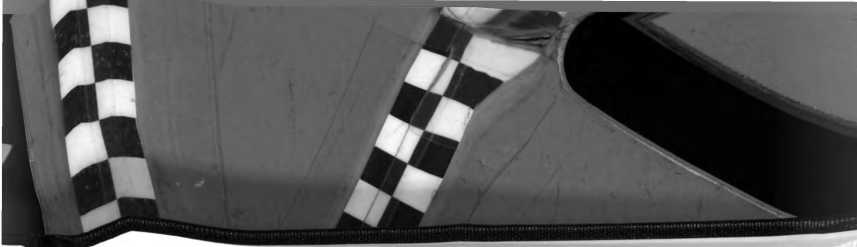
96

LIST OF SCHEMES

Scheme I.1	PFL catalyzed interconversion of pyruvate and CoA to acetyl-CoA and formate	1
Scheme I.2	Structure of the glycyl radical in PFL	1
Scheme I.3	The activation / deactivation of PFL by generation or quenching of the glycyl radical on PFL	3
Scheme I.4	AdoMet-dependent PFL glycyl radical generation by PFL-AE	4
Scheme I.5	Reaction catalyzed by benzylsuccinate synthase activating enzyme	8
Scheme I.6	The interconversion between L-lysine and L- β -lysine catalyzed by lysine 2,3-aminomutase	9
Scheme I.7	Biosynthesis of biotin from dethiobiotin catalyzed by biotin synthase	9
Scheme I.8	Reaction catalyzed by lipoate synthase (LipA)	10
Scheme I.9	General mechanism for radical generation in PFL-AE	12
Scheme III.1	Reductive cleavage of AdoMet by PFL-AE in PFL activation	34
Scheme III.2	AdoMet and the Fe-S cluster of PFL-AE are proposed to be in close proximity during radical generation	35
Scheme III.3	Enzymatic synthesis of <i>S</i> -adenosyl-L-methionine	36
Scheme V.1	Selenoamino acids found in plants	77

10-11-12

10-11-12



LIST OF TABLES

Table II.1	Ratio of absorbances at 426 nm and 280 nm of PFL-AE fractions off the 2nd run of the gel filtration column	28
Table II.2	Summary of activity assay of PFL-AE	30
Table IV.1	<i>T</i> values derived from the dipolar interpretation of the ^2H ENDOR data	73



LIST OF FIGURES

Figure II.1	Chromatograms of purification of PFL	25
Figure II.2	SDS-PAGE analysis of PFL fractions off the Accell Plus QMA anion-exchange column	26
Figure II.3	SDS-PAGE analysis of PFL fractions off the Phenyl-Sepharose hydrophobic column	26
Figure II.4	SDS-PAGE analysis of overexpression of PFL-AE in <i>E. coli</i> cells	27
Figure II.5	Purification of PFL-AE by gel-filtration chromatography	28
Figure II.6	SDS-PAGE analysis of PFL-AE fractions off the 2nd run of the gel filtration column	29
Figure II.7	X-band EPR spectrum of PFL-AE as-isolated in the presence of 1 mM DTT	30
Figure II.8	Activity assay of PFL-AE	31
Figure III.1	SDS-PAGE analysis of AdoMet synthetase	41
Figure III.2	SDS-PAGE analysis of AdoMet synthetase fractions off the Phenyl-Sepharose column	42
Figure III.3	Chromatogram of isolation of CD ₃ -AdoMet by SOURCE 15S cation exchange chromatography	45
Figure III.4	Chromatogram of isolation of ¹³ CH ₃ -AdoMet by SOURCE 15S cation exchange chromatography	46
Figure III.5	Chromatogram of isolation of Se-AdoMet by SOURCE 15S cation exchange chromatography	47
Figure III.6	¹ H NMR (300 MHz) of AdoMet, CD ₃ -AdoMet, ¹³ CH ₃ -AdoMet, and Se-AdoMet	48
Figure IV.1	X-band EPR spectrum of photoreduced PFL-AE in the presence of CD ₃ -AdoMet	60

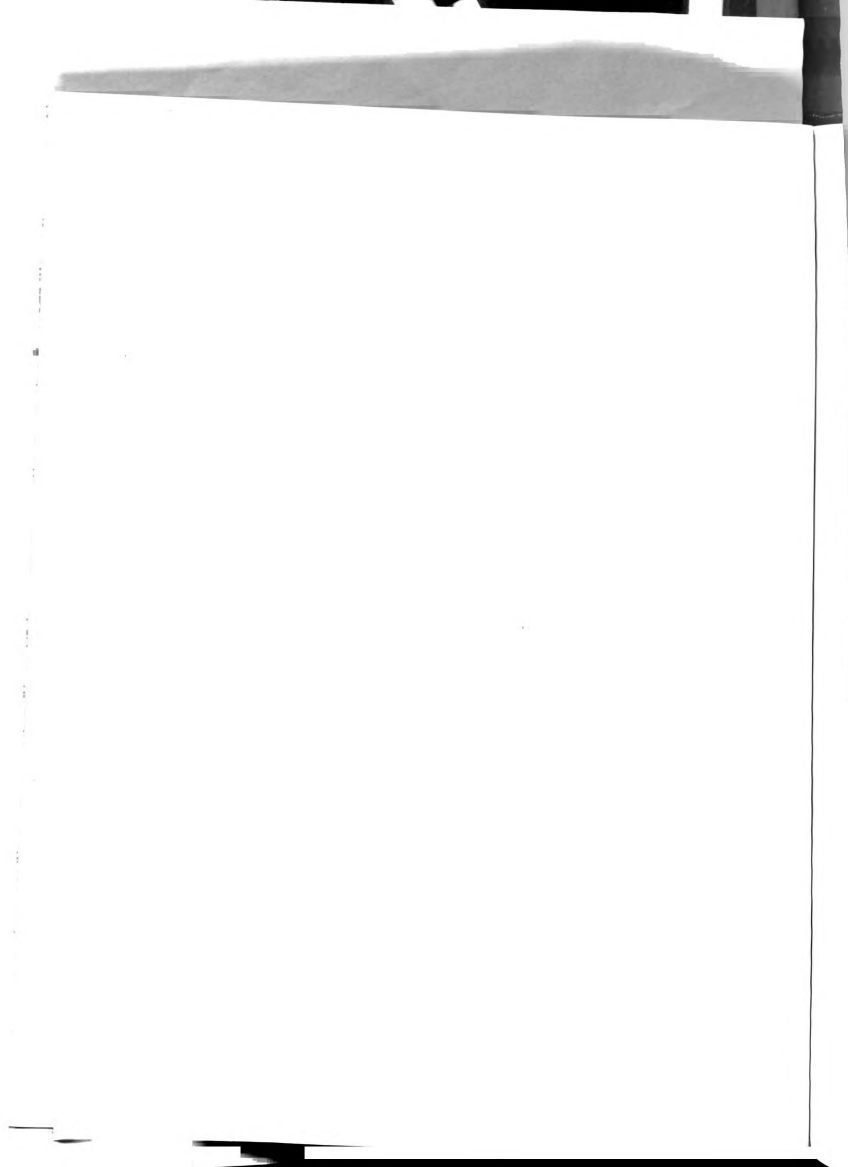


Figure IV.2	X-band EPR spectrum of photoreduced PFL-AE in the presence of $^{13}\text{CH}_3\text{-AdoMet}$	60
Figure IV.3	35 GHz Mims pulsed-ENDOR spectra of PFL-AE with methyl- D_3 AdoMet	68
Figure IV.4	35 GHz Mims pulsed-ENDOR spectra of PFL-AE with methyl- ^{13}C AdoMet	70
Figure IV.5	^{13}C field dependence with simulation of line positions and relative intensities	71
Figure IV.6	Structural model of AdoMet bound to the $[4\text{Fe-4S}]$ cluster of PFL-AE	74
Figure V.1	Activity assay of PFL-AE in the presence of Se-AdoMet	84
Figure V.2	X-band EPR spectra of photoreduced PFL-AE (A) in the presence of Se-AdoMet and (B) in the presence of AdoMet	86
Figure V.3	Se K-edge X-ray absorption spectra (A) and Fourier transforms (B) of Se-Met and Se-AdoMet	88
Figure V.4	Se K-edge X-ray absorption spectra (A) and Fourier transforms (B) of PFL-AE $[4\text{Fe-4S}]^{2+}$ incubated with Se-Met / 5'-dAdo (EPOSA), Se-Met / 5'-dAdo / PFL (EPRPA and EPRPB), Se-AdoMet (EPOEB), and Se-AdoMet / PFL (EPOQA)	90
Figure V.5	Se K-edge X-ray absorption spectra (A) and Fourier transforms (B) of PFL-AE $[4\text{Fe-4S}]^{1+}$ in the presence of Se-AdoMet	91

LIST OF ABBREVIATIONS

5'-dAdo	5'-deoxyadenosine
AdoMet	<i>S</i> -adenosyl-L-methionine
aRNR	anaerobic ribonucleotide reductase
aRNR-AE	anaerobic ribonucleotide reductase activating enzyme
ATP	adenosine triphosphate
β -ME	β -mecaptoethanol
CD ₃ -AdoMet	adenosyl-methyl-D ₃ -methionine
¹³ CH ₃ -AdoMet	adenosyl-methyl- ¹³ C-methionine
CoA	coenzyme A
DTT	dithiothreitol
<i>E. coli</i>	<i>Escherichia coli</i>
ENDOR	electron nuclear double resonance
EPR	electron paramagnetic resonance
ESEEM	electron spin echo envelope modulation
Hepes	<i>N</i> -(2-hydroxyethyl)piperazine- <i>N'</i> -2-ethanesulfonic acid
IPTG	isopropyl- β -D-thiogalactopyranoside
LAM	lysine 2,3-aminomutase
LB	Luria-Bertani
NMR	nuclear magnetic resonance
PFL	pyruvate formate-lyase

PFL-AE pyruvate formate-lyase activating enzyme

PMSF phenylmethylsulfonyl fluoride

SDS-PAGE sodium dodecyl sulfate-polyacrylamide gel electrophoresis


Se-AdoMet Se-adenosyl-L-selenomethionine

Se-Met selenomethionine

Tris tris(hydroxymethyl)aminomethane

XAS X-ray absorption spectroscopy

24-25	24-Met	24-Met	24-Met
26-27	26-Ado	26-Ado	26-Ado
28-29	28-Ado	28-Ado	28-Ado
30-31	30-Ado	30-Ado	30-Ado
32-33	32-Ado	32-Ado	32-Ado
34-35	34-Ado	34-Ado	34-Ado
36-37	36-Ado	36-Ado	36-Ado
38-39	38-Ado	38-Ado	38-Ado
40-41	40-Ado	40-Ado	40-Ado
42-43	42-Ado	42-Ado	42-Ado
44-45	44-Ado	44-Ado	44-Ado
46-47	46-Ado	46-Ado	46-Ado
48-49	48-Ado	48-Ado	48-Ado
50-51	50-Ado	50-Ado	50-Ado
52-53	52-Ado	52-Ado	52-Ado
54-55	54-Ado	54-Ado	54-Ado
56-57	56-Ado	56-Ado	56-Ado
58-59	58-Ado	58-Ado	58-Ado
60-61	60-Ado	60-Ado	60-Ado
62-63	62-Ado	62-Ado	62-Ado
64-65	64-Ado	64-Ado	64-Ado
66-67	66-Ado	66-Ado	66-Ado
68-69	68-Ado	68-Ado	68-Ado
70-71	70-Ado	70-Ado	70-Ado
72-73	72-Ado	72-Ado	72-Ado
74-75	74-Ado	74-Ado	74-Ado
76-77	76-Ado	76-Ado	76-Ado
78-79	78-Ado	78-Ado	78-Ado
80-81	80-Ado	80-Ado	80-Ado
82-83	82-Ado	82-Ado	82-Ado
84-85	84-Ado	84-Ado	84-Ado
86-87	86-Ado	86-Ado	86-Ado
88-89	88-Ado	88-Ado	88-Ado
90-91	90-Ado	90-Ado	90-Ado
92-93	92-Ado	92-Ado	92-Ado
94-95	94-Ado	94-Ado	94-Ado
96-97	96-Ado	96-Ado	96-Ado
98-99	98-Ado	98-Ado	98-Ado
100-101	100-Ado	100-Ado	100-Ado
102-103	102-Ado	102-Ado	102-Ado
104-105	104-Ado	104-Ado	104-Ado
106-107	106-Ado	106-Ado	106-Ado
108-109	108-Ado	108-Ado	108-Ado
110-111	110-Ado	110-Ado	110-Ado
112-113	112-Ado	112-Ado	112-Ado
114-115	114-Ado	114-Ado	114-Ado
116-117	116-Ado	116-Ado	116-Ado
118-119	118-Ado	118-Ado	118-Ado
120-121	120-Ado	120-Ado	120-Ado
122-123	122-Ado	122-Ado	122-Ado
124-125	124-Ado	124-Ado	124-Ado
126-127	126-Ado	126-Ado	126-Ado
128-129	128-Ado	128-Ado	128-Ado
130-131	130-Ado	130-Ado	130-Ado
132-133	132-Ado	132-Ado	132-Ado
134-135	134-Ado	134-Ado	134-Ado
136-137	136-Ado	136-Ado	136-Ado
138-139	138-Ado	138-Ado	138-Ado
140-141	140-Ado	140-Ado	140-Ado
142-143	142-Ado	142-Ado	142-Ado
144-145	144-Ado	144-Ado	144-Ado
146-147	146-Ado	146-Ado	146-Ado
148-149	148-Ado	148-Ado	148-Ado
150-151	150-Ado	150-Ado	150-Ado
152-153	152-Ado	152-Ado	152-Ado
154-155	154-Ado	154-Ado	154-Ado
156-157	156-Ado	156-Ado	156-Ado
158-159	158-Ado	158-Ado	158-Ado
160-161	160-Ado	160-Ado	160-Ado
162-163	162-Ado	162-Ado	162-Ado
164-165	164-Ado	164-Ado	164-Ado
166-167	166-Ado	166-Ado	166-Ado
168-169	168-Ado	168-Ado	168-Ado
170-171	170-Ado	170-Ado	170-Ado
172-173	172-Ado	172-Ado	172-Ado
174-175	174-Ado	174-Ado	174-Ado
176-177	176-Ado	176-Ado	176-Ado
178-179	178-Ado	178-Ado	178-Ado
180-181	180-Ado	180-Ado	180-Ado
182-183	182-Ado	182-Ado	182-Ado
184-185	184-Ado	184-Ado	184-Ado
186-187	186-Ado	186-Ado	186-Ado
188-189	188-Ado	188-Ado	188-Ado
190-191	190-Ado	190-Ado	190-Ado
192-193	192-Ado	192-Ado	192-Ado
194-195	194-Ado	194-Ado	194-Ado
196-197	196-Ado	196-Ado	196-Ado
198-199	198-Ado	198-Ado	198-Ado
200-201	200-Ado	200-Ado	200-Ado
202-203	202-Ado	202-Ado	202-Ado
204-205	204-Ado	204-Ado	204-Ado
206-207	206-Ado	206-Ado	206-Ado
208-209	208-Ado	208-Ado	208-Ado
210-211	210-Ado	210-Ado	210-Ado
212-213	212-Ado	212-Ado	212-Ado
214-215	214-Ado	214-Ado	214-Ado
216-217	216-Ado	216-Ado	216-Ado
218-219	218-Ado	218-Ado	218-Ado
220-221	220-Ado	220-Ado	220-Ado
222-223	222-Ado	222-Ado	222-Ado
224-225	224-Ado	224-Ado	224-Ado
226-227	226-Ado	226-Ado	226-Ado
228-229	228-Ado	228-Ado	228-Ado
230-231	230-Ado	230-Ado	230-Ado
232-233	232-Ado	232-Ado	232-Ado
234-235	234-Ado	234-Ado	234-Ado
236-237	236-Ado	236-Ado	236-Ado
238-239	238-Ado	238-Ado	238-Ado
240-241	240-Ado	240-Ado	240-Ado
242-243	242-Ado	242-Ado	242-Ado
244-245	244-Ado	244-Ado	244-Ado
246-247	246-Ado	246-Ado	246-Ado
248-249	248-Ado	248-Ado	248-Ado
250-251	250-Ado	250-Ado	250-Ado
252-253	252-Ado	252-Ado	252-Ado
254-255	254-Ado	254-Ado	254-Ado
256-257	256-Ado	256-Ado	256-Ado
258-259	258-Ado	258-Ado	258-Ado
260-261	260-Ado	260-Ado	260-Ado
262-263	262-Ado	262-Ado	262-Ado
264-265	264-Ado	264-Ado	264-Ado
266-267	266-Ado	266-Ado	266-Ado
268-269	268-Ado	268-Ado	268-Ado
270-271	270-Ado	270-Ado	270-Ado
272-273	272-Ado	272-Ado	272-Ado
274-275	274-Ado	274-Ado	274-Ado
276-277	276-Ado	276-Ado	276-Ado
278-279	278-Ado	278-Ado	278-Ado
280-281	280-Ado	280-Ado	280-Ado
282-283	282-Ado	282-Ado	282-Ado
284-285	284-Ado	284-Ado	284-Ado
286-287	286-Ado	286-Ado	286-Ado
288-289	288-Ado	288-Ado	288-Ado
290-291	290-Ado	290-Ado	290-Ado
292-293	292-Ado	292-Ado	292-Ado
294-295	294-Ado	294-Ado	294-Ado
296-297	296-Ado	296-Ado	296-Ado
298-299	298-Ado	298-Ado	298-Ado
300-301	300-Ado	300-Ado	300-Ado
302-303	302-Ado	302-Ado	302-Ado
304-305	304-Ado	304-Ado	304-Ado
306-307	306-Ado	306-Ado	306-Ado
308-309	308-Ado	308-Ado	308-Ado
310-311	310-Ado	310-Ado	310-Ado
312-313	312-Ado	312-Ado	312-Ado
314-315	314-Ado	314-Ado	314-Ado
316-317	316-Ado	316-Ado	316-Ado
318-319	318-Ado	318-Ado	318-Ado
320-321	320-Ado	320-Ado	320-Ado
322-323	322-Ado	322-Ado	322-Ado
324-325	324-Ado	324-Ado	324-Ado
326-327	326-Ado	326-Ado	326-Ado
328-329	328-Ado	328-Ado	328-Ado
330-331	330-Ado	330-Ado	330-Ado
332-333	332-Ado	332-Ado	332-Ado
334-335	334-Ado	334-Ado	334-Ado
336-337	336-Ado	336-Ado	336-Ado
338-339	338-Ado	338-Ado	338-Ado
340-341	340-Ado	340-Ado	340-Ado
342-343	342-Ado	342-Ado	342-Ado
344-345	344-Ado	344-Ado	344-Ado
346-347	346-Ado	346-Ado	346-Ado
348-349	348-Ado	348-Ado	348-Ado
350-351	350-Ado	350-Ado	350-Ado
352-353	352-Ado	352-Ado	352-Ado
354-355	354-Ado	354-Ado	354-Ado
356-357	356-Ado	356-Ado	356-Ado
358-359	358-Ado	358-Ado	358-Ado
360-361	360-Ado	360-Ado	360-Ado
362-363	362-Ado	362-Ado	362-Ado
364-365	364-Ado	364-Ado	364-Ado
366-367	366-Ado	366-Ado	366-Ado
368-369	368-Ado	368-Ado	368-Ado
370-371	370-Ado	370-Ado	370-Ado
372-373	372-Ado	372-Ado	372-Ado
374-375	374-Ado	374-Ado	374-Ado
376-377	376-Ado	376-Ado	376-Ado
378-379	378-Ado	378-Ado	378-Ado
380-381	380-Ado	380-Ado	380-Ado
382-383	382-Ado	382-Ado	382-Ado
384-385	384-Ado	384-Ado	384-Ado
386-387	386-Ado	386-Ado	386-Ado
388-389	388-Ado	388-Ado	388-Ado
390-391	390-Ado	390-Ado	390-Ado
392-393	392-Ado	392-Ado	392-Ado
394-395	394-Ado	394-Ado	394-Ado
396-397	396-Ado	396-Ado	396-Ado
398-399	398-Ado	398-Ado	398-Ado
400-401	400-Ado	400-Ado	400-Ado
402-403	402-Ado	402-Ado	402-Ado
404-405	404-Ado	404-Ado	404-Ado
406-407	406-Ado	406-Ado	406-Ado
408-409	408-Ado	408-Ado	408-Ado
410-411	410-Ado	410-Ado	410-Ado
412-413	412-Ado	412-Ado	412-Ado
414-415	414-Ado	414-Ado	414-Ado
416-417	416-Ado	416-Ado	416-Ado
418-419	418-Ado	418-Ado	418-Ado
420-421	420-Ado	420-Ado	420-Ado
422-423	422-Ado	422-Ado	422-Ado
424-425	424-Ado	424-Ado	424-Ado
426-427	426-Ado	426-Ado	426-Ado
428-429	428-Ado	428-Ado	428-Ado
430-431	430-Ado	430-Ado	430-Ado
432-433	432-Ado	432-Ado	432-Ado
434-435	434-Ado	434-Ado	434-Ado
436-437	436-Ado	436-Ado	436-Ado
438-439	438-Ado	438-Ado	438-Ado
440-441	440-Ado	440-Ado	440-Ado
442-443	442-Ado	442-Ado	442-Ado
444-445	444-Ado	444-Ado	444-Ado
446-447	446-Ado	446-Ado	446-Ado
448-449	448-Ado	448-Ado	448-Ado
450-451	450-Ado	450-Ado	450-Ado
452-453	452-Ado	452-Ado	452-Ado
454-455	454-Ado	454-Ado	454-Ado
456-457	456-Ado	456-Ado	456-Ado
458-459	458-Ado	458-Ado	458-Ado
460-461	460-Ado	460-Ado	460-Ado
462-463	462-Ado	462-Ado	462-Ado
464-465	464-Ado	464-Ado	464-Ado
466-467	466-Ado	466-Ado	466-Ado
468-469	468-Ado	468-Ado	468-Ado
470-471	470-Ado	470-Ado	470-Ado

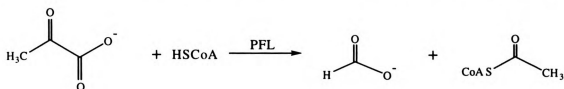


CHAPTER I

INTRODUCTION

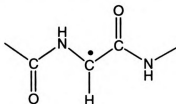
I.1 Pyruvate formate-lyase

Pyruvate formate-lyase (acetyl-CoA:formate C-acetyltransferase, EC 2.3.1.54; PFL) catalyzes the first committed step in anaerobic glucose metabolism in *Escherichia coli* (*E. coli*) cells, the conversion of pyruvate and coenzyme A (CoA) to formate and acetyl-CoA (Scheme I.1) (1-3). Knappe *et al.* identified PFL as the first enzyme known



Scheme I.1 PFL catalyzed interconversion of pyruvate and CoA to acetyl-CoA and formate

to contain a stable glycy radical. The catalytically essential radical of PFL was shown to be located on the α -carbon of glycine 734 through isotopic labeling, EPR spectroscopy, and analysis of the products of oxygenolytic cleavage of the activated PFL (4). The glycy radical (Scheme I.2) is stable in the absence of dioxygen, and its stability can be



Scheme I.2 Structure of the glycy radical in PFL

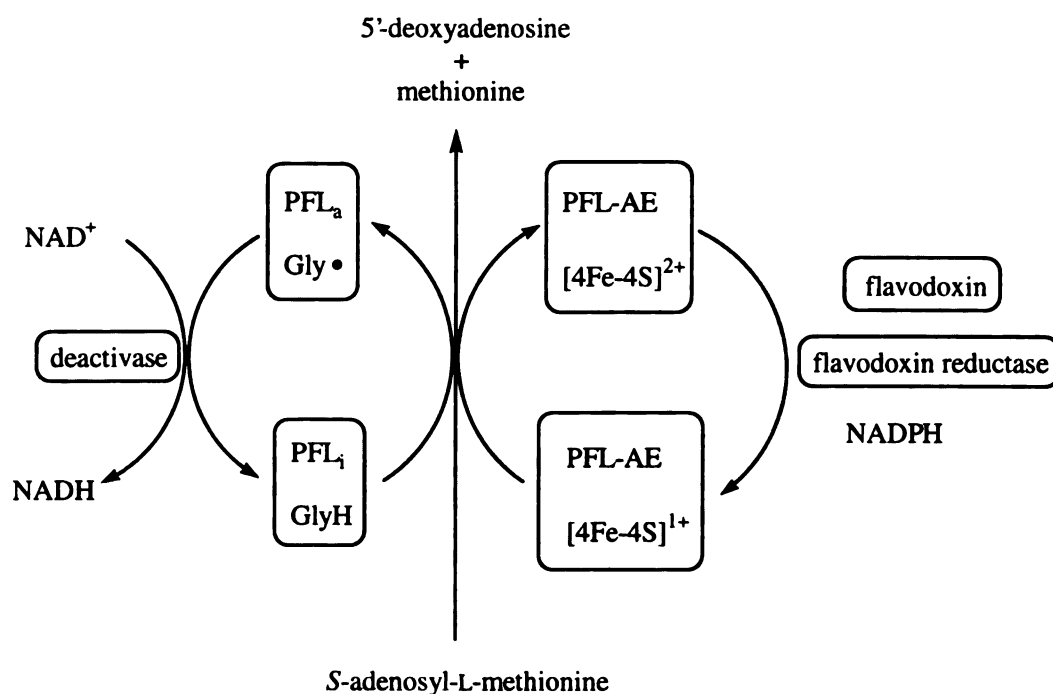
1000

1000

1000

attributed to the summation of the effects of resonance electron withdrawal by the glycyl-carbonyl group and resonance electron donation by the adjacent amide nitrogen through its lone electron pair. Gly734 does not directly participate in catalysis, but rather serves as the source of an unpaired electron that can be relayed to the active site in the form of a cysteinyl-thiyl radical, which is directly involved in homolytic cleavage of the pyruvate C-C bond (5, 6). Based on steric relationships among the amino acid residues, the Gly734 radical was proposed to abstract a hydrogen atom from Cys419, and the Cys419 thiyl radical in turn relays the radical center to Cys418, which is in the pyruvate binding site (7).

PFL from *E. coli* is a homodimeric protein of 170 kDa. The enzyme can exist in an active form (PFL_a), which contains one glycyl radical per dimer, and an inactive form (PFL_i) in which the glycyl radical is reduced (1). The catalytically essential glycyl radical of PFL is post-translationally generated under anaerobic conditions by the stereospecific abstraction of the pro-S hydrogen atom of the Gly734 methylene group (8). The interconversion of PFL between its inactive and active forms requires the pyruvate formate-lyase activating enzyme (PFL-AE), *S*-adenosyl-L-methionine (AdoMet), flavodoxin, and flavodoxin reductase (Scheme I.3) (1). In addition, a “deactivase”, a regulatory component of the PFL system, reduces the glycyl radical of PFL to glycine, preventing its destruction by O₂ (9, 10).

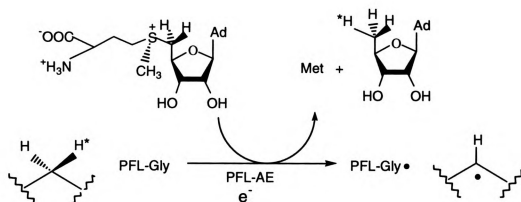


Scheme I.3 The activation / deactivation of PFL by generation or quenching of the glycy radical on PFL.

I.2 Pyruvate formate-lyase activating enzyme

Pyruvate formate-lyase activating enzyme (PFL-AE) generates the glycy radical at G734 on PFL. PFL-AE requires *S*-adenosylmethionine (AdoMet) as a co-substrate in the radical generation, subsequently cleaving it to methionine and 5'-deoxyadenosine (5'-dAdo) (Scheme I.4) (2). The hydrogen atom abstracted from Gly734 of PFL has been shown to be incorporated into the 5'-dAdo product by isotopic labeling, suggesting that the role of AdoMet is to produce an adenosyl radical intermediate as the immediate hydrogen atom abstractor. By using an octapeptide analogous to the Gly734 site of PFL, but with a dehydroalanyl residue in the glycy position, Wagner *et al.* have trapped the adenosyl radical intermediate by *C*-adenosylation of the dehydroalanyl residue (11).

51-148



Scheme I.4 AdoMet-dependent PFL glycyl radical generation by PFL-AE

PFL-AE was initially isolated aerobically from non-overexpressing *E. coli* cells and found to be a 28 kDa monomer with a broad absorbance from 310 to 550 nm suggesting the presence of a covalently bound cofactor (1). The catalytic activity of PFL-AE was shown to be completely dependent on the presence of exogenous iron in the assay, which was the first indication of the role of iron in glycyl radical generation. The first over-expression of PFL-AE in *E. coli* was reported by Kozarich *et al.* (12), but solubility problems made it necessary to purify and then refold the denatured protein. The refolded protein was able to bind stoichiometric quantities of Fe as well as other divalent metals such as Cu(II) and Co(II), but it was found to have enzymatic activity only in the presence of Fe(II) and DTT. A cysteinal coordination sphere for the iron center of PFL-AE was suggested because thiophilic metals such as Cu(II), Zn(II), Hg(II) and Cd(II) were found to be inhibitors of PFL-AE activity.

The first isolation of PFL-AE in its native state under strictly anaerobic conditions and identification of the presence of an iron-sulfur cluster in PFL-AE were achieved by Broderick *et al.* (13, 14). PFL-AE with an intact Fe-S cluster has been purified and a

1871

1872

high specific activity (95 U/mg in the absence of added iron) was obtained for PFL-AE containing 2.65 Fe per protein. When purified under anaerobic conditions in the absence of DTT, PFL-AE was shown to contain primarily a $[3\text{Fe-4S}]^+$ cluster by a combination of UV-visible, EPR and resonance Raman spectroscopic methods (14). A complete description of the states of the cluster present in the enzyme was provided by Mössbauer spectroscopy (15). The major component was confirmed to be the cuboidal $[3\text{Fe-4S}]^+$ cluster, accounting for 66 % of the total iron. Minor contributions from $[2\text{Fe-2S}]^{2+}$ (12 % of the total Fe), $[4\text{Fe-4S}]^{2+}$ (8 % of the total Fe) and linear $[3\text{Fe-4S}]^+$ (~10 % of the total Fe) were also found in the Mössbauer spectrum of as isolated PFL-AE. When PFL-AE was anaerobically reduced with dithionite, complete conversion of all cluster types to $[4\text{Fe-4S}]^{2+/+}$ clusters was observed by Mössbauer spectroscopy.

The above work has clearly demonstrated that the Fe-S cluster of PFL-AE is required for enzymatic activity, and that no ferrous iron is required for activity when an intact cluster is present. Among the mixture of Fe-S clusters present in PFL-AE, the $[4\text{Fe-4S}]$ cluster was considered to be the catalytically relevant cluster, as PFL-AE activity is observed *in vitro* only under anaerobic reducing conditions (1). A definite assignment of the $[4\text{Fe-4S}]^{1+}$ of PFL-AE as the catalytically active cluster was achieved in a “single turnover” experiment (16). Deazariboflavin-mediated photoreduction afforded quantitative reduction of PFL-AE to the $[4\text{Fe-4S}]^{1+}$ state. After the excess reductant was removed by placing the sample in the dark, either AdoMet alone, or AdoMet plus PFL (equimolar to PFL-AE) was added to the reduced PFL-AE. Spin quantitation of the resulting EPR spectra, taken as a function of illumination time, show a 1:1 correspondence between the amount of PFL glycyl radical generated and the amount

of $[4\text{Fe-4S}]^{1+}$ cluster present in the PFL-AE prior to addition of PFL. The $[4\text{Fe-4S}]^{1+}$ was converted to an EPR silent state concomitant with glycy radical formation, and preliminary data suggest that the final cluster state is $[4\text{Fe-4S}]^{2+}$. This is the first direct quantitative spectroscopic evidence that the $[4\text{Fe-4S}]^{1+}$ of PFL-AE is the catalytically relevant cluster, and this cluster provides the electron necessary for AdoMet-dependent glycy radical generation.

Site-directed mutagenesis studies have identified Cys29, Cys33, Cys36 as cluster ligands in PFL-AE (17). In general, a similar cluster-binding motif comprised of only three cysteines (CXXXCXXC) is common to all of the Fe-S/AdoMet-dependent enzymes for which the gene sequence is known (18-23). Considering that the $[4\text{Fe-4S}]$ cluster of PFL-AE is the catalytically relevant cluster, the fourth ligand to the $[4\text{Fe-4S}]$ cluster is presumably non-cysteine, therefore, resulting in a unique iron site, which may be important in binding / interacting with AdoMet.

I.3 Adenosylmethionine-dependent iron-sulfur enzymes

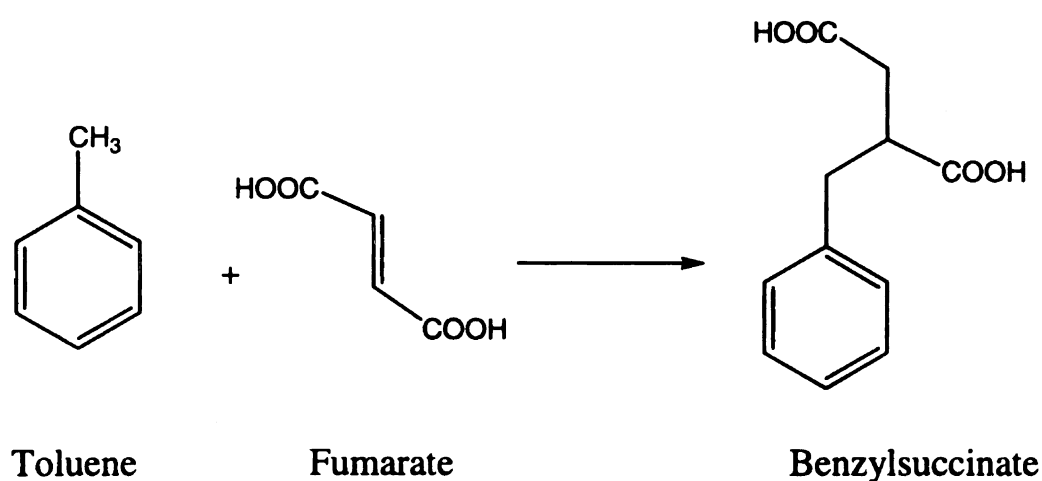
Iron-sulfur clusters are widespread in biological systems and participate in a broad range of functions (24-28), including electron transport, mediating redox catalysis, and non-redox catalysis. Aconitase is one of the most thoroughly studied enzymes that mediate non-redox catalysis, in which a $[4\text{Fe-4S}]^{2+}$ cluster serves as a Lewis acid to catalyze the interconversion between citrate and isocitrate (29). Fe-S clusters also play roles in regulation of gene expression, for example in the iron-responsive protein (IRP) (30), fumarate-nitrate reduction protein (FNR) (31), and SoxR (32) responding to changes in levels of iron, oxygen, and superoxide respectively.

1

A new role for Fe-S clusters has emerged in recent years as a number of enzymes have been identified that utilize Fe-S clusters and AdoMet to initiate radical catalysis. This Fe-S cluster-mediated radical catalysis includes the generation of catalytically essential glycy radical (4, 13, 33, 34), the generation of substrate radical intermediates (35), cofactor biosynthesis (36-39), and repair of DNA damage (40). Amazingly, a novel protein superfamily of more than 600 related enzymes that involve AdoMet-derived radical biochemistry has very recently been discovered by iterative profile searches and analyzed with bioinformatics and information visualization methods (41). This radical SAM superfamily, as named by Sofia *et al.*, has highly diverse functions in biochemical pathways and reflects an ancient conserved mechanistic approach to difficult chemistries. The following is a brief introduction of some defining members of the superfamily, besides PFL-AE, that are being investigated in various laboratories.

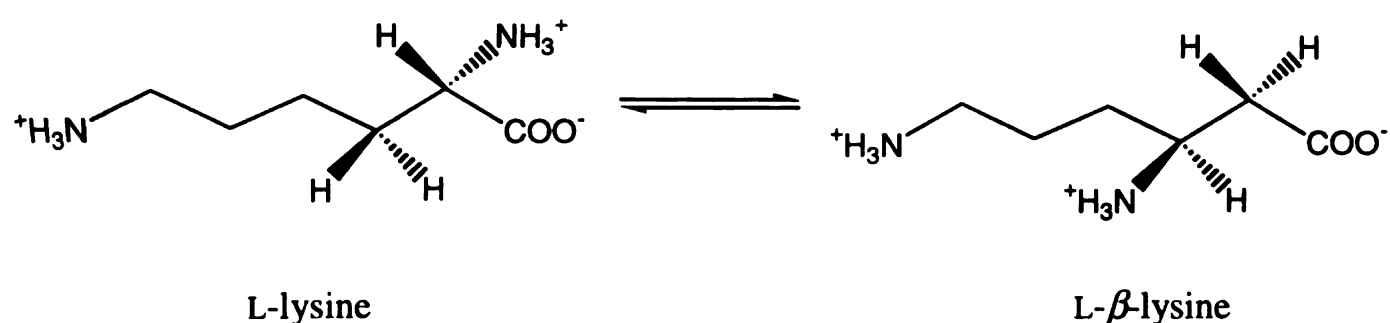
The reduction of ribonucleotides into deoxyribonucleotides is catalyzed by ribonucleotide reductases (RNRs) in order to supply DNA precursors to cells (42-45). All known RNRs fall into four distinct classes according to their metal cofactor, but all use a protein radical to activate the ribonucleotide substrate (45). Class III RNRs are utilized under anaerobic conditions by certain microbes, and are similar to PFL / PFL-AE in that they have a glycy radical and are AdoMet dependent. The anaerobic RNR (aRNR) from *E.coli* was originally purified in an inactive dimeric α_2 form. In its active form, a glycy radical is generated by an activating enzyme, the β protein, which contains an Fe-S cluster (46-49). Evidence has suggested that the $[4\text{Fe-4S}]^{1+}$ cluster of aRNR-AE is catalytically relevant (34).

The activating enzyme of benzylsuccinate synthase is another probable member of the Fe-S / AdoMet enzyme groups, which was found to have a high degree of sequence homology with both PFL-AE and aRNR-AE, especially in the region of the cluster-binding site (50). Benzylsuccinate synthase catalyzes the first step in anaerobic degradation of toluene, the addition of the toluene methyl carbon to the double bond of fumarate to form benzylsuccinate (Scheme I.5) through a glycy radical mechanism (51). The sequence of benzylsuccinate synthase is significantly similar to that of PFL and aRNR, with a highly conserved region around the glycy radical site and an active-site cysteine.



Scheme I.5 Reaction catalyzed by benzylsuccinate synthase activating enzyme

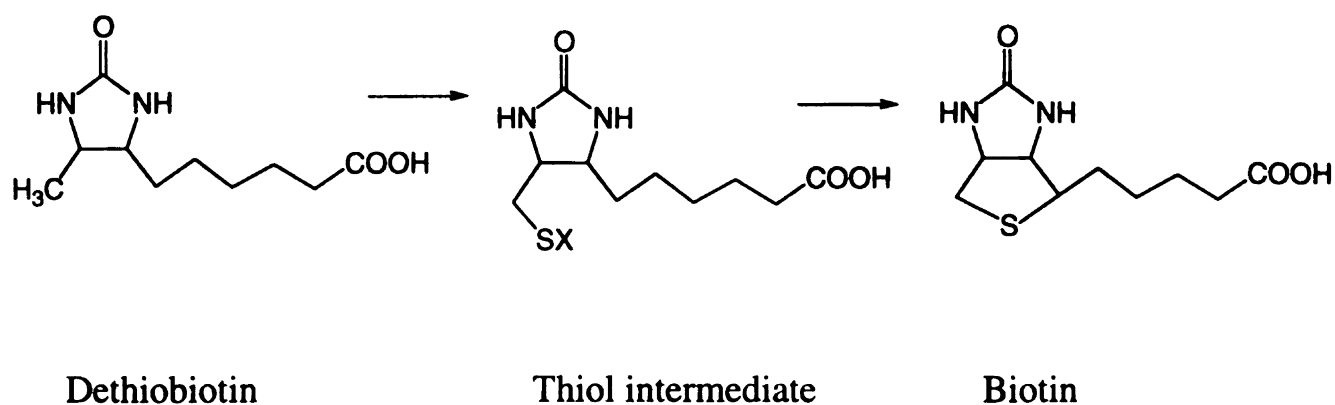
Lysine 2,3-aminomutase (LAM) from *Clostridiumsubterminale* SB4 catalyzes the interconversion between L-lysine and L- β -lysine (Scheme I.6). The reaction catalyzed by LAM is analogous to those that are catalyzed by adenosylcobalamin-dependent aminomutases, as well as other adenosylcobalamin isomerases. However, LAM reactivity does not depend on adenosylcobalamin, but instead requires AdoMet, a Fe-S cluster, and pyridoxal 5'-phosphate (PLP) (52-54). The $[4\text{Fe-4S}]^{1+}$ cluster generated in



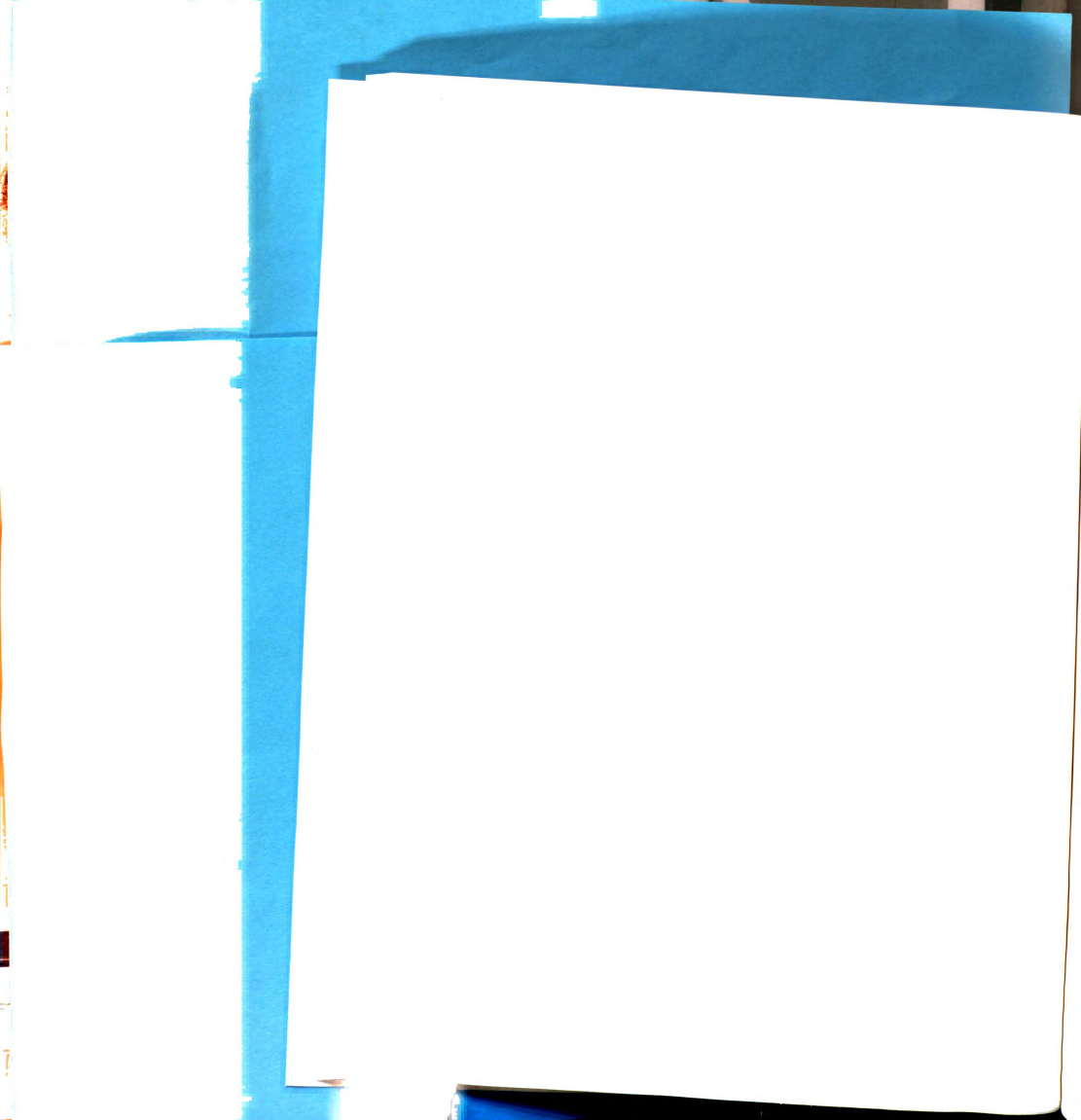
Scheme I.6 The interconversion between L-lysine and L- β -lysine catalyzed by lysine 2,3-aminomutase


the presence of AdoMet has been demonstrated to be the catalytically active species of the enzyme that is directly involved in the generation of a substrate radical intermediate (35). By using the cofactor analog *S*-3',4'-anhydroadenosyl-L-methionine, Magnusson *et al.* have recently provided the first spectroscopic evidence for an analog of the adenosyl radical intermediate in the Fe-S / AdoMet enzymes (55, 56).

The biosynthesis of biotin from dethiobiotin (Scheme I.7) is catalyzed by the enzyme biotin synthase (BioB, the *bioB* gene product) with the absolute requirement of AdoMet as a co-substrate and the presence of an Fe-S cluster (37, 57). Isotopic labeling studies have demonstrated that the Fe-S cluster is actually the sulfur donor (37), and an AdoMet-derived deoxyadenosyl radical is involved in the cleavage of the C-H bonds of dethiobiotin (58).



Scheme I.7 Biosynthesis of biotin from dethiobiotin catalyzed by biotin synthase

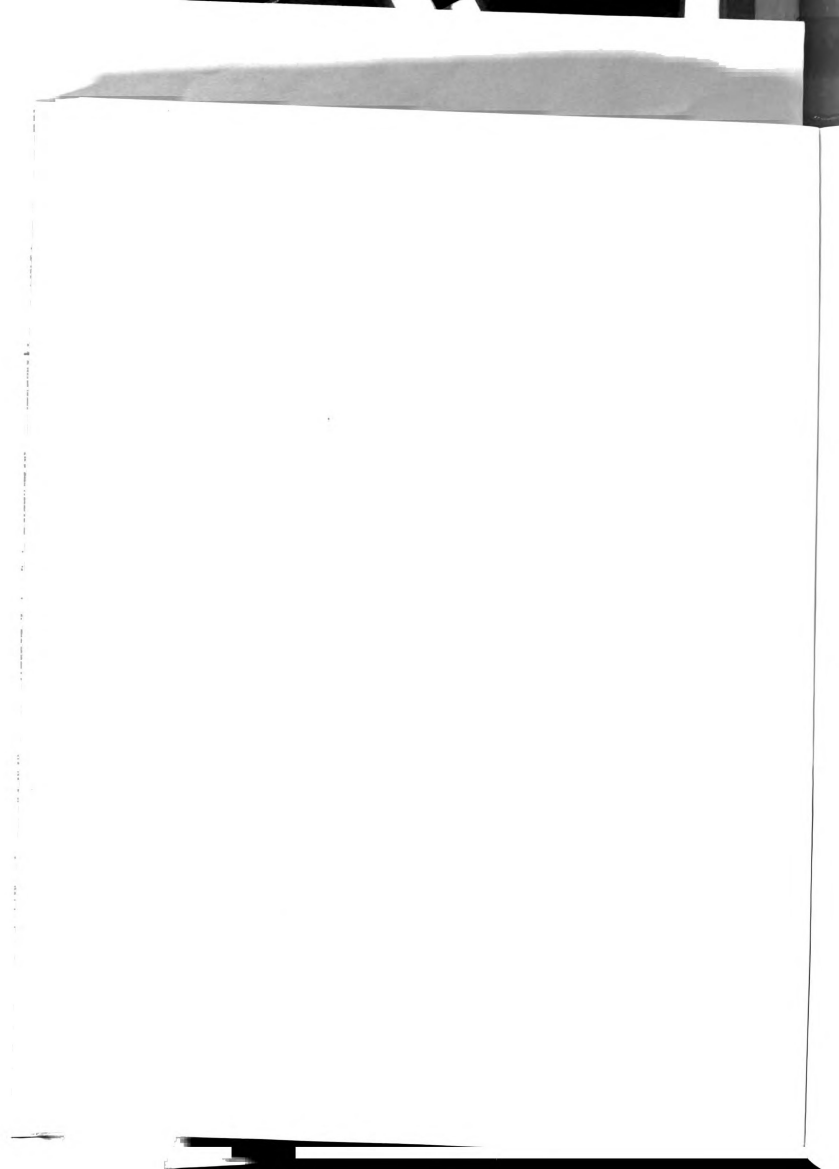




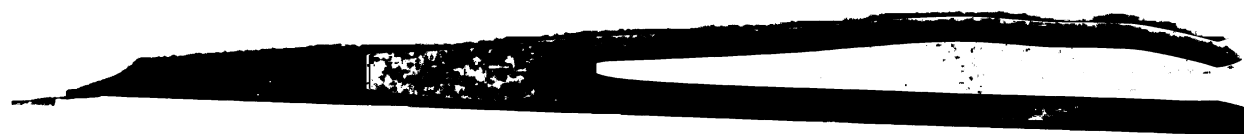
Octanoic Acid
 Lipoic acid

Despite the differences in cluster properties for the AdoMet-dependent Fe-S

10



generated from the much simpler cofactor, AdoMet, through an interaction with an Fe-S cluster is an intriguing mechanistic question. It has been shown for LAM (35), PFL-AE (16), and aRNR-AE (34) that the $[4\text{Fe-4S}]^{1+}$ is the cluster that interacts with AdoMet to initiate radical chemistry, and one-electron oxidation of the cluster appears to accompany radical generation (16, 35). Based on this information, a general mechanistic framework for the adenosyl radical generation in PFL-AE, as well as these related enzymes is proposed (Scheme I.9). In this scheme, the unidentified ligand to the labile iron site is denoted as "X". This ligand is likely to be an exogenous ligand in the resting enzyme or in the environment, such as H_2O , but may be displaced by AdoMet in its catalytically relevant state (Step 1). The presence of AdoMet has been shown to dramatically affect the EPR signal of the PFL-AE $[4\text{Fe-4S}]^{1+}$ (15, 16), suggesting the possibility of a direct interaction between AdoMet and Fe-S cluster of PFL-AE, though the nature of the enzyme-AdoMet complex is not clear. This direct interaction could occur through either the iron or the sulfides of the cluster, and could involve the sulfonium, 5'-carbon, hydroxyls, or amino and carboxylate functionalities of AdoMet. In the central and most intriguing mechanistic step, the reduced cluster donates an electron to convert AdoMet to methionine and 5'-deoxyadenosyl radical intermediate (Step 2). Label-transfer from the glycine residue of PFL to 5'-dAdo product has provided indirect evidence for an adenosyl radical intermediate (8), but direct spectroscopic evidence for the existence of the adenosyl radical intermediate is not available due to the instability of this radical intermediate. An allylic analog of the 5'-deoxyadenosyl radical has been detected in the LAM catalyzed reaction (55, 56). The adenosyl radical intermediate then abstracts a hydrogen atom from PFL Gly734 to generate 5'-dAdo and the glycy radical (Step 3).

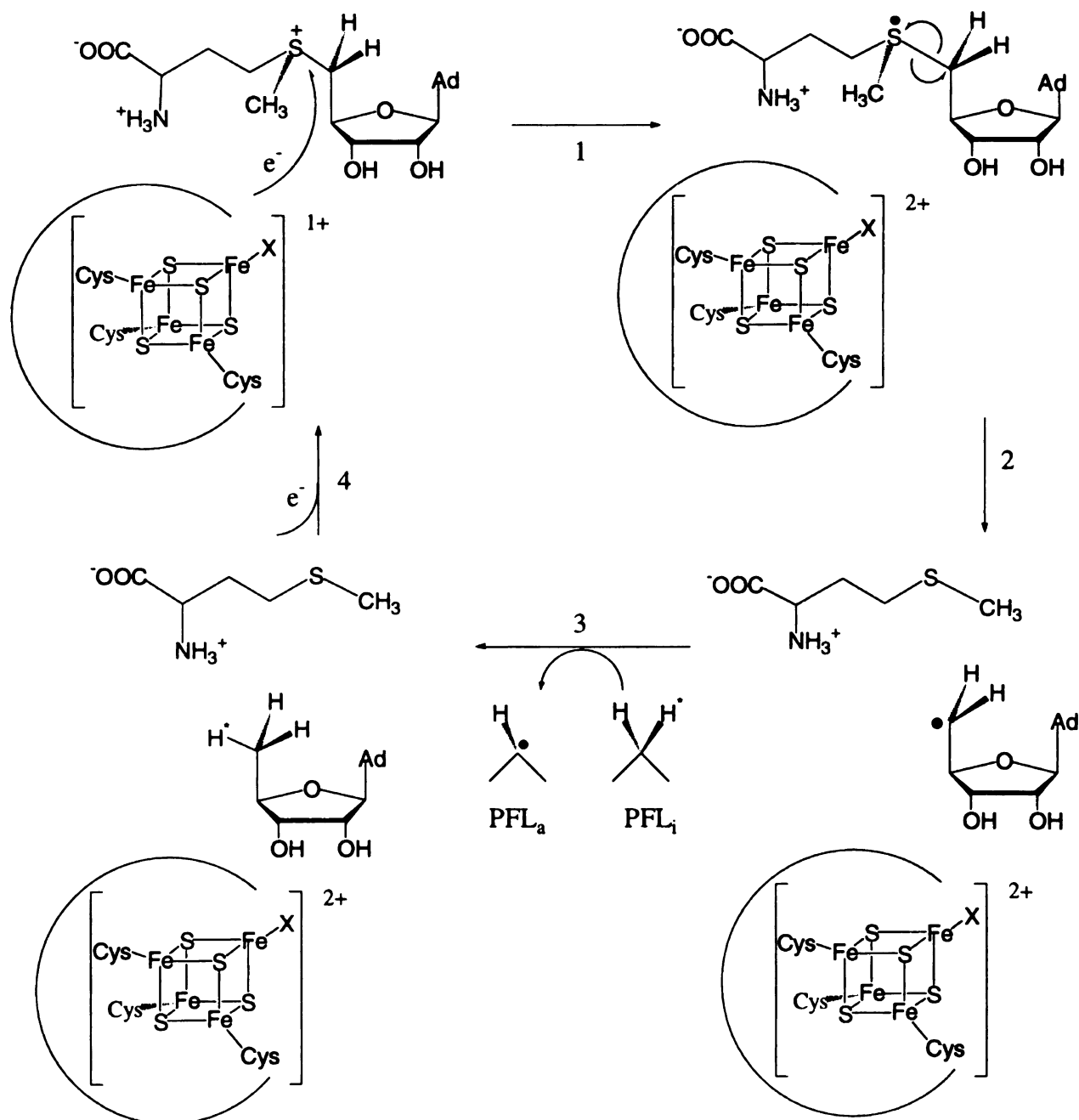


100

100

100

PFL-AE consumes one AdoMet per turnover, and therefore, after release of methionine of 5'-dAdo, an external reductant is necessary to reduce the $[4\text{Fe-4S}]^{2+}$ to the $[4\text{Fe-4S}]^{1+}$ cluster, enabling further turnover. *In vivo*, the source of reductant is flavodoxin / flavodoxin reductase (1).



Scheme I.9 General mechanism for radical generation in PFL-AE

The key question regarding the mechanism by which the Fe-S cluster interacts with adenosylmethionine to generate an adenosyl radical intermediate remains to be answered. As the sulfur-5'-deoxyadenosyl carbon bond is reductively cleaved during the radical generation, the sulfonium center of AdoMet is likely to be positioned close to the Fe-S cluster. In the work described here, the putative interaction between AdoMet and the Fe-S cluster was probed. The sulfonium center of AdoMet was synthetically modified, and used along with a variety of spectroscopic methods to investigate the interaction between AdoMet and the Fe-S cluster of PFL-AE. Specifically, the methyl group of AdoMet was labeled with ^2H and ^{13}C , and the sulfur was replaced by selenium to take advantage of the natural abundance of ^{77}Se (7.50 %). All of these nuclei have non-zero nuclear spins, and therefore, are effective probes in spectroscopic studies, such as electron paramagnetic resonance (EPR) and electron nuclear double resonance (ENDOR) spectroscopy, to demonstrate the possible interaction between AdoMet and the Fe-S cluster of PFL-AE.

.

(2)

47

CHAPTER II

OVEREXPRESSION AND CHARACTERIZATION OF PYRUVATE FORMATE-LYASE AND PYRUVATE FORMATE-LYASE ACTIVATING ENZYME

II.1 Introduction

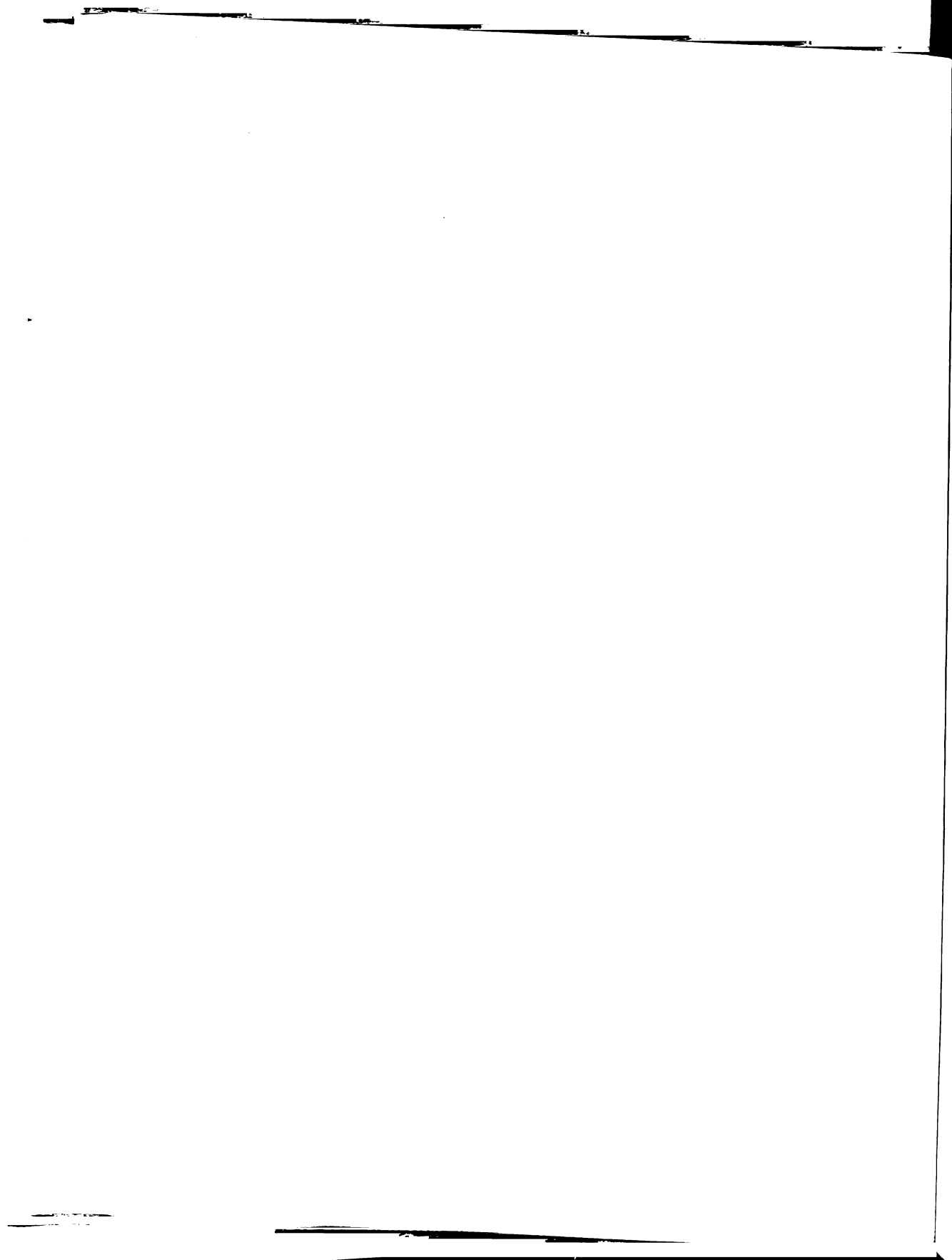
Pyruvate formate-lyase (PFL) plays a central role in anaerobic glucose fermentation, catalyzing the reversible conversion of pyruvate and coenzyme A (CoA) to acetyl-CoA and formate (Scheme I.1). The catalytic activity of PFL is regulated at both the transcriptional and post-translational levels (66, 67). Under aerobic conditions, PFL is expressed constitutively but is inactive; conversion of the inactive form to the active form occurs post-translationally upon a shift to anaerobic conditions, and is catalyzed by the pyruvate formate-lyase activating enzyme (PFL-AE) (Scheme I.4), which requires S-adenosylmethionine and flavodoxin as cosubstrates. Pyruvate or oxamate is also required as an allosteric effector for PFL activation (66-68). The inactive form of PFL has an α_2 oligomeric structure (2x85 kDa) and contains no cofactor (2). The active form of PFL contains a stable glycyl radical located at residue 734 (4). During the PFL activation reaction, the glycyl radical is formed by abstraction of the pro-S hydrogen atom of G734 of PFL, and AdoMet is converted stoichiometrically to methionine and 5'-deoxyadenosine (5'-dAdo) (2, 8).

PFL-AE was first isolated by Knappe *et al.* from non-overexpressing *E. coli* cells (2). The *E. coli* cells were grown anaerobically, but the enzyme was purified aerobically and shown to be a 28 kDa monomer. A broad absorbance from 310 to 550 nm suggested

the presence of a covalently bound chromophore. The enzymatic activity was shown to be completely dependent on the presence of exogenous iron in the assay.

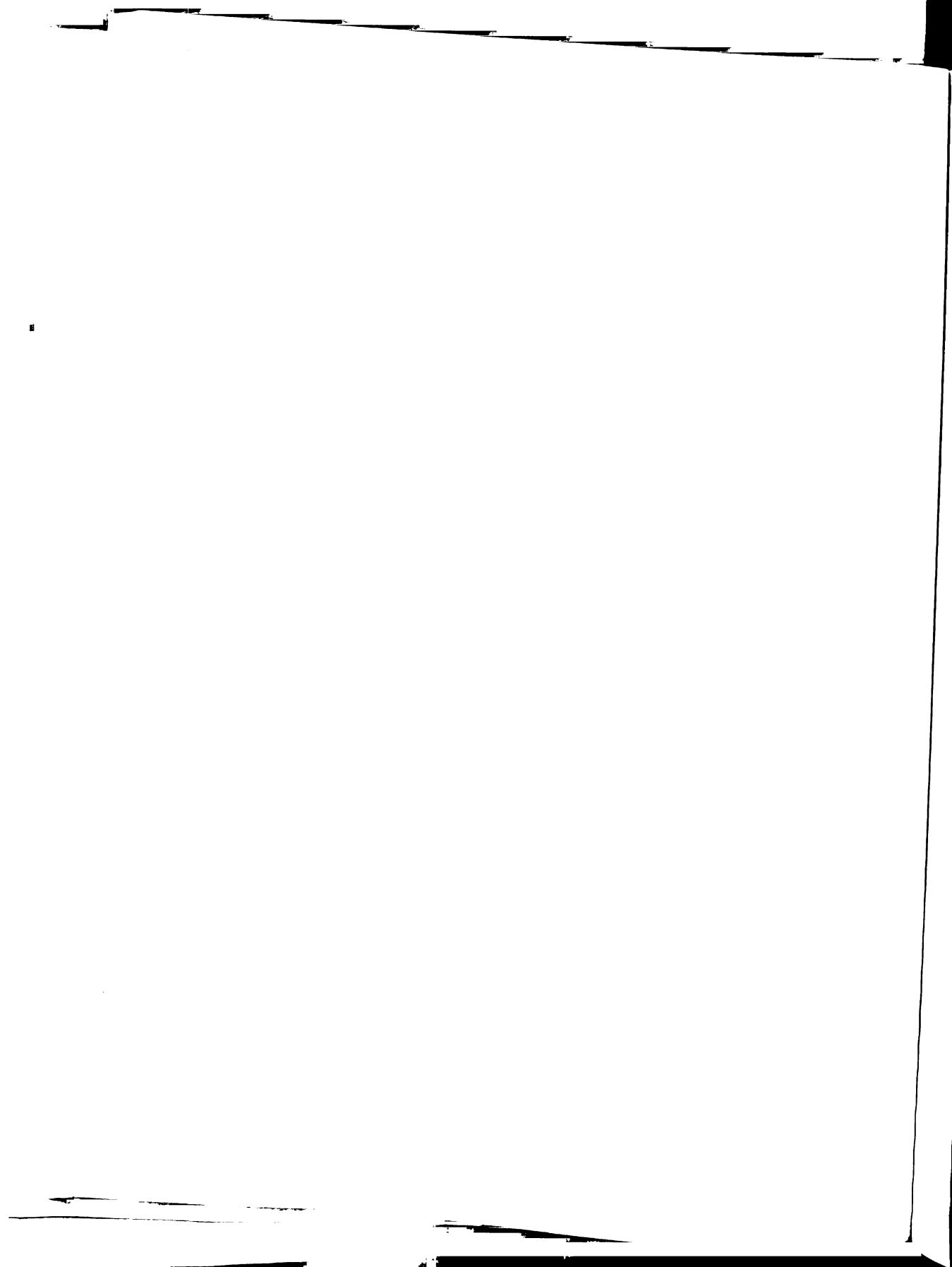
The first over-expression of PFL-AE in *E. coli* was reported by Wong *et al.* (12). The majority of the overexpressed protein, however, was found in the form of insoluble inclusion bodies. PFL-AE was purified from these inclusion bodies by denaturation in guanidine-HCl, followed by gel-filtration chromatography and refolding under anaerobic conditions. Fe(II) was not required for refolding but could be included with a stoichiometry of approximately 1:1, and was again an absolute requirement for activation of PFL. The apo-enzyme could also be reconstituted with various divalent metals, although none of these metal-substituted proteins showed activity in the absence of added iron. Thiophilic metals such as Cu(II), Zn(II), Hg(II) and Cd(II) were found to be inhibitors of PFL-AE activity, which was consistent with the proposal that cysteines are the metal ligands.

The ability to isolate large quantities of native PFL-AE, without resorting to denaturation and artificial reconstitution, is critical to understanding the nature of the iron center in PFL-AE and its role in radical generation. The first isolation of PFL-AE in its native state under strictly anaerobic conditions and identification of the presence of an iron-sulfur cluster in PFL-AE were achieved by Broderick *et al.* (13, 14). When purified under anaerobic conditions in the absence of DTT, PFL-AE was shown to contain primarily a $[3\text{Fe-4S}]^+$ cluster by a combination of UV-visible, EPR and resonance Raman spectroscopic methods (14). A complete description of the states of the cluster present in the enzyme was provided by Mössbauer spectroscopy (15), a method that can detect and quantify all iron species in the samples. Detailed analysis of the Mössbauer data



indicates a mixture of Fe-S clusters with the cuboidal $[3\text{Fe-4S}]^+$ cluster as the primary cluster form, accounting for 66 % of the total iron. Also present are $[2\text{Fe-2S}]^{2+}$ (12 % of the total Fe), $[4\text{Fe-4S}]^{2+}$ (8 % of the total Fe) and linear $[3\text{Fe-4S}]^+$ (~10 % of the total Fe). The isolated native enzyme has nearly a full complement of Fe-S cluster with approximately 3 irons and 3 sulfides per protein molecule. It exhibits a high specific activity (95 U/mg) in the absence of added iron, while the apo-enzyme exhibits no such activity, indicating the cluster present in native enzyme is essential and sufficient for enzymatic activity.

In the dithionite-reduced form of PFL-AE, all cluster types were converted into the $[4\text{Fe-4S}]$ form (15). By analogy to aconitase (69), the $[4\text{Fe-4S}]$ cluster was expected to be the catalytically relevant cluster, which is generated under the reducing conditions present in the activity assay. Recently, Henshaw *et al.* have demonstrated that the $[4\text{Fe-4S}]^{1+}$ is the catalytically active cluster of PFL-AE and that it donates the electron required for reductive cleavage of AdoMet (16). The purification of PFL-AE containing primarily $[3\text{Fe-4S}]^+$ clusters implies a labile fourth iron site, and is consistent with the observation that only three cysteines have been implicated in cluster coordination (17). These three cysteines exist in a $\text{CX}_3\text{CX}_2\text{C}$ motif that is common to all of the AdoMet dependent Fe-S enzymes for which a sequence has been determined (18-23). The identity of the fourth ligand to the $[4\text{Fe-4S}]$ cluster in PFL-AE and these related enzymes is currently unknown. By analogy to aconitase, in which substrate coordinates to the unique iron site (70-72), and solvent binds in the absence of substrate or product (70), it is reasonable to propose that exogenous ligands such as water or substrate may bind to the unique labile iron site in PFL-AE.



Currently, PFL-AE is purified under anaerobic reducing conditions in the presence of DTT to yield essentially EPR-silent clusters, presumably in the $[4\text{Fe-4S}]^{2+}$ state, which can be readily reduced to $[4\text{Fe-4S}]^{1+}$ – the cluster that is responsible for providing the electron necessary for AdoMet dependent glycyl radical generation on PFL.

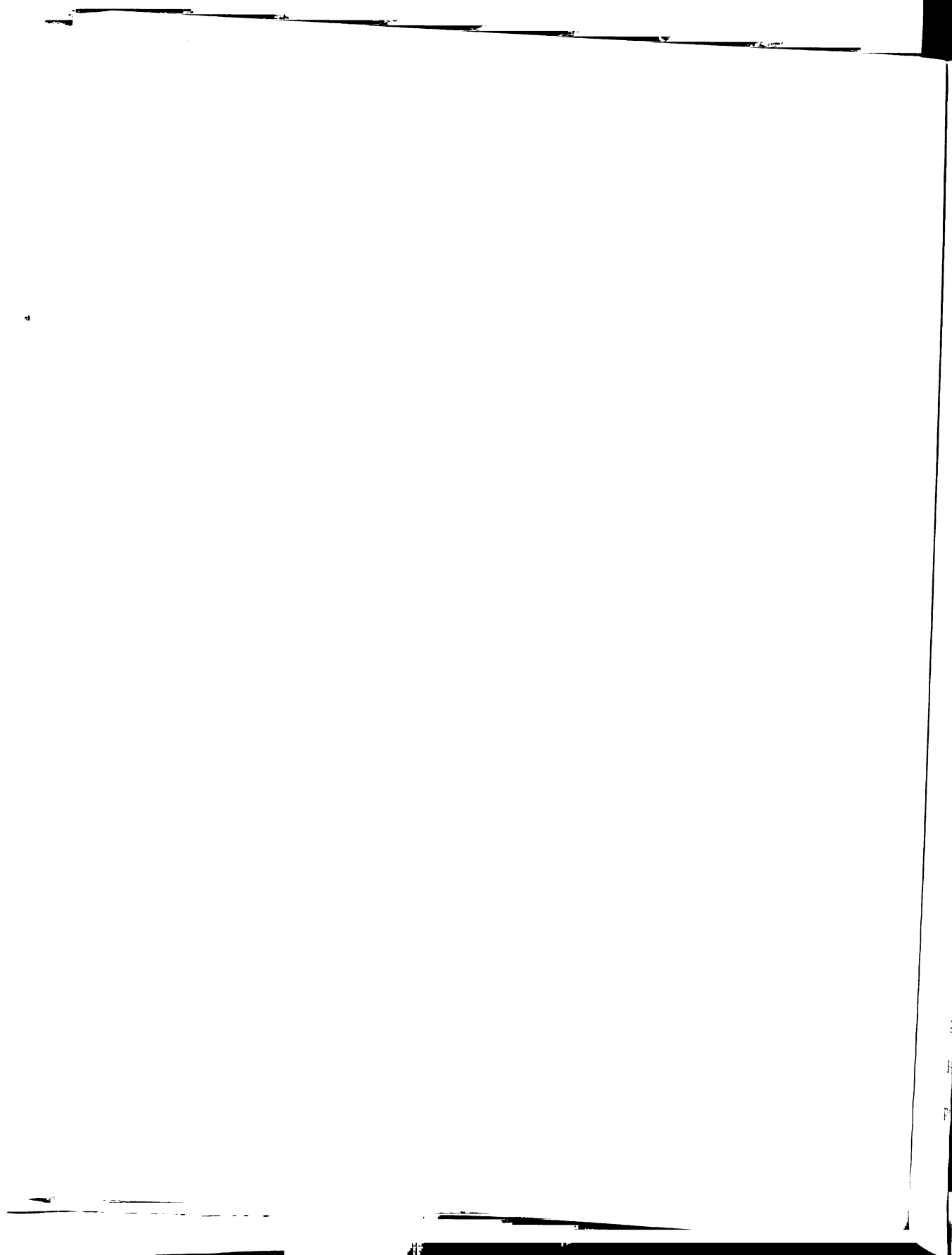
II.2 Experimental methods

II.2.1 Materials

The plasmids pMG-AE and pKK-PFL were obtained as a generous gift from John Kozarich (Merck). The *Escherichia coli* BL21(DE3)pLysS strain and pCAL-n-EK expression vector were obtained from Stratagene. 5-Deazariboflavin was previously synthesized in our laboratory according to published procedures (73-75), and characterized using NMR and TLC. All other chemicals were obtained commercially and used as received.

II.2.2 Growth and expression of PFL

pKK-PFL was used to transform BL21(DE3)pLysS. A single colony of transformed cells was used to inoculate 50 mL LB media containing 50 $\mu\text{g/mL}$ ampicillin (LB/Amp). This culture was grown for 16 h to saturation and then used to inoculate LB/Amp in a 9 L bench-top fermentor (New Brunswick). The 9 L culture was grown at 37 °C with continuous air purge and vigorous agitation to early log phase ($\text{OD}_{600} \sim 0.6$ -0.8), and then induced by addition of isopropyl- β -D-thiogalactopyranoside (IPTG) to



1 mM. The culture was grown for 2 more hours before harvesting by centrifugation at $10,816 \times g$ (8,000 rpm, Sorvall GS3 rotor). The supernatant was decanted and the cells stored at $-80\text{ }^{\circ}\text{C}$.

II.2.3 Purification of PFL

PFL was purified from the BL21(DE3)pLysS/pKK-PFL cells. Cell paste (typically approximately 10 g) was suspended in enzymatic lysis buffer (5 mL per gram of cell paste) containing 20 mM Hepes, pH 7.2, 1 % (w/v) Triton X-100, 5 % (w/v) glycerol, 10 mM MgCl_2 , 8 mg lysozyme, 1 mM PMSF, and trace amounts (approximately 0.1 mg each) RNase A and DNase I. The suspension was agitated and then incubated at ambient temperature for 1 hour. The lysed cells were centrifuged at $26,892 \times g$ (15,000 rpm, SS34) for 20 min at 4°C . The crude extract (typically approximately 50 mL) was decanted and loaded onto an Accell Plus QMA Anion Exchange column (Quaternary Methylamine, 300 Å, Waters Corp., 5 x 30 cm) equilibrated with Buffer A (20 mM Hepes, pH 7.2, 1 mM DTT). The column was washed with 300 mL of the same buffer prior to running a gradient from Buffer A to Buffer B (20 mM Hepes, pH 7.2, 500 mM NaCl, 1 mM DTT) over 900 mL. PFL eluted at approximately 240 mM NaCl. Fractions containing $\geq 75\%$ pure PFL (as judged by SDS-PAGE on a 5 % - 14 % Tris-HCl gel) were combined, flash frozen and stored at $-80\text{ }^{\circ}\text{C}$. Another 50 mL of crude extract was run through the same procedure, and the $\geq 75\%$ pure fractions from both runs were combined, dialyzed against Buffer C (40 mM Hepes, pH 7.2, 1 M ammonium sulfate, 1 mM DTT), and centrifuged to remove precipitated protein. The supernatant was loaded onto a Phenyl-Sepharose column

and the column was

100% $\pm 10,000$ per

used in 80°C

8.3.3. Fractionation

FFL was fractionated

(possibly appropriate

in cell nuclei) contain

spectro, 10 mM HEPES

approximately 0.1

then incubated in air

20,000 \pm (12,000) g

approximately 50 ml

Electrophoresis (C

equipped with Buffer A

washed with 500 ml

buffer B (20 mM HEPES

approximately 540 ml

20S-PAGE on a 7.5

-80°C. Another 50 ml

± 75 pure fraction from both

HeLa cell 7.5 M ammonium

precipitated protein. The supernatant

(Pharmacia 16/10) equilibrated with Buffer C. The column was washed with 50 mL of Buffer C prior to running a gradient from Buffer C to Buffer A over 50 mL, followed by a wash with 50 mL of Buffer A. PFL was eluted through the last half of the gradient. Fractions containing ≥ 95 % pure PFL (as judged by SDS-PAGE) were combined, dialyzed against Buffer A, concentrated, flash-frozen and stored at -80 °C.

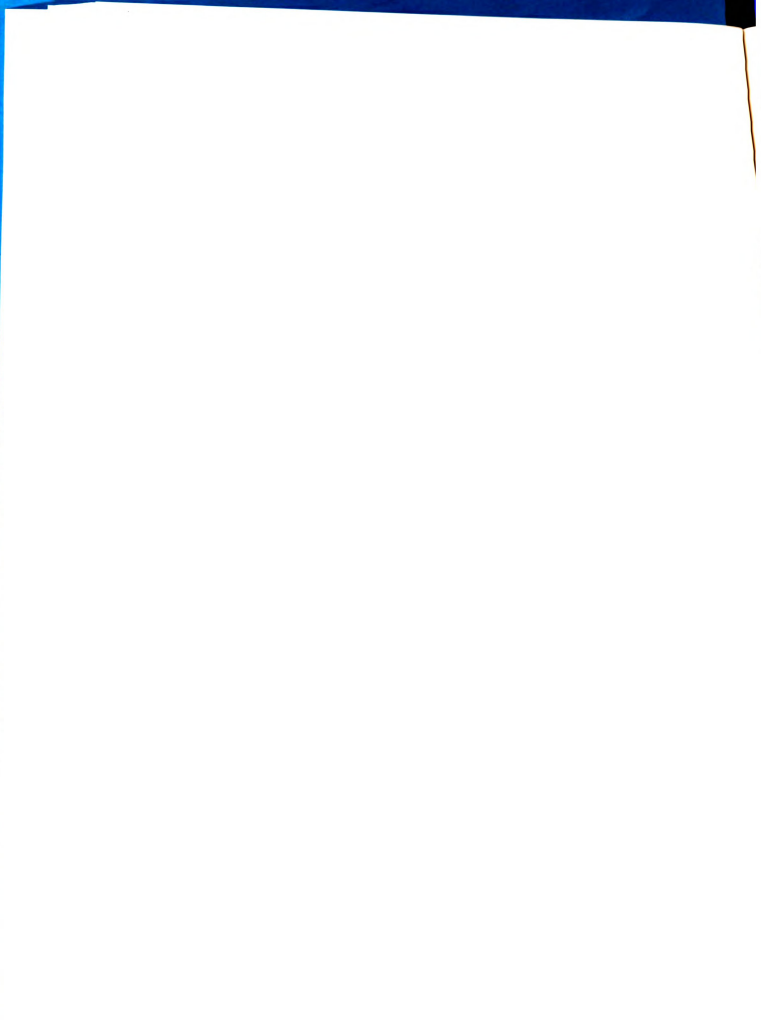
II.2.4 Growth and expression of PFL-AE

A single colony of transformed BL21(DE3)pLysS/pCAL-n-AE3 was used to inoculate 50 mL LB/Amp. This culture was grown for 16 h to saturation at 37 °C and then used to inoculate 9 L of defined MOPS medium based on one previously described (76). The media was modified to include (per 9 L) 75.6 g MOPS, 99 g casamino acid, 7.2 g tricine, 26.3 g NaCl, 14.4 g KOH, 4.6 g NH_4Cl , 200 mL of 20 % glucose, 20 mL of “O” solution, 20 mL of 1 M KH_2PO_4 , 10 mL of 276 mM K_2SO_4 , and 50 mL of 0.1 M CaCl_2 . The “O” solution consists of 0.1 g $\text{FeCl}_2 \cdot 4\text{H}_2\text{O}$ in 10 mL concentrated HCl, 1 mL of “T” solution which includes 8 mL concentrated HCl, 18.4 mg of $\text{CaCl}_2 \cdot 2\text{H}_2\text{O}$, 64 mg H_3BO_3 , 40 mg $\text{MnCl}_2 \cdot 4\text{H}_2\text{O}$, 18 mg $\text{CoCl}_2 \cdot 6\text{H}_2\text{O}$, 4 mg $\text{CuCl}_2 \cdot 2\text{H}_2\text{O}$, 340 mg ZnCl_2 , 605 mg $\text{Na}_2\text{MoO}_4 \cdot 2\text{H}_2\text{O}$, and 2.68 g $\text{MgCl}_2 \cdot 6\text{H}_2\text{O}$. Ampicillin (9 mL of 50 mg/mL) and 10 mg each of riboflavin, thioctic acid, vitamin B12, niacinamide, pantothenic acid, piridoxine and folic acid were added to the 9 L culture right before the inoculation. The 9 L culture was grown at 37 °C in a bench-top fermentor (New Brunswick) with a continuous air purge and vigorous agitation to early log phase ($\text{OD}_{600} \sim 0.5$), and then induced by addition of IPTG to 1 mM. At this time the medium was supplemented with 750 mg $\text{Fe}(\text{NH}_4)_2(\text{SO}_4)_2$. The culture was allowed to grow for an additional 2 h, purging

with air before cooling down and purging with nitrogen for 20 min. The medium was then supplemented with another 750 mg $\text{Fe}(\text{NH}_4)_2(\text{SO}_4)_2$. When the temperature was reduced to 20 °C, the culture was incubated for 14-17 hours at 4 °C under argon. The cells were harvested by centrifugation at $10,816 \times g$ (8,000 rpm, GS3) under anaerobic conditions. The harvested cells were stored under nitrogen at -80°C until used for purification.

II.2.5 Purification of PFL-AE

PFL-AE was purified from *E.coli* BL21(DE3)pLysS transformed with pCAL-n-AE3, prepared as described above. All steps in the purification were performed in a single day under strictly anaerobic conditions in a Coy anaerobic chamber (Coy Laboratories, Grass Lake, MI) at ambient temperature except where noted. Solutions and buffers used in the purification were thoroughly degassed or purged with nitrogen prior to bringing them into the Coy chamber. Cell paste was suspended in enzymatic lysis buffer (2 mL per gram of cells) containing 50 mM Tris-sulfate, pH 7.5, 200 mM NaCl, 1 % Triton X-100, 5 % glycerol, 10 mM MgCl_2 , 1 mM DTT, 8 mg lysozyme, 1 mM PMSF and trace amounts (approximately 0.1 mg each) of RNase A and DNase I. The suspension was agitated with a 10 mL syringe and then incubated at ambient temperature for 1 h. The suspension was centrifuged at $38,724 \times g$ (18,000 rpm, SS34) for 30 min at 4 °C. The extract was decanted and used directly in purification. Up to 30 mL of the crude extract was loaded onto a Sephacryl S-200 HR column (5 x 60 cm) equilibrated with 50 mM Hepes, pH 7.5, 200 mM NaCl, 1 mM DTT. The protein was eluted with this same buffer at 3 mL/min. PFL-AE eluted from the column in a relatively sharp peak at



approximately 680 mL after injection. The fractions that had fairly dark red/brown color were pooled and concentrated down to less than 10mL using an Amicon concentrator with YM10 filter membranes. Another aliquot of crude extract was run through the same procedure. Fractions pooled from both runs were combined, concentrated to less than 20 mL, and re-run on the same column as above. The final fractions were checked by the ratio of UV absorbance at 426 nm and 280 nm. Fractions that have the highest ratio (greater than 0.15, but fractions with a blue-shifted 280 nm peak, indicating nucleic acid contaminants, were avoided) were pooled, concentrated, flash-frozen, and stored at -80°C .

II.2.6 Protein assays

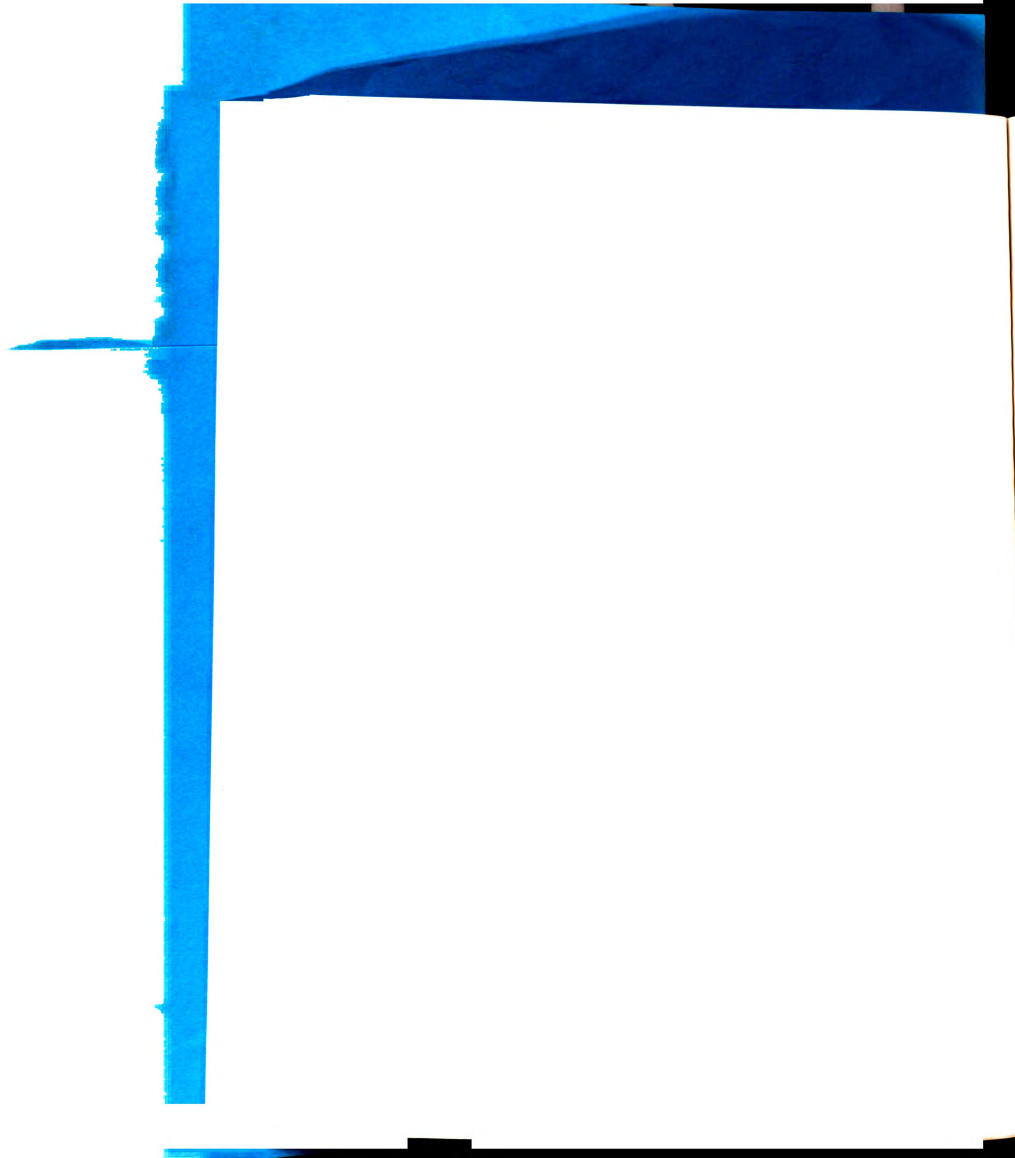
Routine determinations of protein concentrations were done by the method of Bradford (77), using a kit purchased from Bio-Rad, and bovine serum albumin as a standard. Calibration of the results from the Bradford assays of PFL-AE was obtained by amino acid hydrolysis of the purified enzymes, performed at the MCB Core Facility, University of Massachusetts, Amherst. Actual protein concentrations could then be determined by applying a correction factor of 0.65 to the Bradford assays.

II.2.7 Iron assays

Iron assays were carried out by using the method of Beinert (78).

II.2.8 Sulfide assays

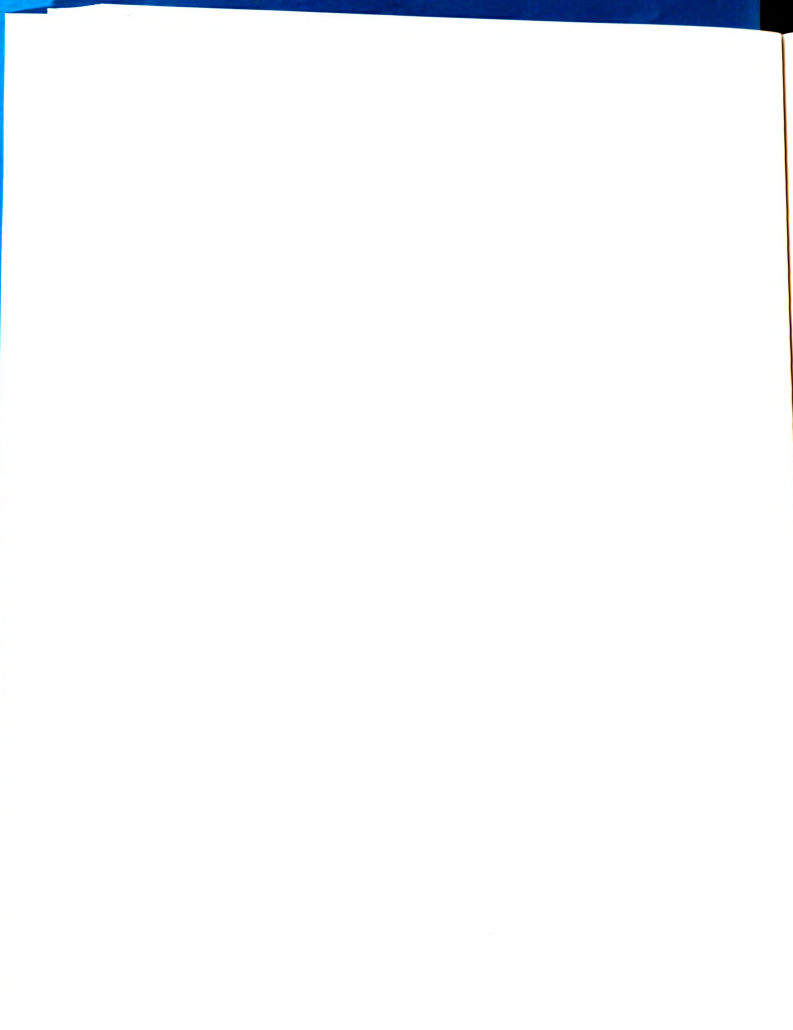
Sulfide assays were carried out with a modification of the method of Beinert (14, 79). The use of siliconized Eppendorf tubes was found to yield more reproducible



results, perhaps due to the minimized head space for loss of sulfide as H_2S . The tubes were kept tightly capped except when adding reagents. Rather than using stir bars, the tubes were closed and vortexed when mixing was called for. The procedure used was as follows. The sample volumes were brought to 100 μL with MQ H_2O , pH 8.1. One at a time, each tube was opened, 300 μL 1 % ZnOAc and 15 μL 12 % NaOH were added simultaneously, the tube was closed tightly and vortexed. When all tubes had been treated in this way, they were allowed to sit for 12 to 15 h before addition (again, one tube processed at a time) of 75 μL DMPD (0.1 % in 5 M HCl) and 2 μL FeCl_3 (23 mM in 1.2 M HCl). $\text{Na}_2\text{S}\cdot 9\text{H}_2\text{O}$ was used as standard and prepared as follow: a small-to-medium chunk of $\text{Na}_2\text{S}\cdot 9\text{H}_2\text{O}$ was rinsed with MQ H_2O , pH 8.1, dried by gently patting with Kim-wipe, weighed to 4 decimal places, and dissolved in 100 mL deoxygenated 0.1 M NaOH solution to make a standard solution of concentration between 1.2 to 2.7 mM. The standard solution was sealed with septum, purged thoroughly with nitrogen, and was good for at least a month.

II.2.9 Activity assay of PFL-AE

The activity of PFL-AE was assayed using a direct enzyme assay in which the amount of glycyl radical on PFL generated by PFL-AE as a function of time was quantified by EPR spectroscopy. The PFL-AE reaction mix contained in a final volume of 1 mL: 0.1 M Tris- HCl , pH 7.6, 0.1 M KCl , 10 mM DTT, 10 mM oxamate (allosteric effector), 10.01 mg PFL, 200 μM 5-deazariboflavin, 0.2 mM AdoMet, and 0.186 μM PFL-AE. This mix was made in an anaerobic chamber by combining reagents from anoxic stock solutions in the order listed to the final concentrations indicated. The 1 mL



mix was split into 5 EPR tubes and the reaction was initiated by illumination of the samples with a 500 W halogen lamp. The samples were situated at a distance of 5 cm from the lamp and maintained at ambient temperature (20-26 °C) during illumination by immersion in a water bath to which ice was added as needed. After specified periods of illumination, typically 5, 10, 20, 30, and 40 min, the samples were flash-frozen to stop the reaction. The amount of glycy radical generated was determined by EPR spectroscopy. One unit of PFL-AE activity was defined as 1nmol of glycy radical generated per min, and the specific activity of PFL-AE was defined as the number of units per mg of PFL-AE.

II.2.10 EPR spectroscopy

EPR first-derivative spectra were obtained at X-band on a Bruker ESP300E spectrometer equipped with a liquid He cryostat and a temperature controller from Oxford Instruments. Spectra were recorded at 12 K for $[3\text{Fe-4S}]^{1+}$ and $[4\text{Fe-4S}]^{1+}$, and at 60 K to detect glycy radical. Spin quantifications were done as described previously (80). The double integrals of the EPR signals were evaluated by using a computer on-line with the spectrometer. Spin concentrations in the protein samples were determined by calibrating double integrals of the EPR spectra recorded under nonsaturating conditions (i) with a standard sample of 0.1 mM Cu(II) and 1 mM EDTA solution for the cluster signals, or (ii) with a 1.04 mM $\text{K}_2(\text{SO}_3)_2\text{NO}$ solution for the glycy radical signals. The concentration of the $\text{K}_2(\text{SO}_3)_2\text{NO}$ standard was determined using the optical extinction coefficient (81).

the new vinyl group (PPV).

samples were 200-250 μ thick.

the film was washed

in a water bath

temperature (20°C).

the reaction. The

polymer. One

product for each

was not of PTFE.

11.3.1. EPR spectra

EPR (first-derivative

derivative) spectra

(first-derivative

of the first-derivative

of the first-derivative

of the first-derivative

of the first-derivative

of the first-derivative

of the first-derivative

of the first-derivative

of the first-derivative

of the first-derivative

of the first-derivative

of the first-derivative

of the first-derivative

II.3 Results and Discussion

II.3.1 Expression and purification of PFL

PFL was purified from BL21(DE3)pLysS cells harboring the pKK-PFL plasmid. The cells were lysed by an enzymatic procedure. Two portions of partially purified PFL from the first ion-exchange column (chromatogram see Fig. II.1; SDS-PAGE gel see Figure II.2) were combined, dialyzed, and run on an hydrophobic column to yield $\geq 95\%$ pure PFL (chromatogram see Fig. II.2; SDS-PAGE gel see Figure II.3). Yield was approximately 50 mg of purified PFL per liter of bacterial culture.

11. Results and Discussion

11.1. Experimental results

11.1.1. PFT with low flow

The cells were fixed with 10% formalin and embedded in paraffin. The cells were then stained with hematoxylin and eosin (H&E) and mounted on glass slides. The cells were then examined under a light microscope.

Figure 1 shows the results of the PFT with low flow. The cells were fixed with 10% formalin and embedded in paraffin. The cells were then stained with hematoxylin and eosin (H&E) and mounted on glass slides. The cells were then examined under a light microscope.

Figure 2 shows the results of the PFT with low flow. The cells were fixed with 10% formalin and embedded in paraffin. The cells were then stained with hematoxylin and eosin (H&E) and mounted on glass slides. The cells were then examined under a light microscope.

Figure 3 shows the results of the PFT with low flow. The cells were fixed with 10% formalin and embedded in paraffin. The cells were then stained with hematoxylin and eosin (H&E) and mounted on glass slides. The cells were then examined under a light microscope.

Figure 4 shows the results of the PFT with low flow. The cells were fixed with 10% formalin and embedded in paraffin. The cells were then stained with hematoxylin and eosin (H&E) and mounted on glass slides. The cells were then examined under a light microscope.

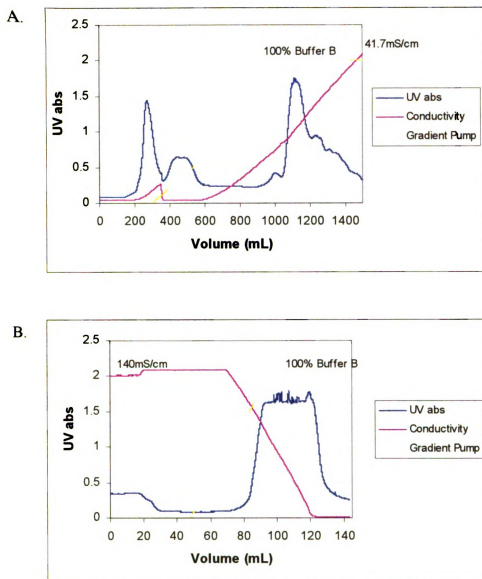
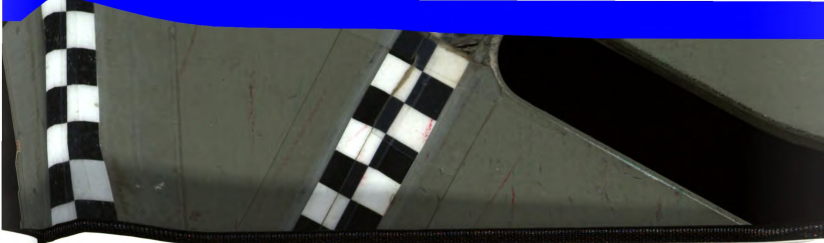


Figure II.1 Chromatograms of purification of PFL. **A.** Elution profile for the Accell Plus QMA Anion Exchange column (Quaternary Methylamine, 300 Å, Waters Corp., 5 x 30 cm), gradient from Buffer A (20 mM Hepes, pH 7.2, 1 mM DTT) to Buffer B (20 mM Hepes, pH 7.2, 500 mM NaCl, 1 mM DTT) over 900 mL, flow rate 5 mL/min. PFL eluted at approximately 240 mM NaCl, and was dialyzed against Buffer C (40 mM Hepes, pH 7.2, 1 M ammonium sulfate, 1mM DTT). **B.** Elution profile for the Phenyl-Sepharose column (Pharmacia 16/10), gradient from Buffer C to Buffer A over 50 mL, followed by a wash with 50 mL of Buffer A, flow rate 1 mL/min. PFL was eluted through last half of the gradient. (Images in this thesis are presented in color.)

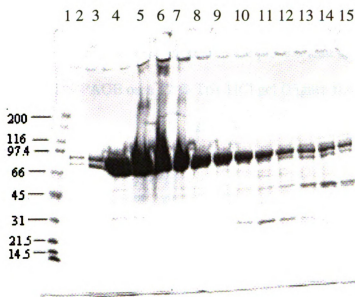


Figure II.2 SDS-PAGE analysis of PFL fractions off the Accell Plus QMA anion-exchange column. Lane 1, molecular marker (kDa); lane 2-15, fractions 19-45 (every other one). Fractions 23-43 were pooled.

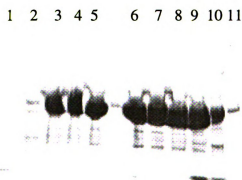
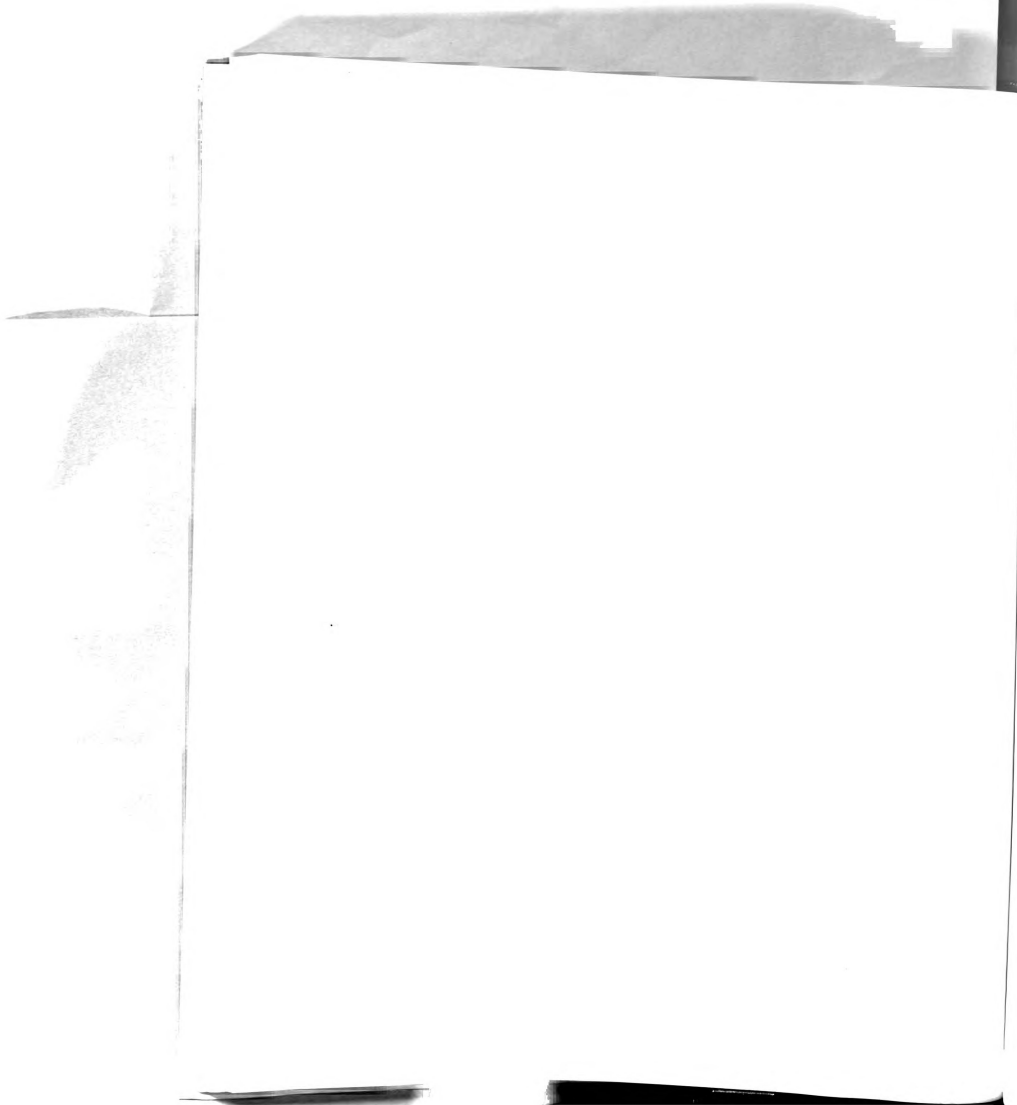


Figure II.3 SDS-PAGE analysis of PFL fractions off the Phenyl-Sepharose hydrophobic column. Lane 1-11, fractions 7-27 (every other one). Fractions 11-21 were pooled.



II.3.2 Expression and purification of PFL-AE

PFL-AE was purified from BL21(DE3)pLysS cells harboring the pCAL-n-AE3 expression vector. Overexpression of the protein in the pre-induced and post-induced cells were checked by SDS-PAGE on a 12 % Tris-HCl gel (Figure II.4). The cells were

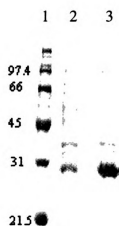


Figure II.4 SDS-PAGE analysis of overexpression of PFL-AE in *E. coli* cells. Lane 1, molecular marker (kDa); lane 2, pre-induced cells; lane 3, post-induced cells.

lysed by an enzymatic procedure, and PFL-AE was purified from this crude extract by two passages through a preparative gel filtration column (Figure II.5). The enzyme eluted as a reddish-brown peak, and pure fractions from the final run of the column were identified by the highest ratio of absorbance at 426 nm and 280 nm. Both $[3\text{Fe-4S}]^{1+}$ and $[4\text{Fe-4S}]^{2+}$, the major cluster forms found in purified PFL-AE, have significant absorbance at 426 nm. All proteins have maximal absorbance at 280 nm. The high iron content in the enzyme, thus, is indicated by the high ratio of the absorbance values (Table II.1). Fraction purity was confirmed by SDS-PAGE (Figure II.6), and the purest fractions were combined, concentrated, and stored under nitrogen in small aliquots at -80°C . Yield was typically 40-50 mg of purified PFL-AE per liter of bacterial culture.

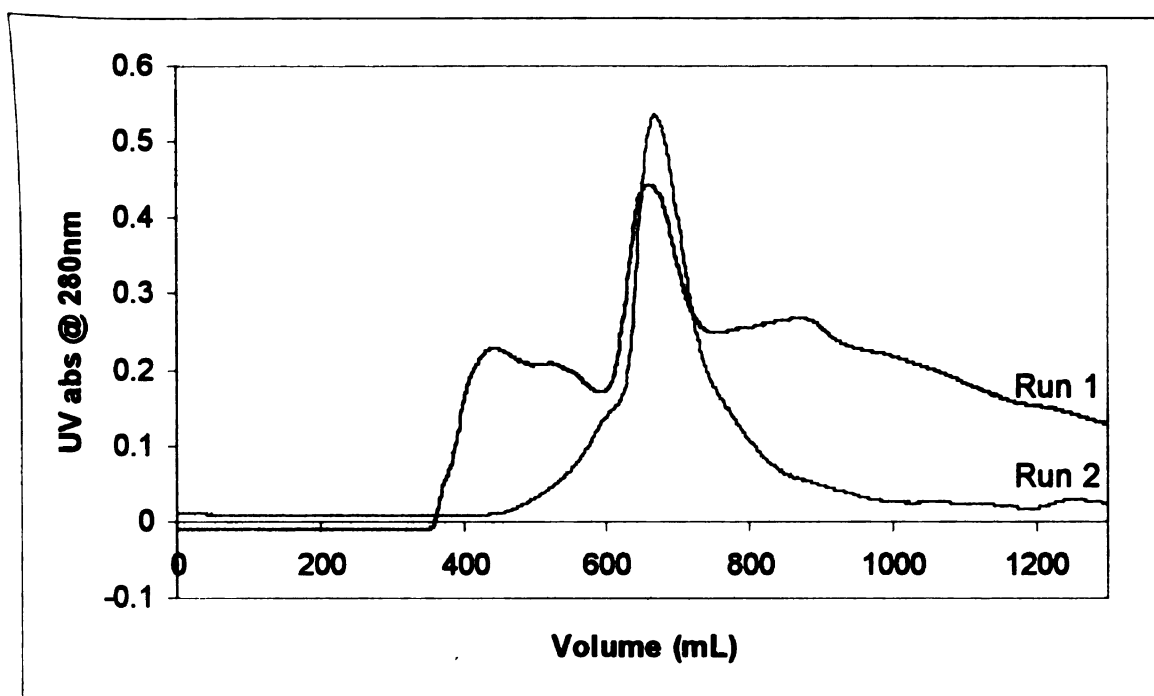
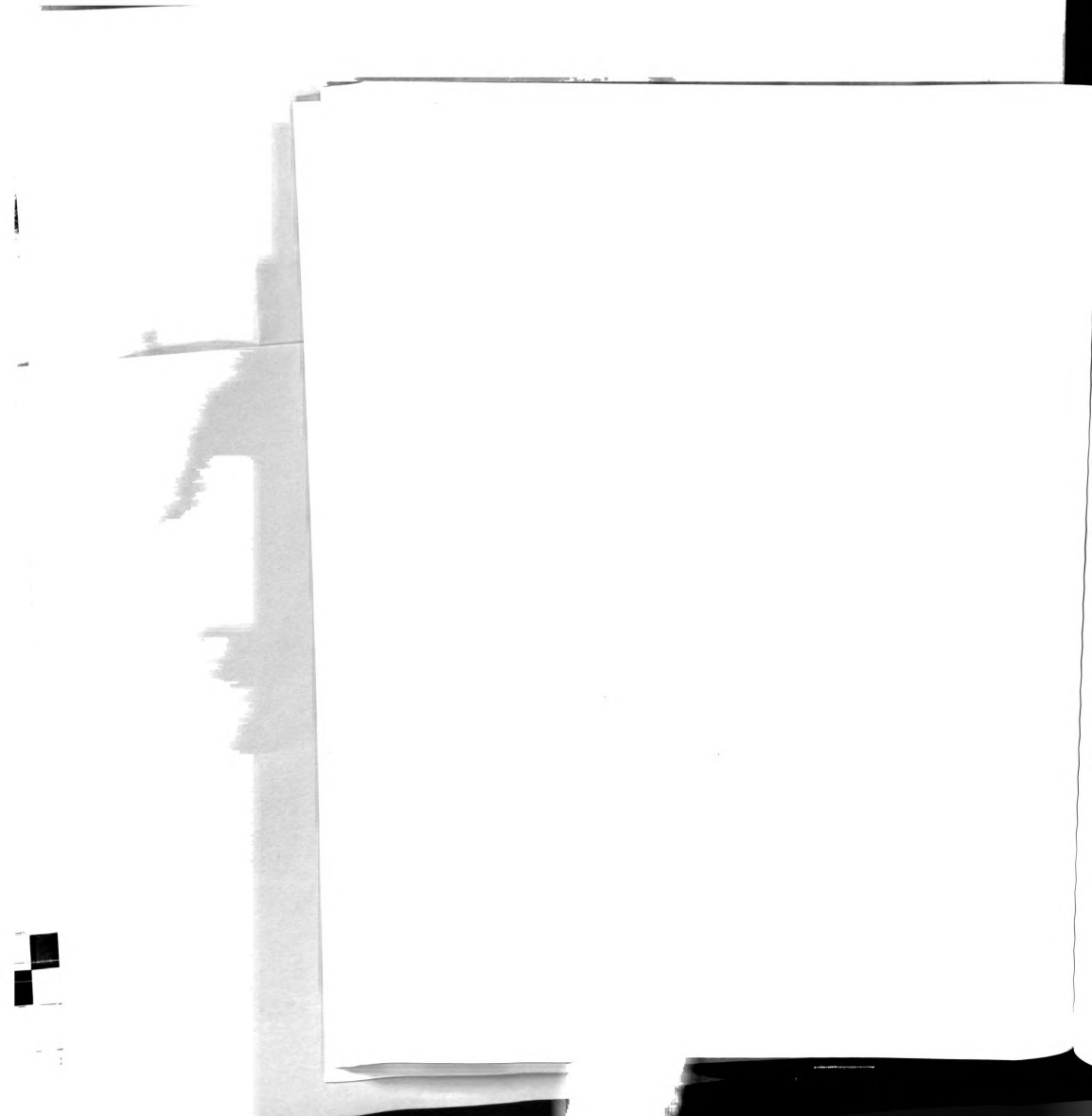


Figure II.5 Purification of PFL-AE by gel-filtration chromatography (Sephacryl S-200 HR column, 5 x 60 cm). The protein was eluted with 50 mM Hepes, pH 7.5, 200 mM NaCl, 1 mM DTT at 3 mL/min. PFL-AE eluted from the column in a relatively sharp peak at approximately 680 mL after injection. The chromatogram labeled “Run 2” shows the final purification of the pooled fractions from two first runs on the column.

Fraction	Ratio 426 nm / 280 nm	Abs at 426 nm	Abs at 280 nm
17	0.085	0.022	0.255
18	0.128	0.046	0.359
19	0.154	0.067	0.435
21	0.184	0.069	0.378
23	0.213	0.046	0.216
25	0.153	0.019	0.125
27	0.101	0.009	0.091
28	0.095	0.008	0.080

Table II.1 Ratio of absorbances at 426 nm and 280 nm of PFL-AE fractions off the 2nd run of the gel filtration column.



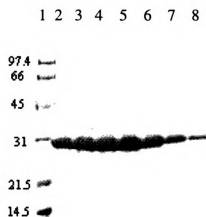


Figure II.6 SDS-PAGE analysis of PFL-AE fractions off the 2nd run of the gel filtration column. Lane 1, molecular marker (kDa); lane 2-8, fractions 17, 18, 19, 20, 22, 24, 26. Fractions 19-25 were pooled.

II.3.3 Characterization of purified PFL-AE

PFL-AE purified under anaerobic reducing conditions in the presence of 1mM DTT was essentially EPR-silent, presumably in the $[4\text{Fe-4S}]^{2+}$ state, containing approximately 2 % $[3\text{Fe-4S}]^{1+}$ as indicated by EPR spectroscopy (Figure II.7). The protein was found to contain 2.5-3.8 mol Fe / mol protein and a stoichiometric amount of acid-labile sulfide.



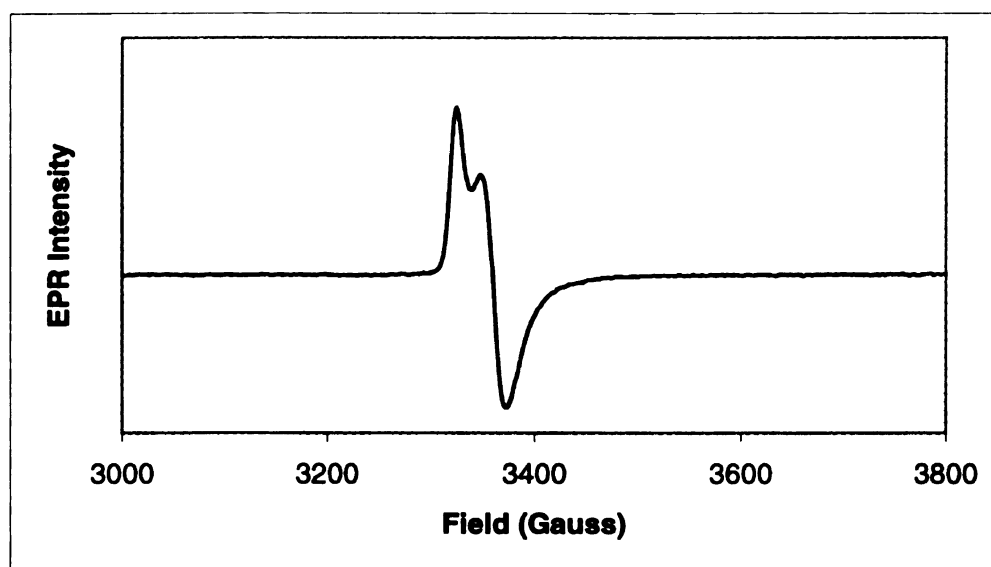
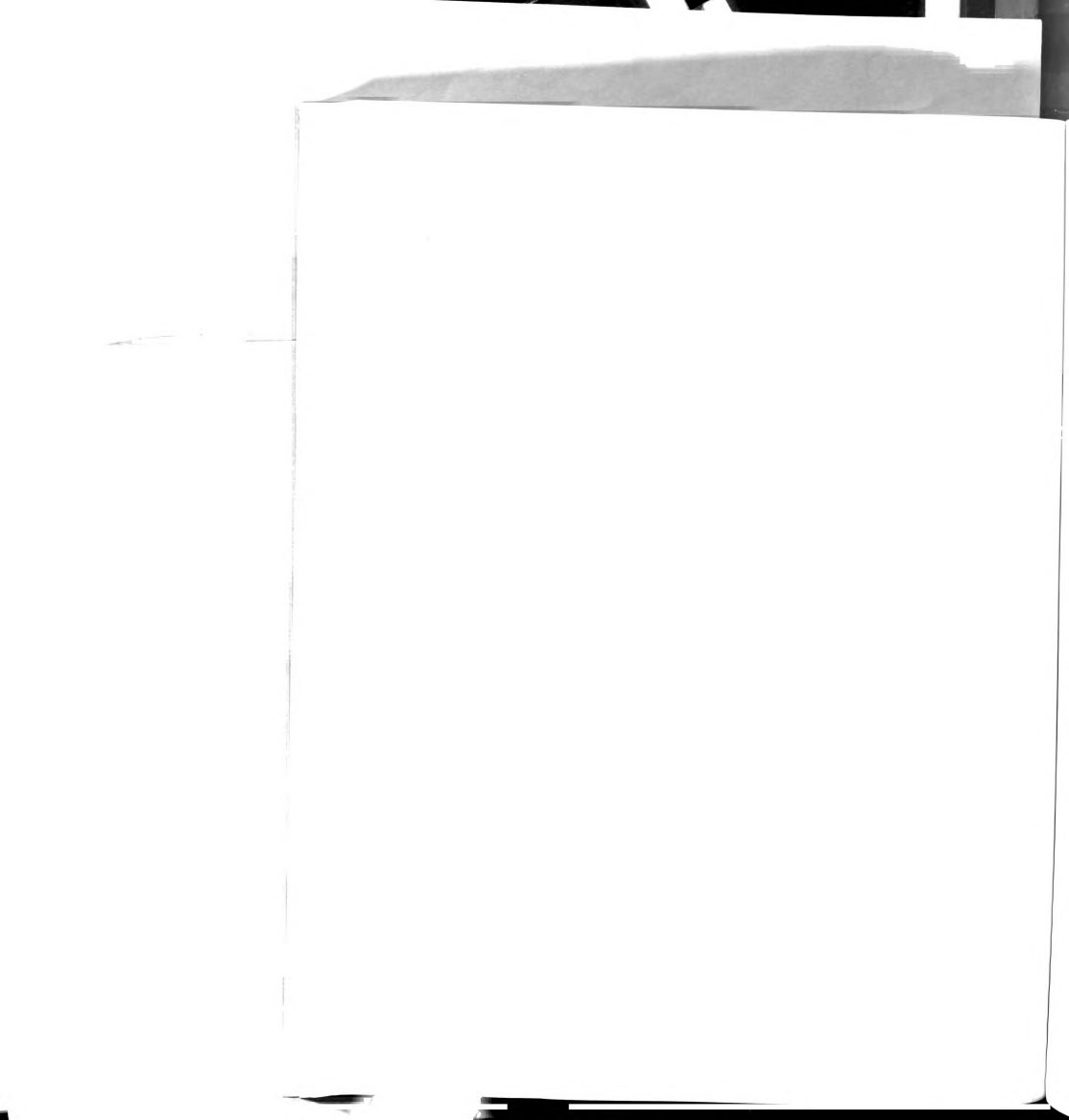


Figure II.7 X-band EPR spectrum of PFL-AE as-isolated in the presence of 1 mM DTT. Protein concentration, 400 μM ; $[\text{3Fe-4S}]^{1+}$ concentration, 8.3 μM , $g_{\perp} = 2.017$, $g_{\parallel} = 2.038$. Conditions of measurement, $T = 12\text{ K}$; microwave power, 2 mW; microwave frequency, 9.49 GHz; modulation amplitude, 9.57 G; modulation frequency, 100 kHz, single scan.

Using purified PFL and PFL-AE, a specific activity for PFL-AE of 109 units / mg was achieved using the direct activity assay (Figure II.8), and the specific activity per holoenzyme was calculated to be 115 U/mg based on 3.8 mol Fe/mol protein (Table II.2).

Rate (μM glcyl radical/ min)	0.5697
Units (nmol PFL/ min)	0.5697
Specific Activity (U/ mg PFL-AE)	109
Number of Fe in PFL-AE (mol Fe/ mol PFL-AE)	3.8
Specific Activity per holoenzyme (U/ mg)	115

Table II.2 Summary of activity assay of PFL-AE



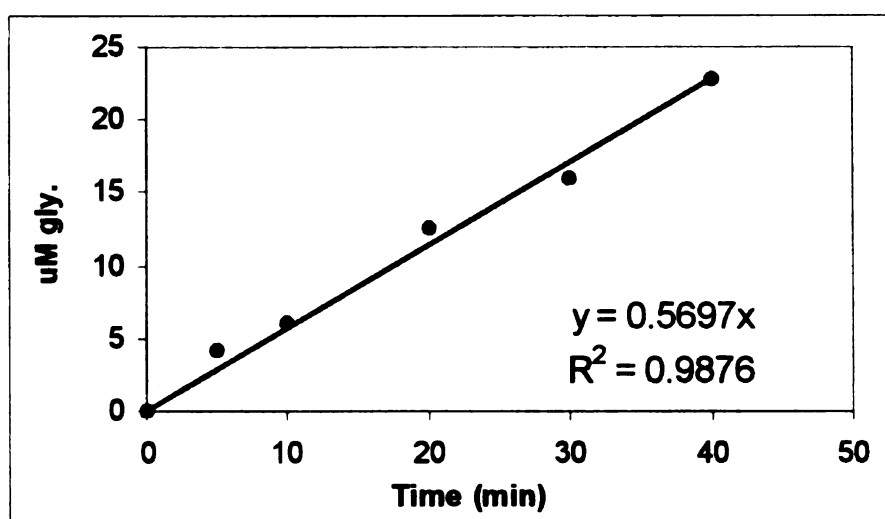
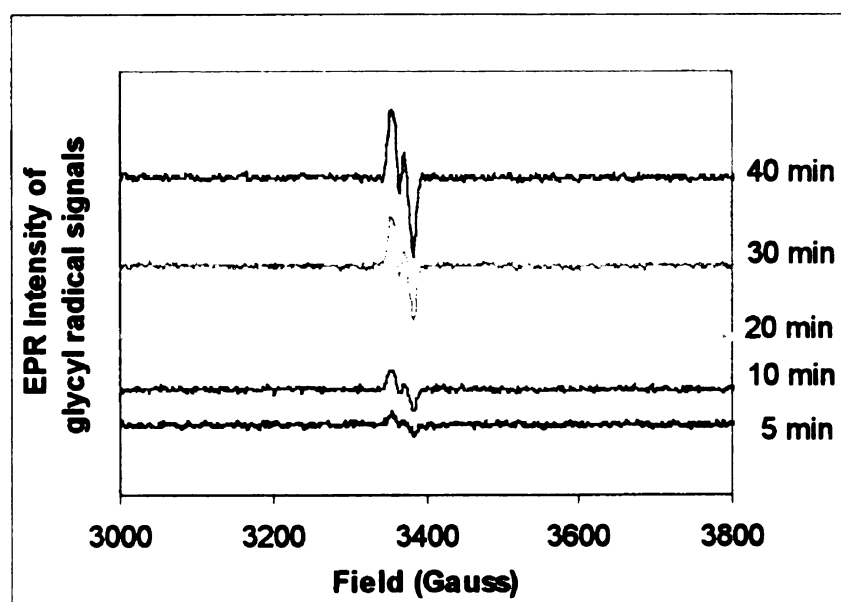


Figure II.8 Activity assay of PFL-AE. The assay mix (1 mL) contained 10.01 mg/mL (58.9 mM) PFL, 0.1 M Tris-HCl, pH 7.6, 0.1 M KCl, 10 mM DTT, 10 mM oxamate, 0.2 mM deaza, 0.2 mM AdoMet, and 0.186 μM PFL-AE (3.8 mol Fe/ mol PFL-AE, 4.0 mol S/ mol PFL-AE). The assay mix was illuminated for 5, 10, 20, 30, and 40 min, and the amount of glycy radical generated was determined by EPR spectroscopy. The glycy radical is indicated by a doublet signal at $g = 2.007$. Conditions of measurement, $T = 60$ K; microwave power, 20 μW ; microwave frequency, 9.47 GHz; modulation amplitude, 5.04 G; modulation frequency, 100 kHz. The spectra shown are single scans.

1000

The optimization of the growth and purification conditions for PFL-AE has been a long and evolving process in our laboratory. Inducing at an earlier log phase ($OD_{600} \sim 0.5$ vs. ~ 0.8) and supplementing iron to the medium after making the culture anaerobic contributed to better overexpression and iron inclusion of PFL-AE. The component of holoenzyme in the isolated native enzyme that contains full complement of iron was also improved in the purification procedure. The enzyme was purified by passing through the gel filtration column twice under strictly anaerobic conditions in the presence of 1 mM DTT, and pooling fractions based not only on SDS-PAGE analysis but also on the UV absorbance ratio at 426 nm and 280 nm. In summary, under current growth and purification conditions, approximately 400 mg of purified PFL-AE was obtained from a 9 L bacteria culture; this represents a 2-3-fold improvement over earlier procedures. The PFL-AE contains 2.5 – 3.8 mol Fe/ mol protein and a stoichiometric amount of acid-labile sulfide. The F-S clusters in the isolated protein are essentially EPR-silent, presumably in the $[4Fe-4S]^{2+}$ form, with about 2 % of $[3Fe-4S]^{1+}$ cluster. A high specific activity of 109 U/ mg enzyme was achieved for PFL-AE containing 3.8 mol Fe/ mol protein.

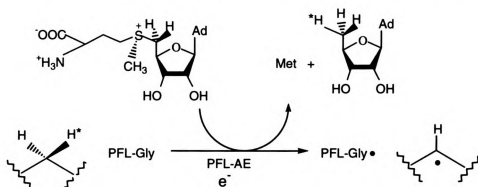
CHAPTER III

SYNTHESES AND CHARACTERIZATION OF ISOTOPICALLY LABELED *S*-ADENOSYL-L-METHIONINES AND Se-ADENOSYL-L-SELENOMETHIONINE

III.1 Introduction

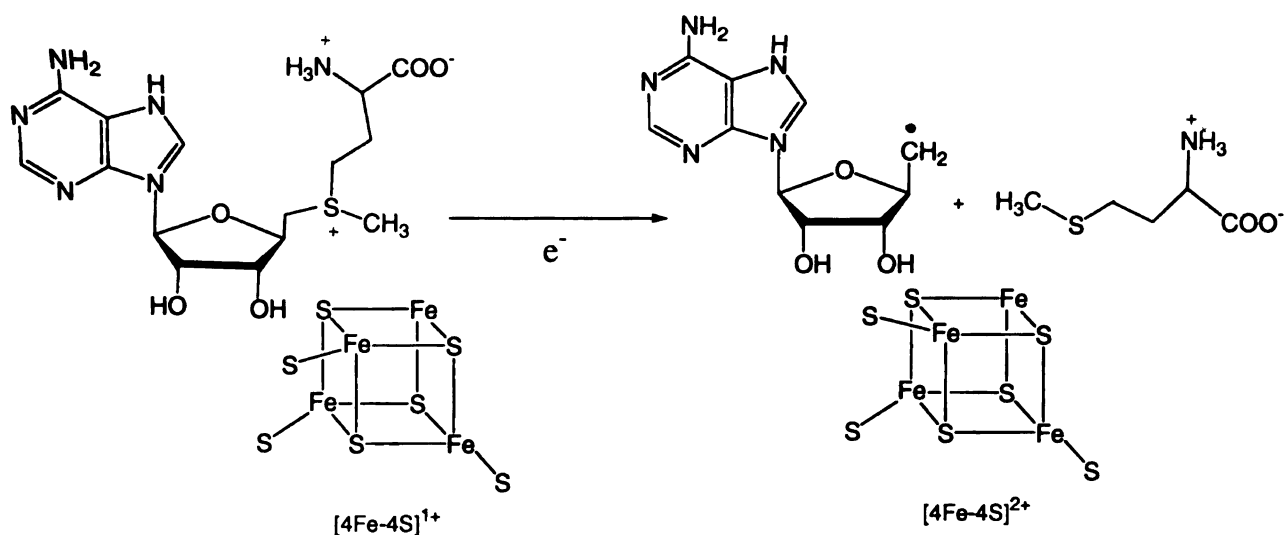
S-adenosyl-L-methionine (AdoMet) was first discovered and identified in 1953 by Cantoni (82), and a great deal of research has been directed towards its synthesis and biological functions since then. AdoMet plays various roles in biological systems. It is the primary methyl donor in the methylation of DNA, RNA, proteins, lipids, vitamin B₁₂ and many other substrates, by AdoMet-dependent methyltransferases (83). Alternatively, AdoMet can undergo decarboxylation to act as three-carbon donor. The three carbon aminopropyl group is incorporated into the polyamines, spermine and spermidine (84), and is also a precursor of the plant hormone, ethylene (85). As a five-carbon donor, the adenosyl moiety of AdoMet is the precursor of the cyclopentenediol of the *t*RNA wobble base queuosine (86). AdoMet also has clinical applications as a therapeutic drug in the treatment of liver disease, as a potential cancer chemo-preventive agent (87), and as an antidepressant (88-90). Another important function of AdoMet resides in the newly emerging group of AdoMet dependent iron-sulfur enzymes, where AdoMet participates in radical generation, with evidence suggesting a common mechanism involving an intermediate 5'-deoxyadenosyl radical (4, 34, 35, 55). A superfamily of more than 600 related enzymes that involve radical-based biochemistry has very recently been identified and named the radical SAM superfamily (41).

During the PFL activation reaction, PFL-AE requires AdoMet as a cosubstrate, cleaving it to methionine and 5'-deoxyadenosine (2). Knappe *et al.* have shown that the hydrogen atom abstracted from Gly734 of PFL is incorporated into the 5'-dAdo product (Scheme III.1), indicating that the role of AdoMet is to produce an adenosyl radical



Scheme III.1 Reductive cleavage of AdoMet by PFL-AE in PFL activation

intermediate as the immediate hydrogen atom abstractor (8). Recently, Henshaw *et al.* have demonstrated that the $[4\text{Fe-4S}]^{1+}$ is the catalytically active cluster of PFL-AE and that it donates the electron required for reductive cleavage of AdoMet (16). The presence of AdoMet has also been shown to dramatically affect the EPR signal of the $[4\text{Fe-4S}]^{1+}$ of PFL-AE (15, 16), suggesting the possibility of a direct interaction between AdoMet and Fe-S cluster of PFL-AE. The mechanistic question of how the Fe-S cluster of PFL-AE interacts with AdoMet to generate the putative adenosyl radical, however, still remains unclear. As the S-C bond is reductively cleaved during the radical generation, the sulfonium center of AdoMet is likely to be positioned close to the Fe-S cluster (Scheme III.2). Using isotopically labeled AdoMets and AdoMet analogs in which

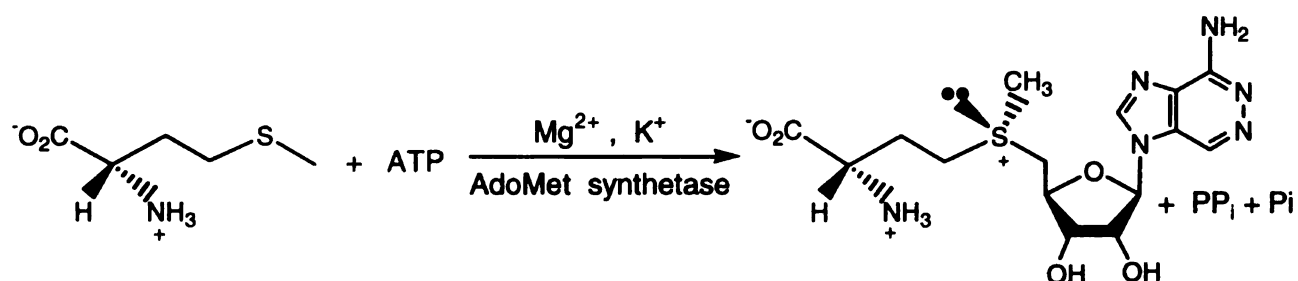


Scheme III.2 AdoMet and the Fe-S cluster of PFL-AE are proposed to be in close proximity during radical generation.

atoms in the sulfonium center are substituted with nuclei that have non-zero nuclear spins, hyperfine interactions with the Fe-S cluster of PFL-AE can be displayed if AdoMet coordinates or is in close proximity to the cluster. In order to probe hyperfine interactions between AdoMet and the cluster, the methyl group of AdoMet was labeled with ²H and ¹³C, and the sulfur was replaced by selenium to take advantage of the natural abundance of ⁷⁷Se (7.50 %). These isotopically labeled AdoMets and AdoMet analog are effective probes in spectroscopic studies to demonstrate the possible interaction between AdoMet and the Fe-S cluster of PFL-AE.

AdoMet contains a chiral sulfonium center and thus exists in two diastereoisomeric forms, (-)- and (+)-AdoMet. (-)-AdoMet is the only form enzymatically synthesized (91), and the only methyl donor *in vivo* (92). Chemical coupling reactions between adenosyl homocysteine and methyl group donating agents can produce AdoMet, however the diastereoselectivity is poor (91). The formation of (-)-AdoMet is catalyzed by S-Adenosylmethionine synthetase (ATP:L-methionine S-adenosyltransferase

EC2.5.1.6; AdoMet synthetase) (Scheme III.3). AdoMet synthetase from *E.coli* has a molecular weight of 180 kDa, and the native enzyme is a tetramer of 4 identical subunits (93).



Scheme III.3 Enzymatic synthesis of *S*-adenosyl-L-methionine

Kinetic experiments have demonstrated that the enzymatic reaction proceeds sequentially in 4 steps: (i) random addition of methionine and MgATP; (ii) formation of AdoMet and tripolyphosphate; (iii) oriented cleavage of tripolyphosphate to yield orthophosphate (Pi) and pyrophosphate (PPi); (iv) product release with orthophosphate and pyrophosphate dissociation before AdoMet (93). Two divalent metal ions, such as Mg^{2+} , bind to the enzyme active site in the presence of ATP, and both are required for activity (82, 94, 95). A single divalent cation, such as K^+ , binds in the presence of AdoMet, and stimulates the rate of AdoMet formation up to 100-fold (93).

Prior to a report by Park *et al.* (96), preparative scale synthesis of AdoMet was infeasible, due to product inhibition at substrate concentrations >1 mM, which may result from the formation of inactive AdoMet-bound-enzyme complexes (93-95, 97-99). The inhibition problem was successfully overcome in incubations using 10 mM substrate in the presence of various additives, including *p*-toluenesulfonate (*p*-TsONa), and more efficiently, a high concentration of β -mercaptoethanol (β -ME), acetonitrile or urea (96).

In the work described here, 8 % β -ME was used as additive to overcome product inhibition. Pyrophosphate also acts as an inhibitor of AdoMet synthetase (93). Though it is a weaker inhibitor than AdoMet, it is still strong enough to show an inhibitory effect in reactions containing > 1 mM substrate. Therefore, a small amount of pyrophosphatase was added to the reaction mixture to hydrolyze pyrophosphate to orthophosphate, a weaker non-competitive inhibitor of AdoMet synthetase (93).

III.2 Experimental methods

III.2.1 Materials

AdoMet synthetase overproducing strain DM22 (pK8) was a general gift from Dr. George D. Markham (Fox Chase Cancer Center). Methyl-D₃- L-methionine and methyl-¹³C-L-methionine were purchased from Isotech Inc. Seleno-L-methionine, ATP, and inorganic pyrophosphatase were purchased from Sigma. These and all other chemicals were of the highest purity obtainable from commercial sources.

III.2.2 Growth and purification of AdoMet synthetase

Expression of E. coli AdoMet synthetase

AdoMet synthetase overproducing strain DM22 (pK8) was stored in 50 % glycerol at -80 °C. A single colony of transformed cells was used to inoculate 50 mL LB media containing 30 μ g/mL oxytetracycline (LB/Tet). This culture was grown for 12 - 14 h to saturation and then used to inoculate 700 mL LB/Tet in each of 5 2800 mL Fernbach culture flasks. The culture was grown at 37 °C with vigorous shaking for 12 - 14 h before harvesting by centrifugation at $10,816 \times g$ (8,000 rpm, GS3 rotor). The supernatant was decanted and the cells stored at -80 °C.

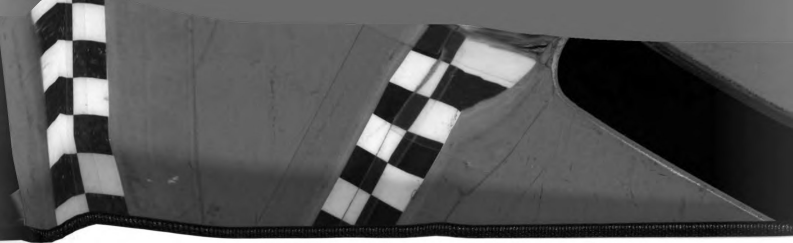
Preparation of cell lysate for AdoMet synthesis

Cell paste was suspended in 100mM Tris-HCl, pH 8.0 containing 1 mM EDTA (3 – 3.5 mL/g cell). Lysozyme was added to 50 $\mu\text{g/mL}$ and the suspension was incubated at room temperature for 30 min. Phenylmethylsulfonyl fluoride (PMSF) was added to a final concentration of 0.1 mM. Cells were lysed by sonication (10 cycles of 1 min sonication with 1 min rest in between) in an ice bath. The suspension was centrifuged at $26,892 \times g$ (15,000 rpm, SS34) for 20 min. The supernatant was decanted and the cells stored at $-80\text{ }^{\circ}\text{C}$ until needed. Protein concentrations were determined by the method of Bradford (77), using a kit purchased from Bio-Rad.

Purification of AdoMet synthetase

Preparation of cell lysate: Cell paste was suspended in 100 mM Tris-HCl, pH 8.0 containing 10 % glycerol, 1 mM EDTA, 0.1 % β -ME (4 mL/g cell). PMSF was added to a final concentration of 0.1 mM, followed by lysozyme (50 $\mu\text{g/mL}$) and trace amount of DNase and RNase (about 0.1 mg each). The lysate was incubated in ice for 1-1.5 hours, and then centrifuged at $10,816 \times g$ (8,000 rpm, GS3) for 20 min. The supernatant was decanted and used for the next step.

Ammonium sulfate fractionation: For each 100 mL of the supernatant solution, 22 g of ammonium sulfate were added. After stirring at $4\text{ }^{\circ}\text{C}$ for 20 min the suspension was centrifuged. The supernatant was decanted and for each 100 mL of the supernatant, 12 g of ammonium sulfate were added. After stirring at $4\text{ }^{\circ}\text{C}$ for 20 min the precipitated protein was collected by centrifugation.



Phenyl-Sepharose chromatography: The protein was dissolved in 10 mM Tris-HCl, pH 8.0, containing 10 % glycerol, 1 mM EDTA, 0.1 % β -ME, and 0.75 M ammonium sulfate. The protein solution was then loaded onto a Phenyl-Sepharose column (Pharmacia 16/10), which had been equilibrated with the above buffer. The column was washed with 2 volumes of the above buffer prior to running a reverse linear gradient of 0.75 M to 0 M ammonium sulfate in 200 mL 10 mM Tris-HCl, pH 8.0 containing 10 % glycerol, 1 mM EDTA, 0.1 % β -ME. Fractions containing AdoMet synthetase, which were eluted at the middle of the gradient (as judged by SDS-PAGE on a 12 % Tris-HCl gel), were pooled and concentrated in an Amicon concentrator with YM30 filter membranes. The purified protein was flash-frozen and stored at -80°C .

III.2.3 Synthesis and purification of isotopically labeled AdoMets and Se-AdoMet

AdoMet synthesis reactions (10 mL) were carried out at room temperature with moderate stirring in 100 mM Tris-HCl, pH 8.0 containing 50 mM KCl, 26 mM MgCl_2 , 13 mM ATP, 1 mM EDTA, 8 % β -ME, 10 mM isotopically labeled methionine or seleno-L- methionine, a small amount of inorganic pyrophosphatase (about 0.25 U) and 1 mL AdoMet synthetase lysate (approximately 13 mg of total protein). All reagents were added in the order as listed. The reaction was monitored by thin-layer chromatography (TLC) on silica plates developed in butanol /acetic acid /water (4:1:1). The reaction was terminated by addition of 1 mL of 1 M HCl and precipitated protein was removed by centrifugation at $26,892\times g$ (15,000 rpm, SS34) for 20 min at 4°C . The supernatant was decanted and split in half. Half of the supernatant was loaded onto a SOURCE 15S cation exchange column (Pharmacia, 8 mL), which had been charged with 1 M HCl and equilibrated with MQ H_2O . The column was run with a linear gradient of



0.1 M HCl, and AdoMet eluted from 38 – 56 % of the gradient as a distinct peak. The other half of the supernatant was run through the same procedure. Fractions containing products were pooled, lyophilized, and stored at -80°C until needed.

Adenosyl-methyl- D_3 -methionine (CD_3 -AdoMet) was synthesized overnight as described above with 10 mM methyl- D_3 -L-methionine.

Adenosyl-methyl- ^{13}C -methionine ($^{13}\text{CH}_3$ -AdoMet) was synthesized overnight as described above with 10 mM methyl- ^{13}C -L-methionine.

Se-adenosyl-L-selenomethionine (Se-AdoMet) was synthesized either at room temperature for 2-3 hours or at 4°C for 6-7 hours with 10 mM seleno-L-methionine.

III.2.4 NMR spectroscopy

^1H , ^{13}C and ^2H NMR spectra were recorded at room temperature on a Varian Inova-300 or a VXR-300 spectrometer (300.11, 75.43 and 46.04 MHz respectively).

III.2.5 Mass spectroscopy

Mass spectral data were obtained at the Michigan State University Mass Spectrometry Facility, which is supported, in part, by a grant (DRR-00480) from the Biotechnology Research Technology Program, National Center for Research, National Institutes of Health.

III.3 Results and Discussion

III.3.1 Growth and purification of AdoMet synthetase

AdoMet synthetase was purified from DM22(pK8) overproducing strain.

Overexpression of the protein in the *E. coli* cells was checked by SDS-PAGE on a 12 % Tris-HCl gel (Figure III.1). Typical yields were 5-8.5 g of cells per liter of bacterial culture. The cell lysate for AdoMet synthesis was prepared by a conjunction of enzymatic and physical lysis procedures. The purity of the crude extract was checked by SDS-PAGE on a 12 % Tris-HCl gel (Figure III.1). The crude extract was concentrated to approximately 13 mg/mL for AdoMet synthesis.

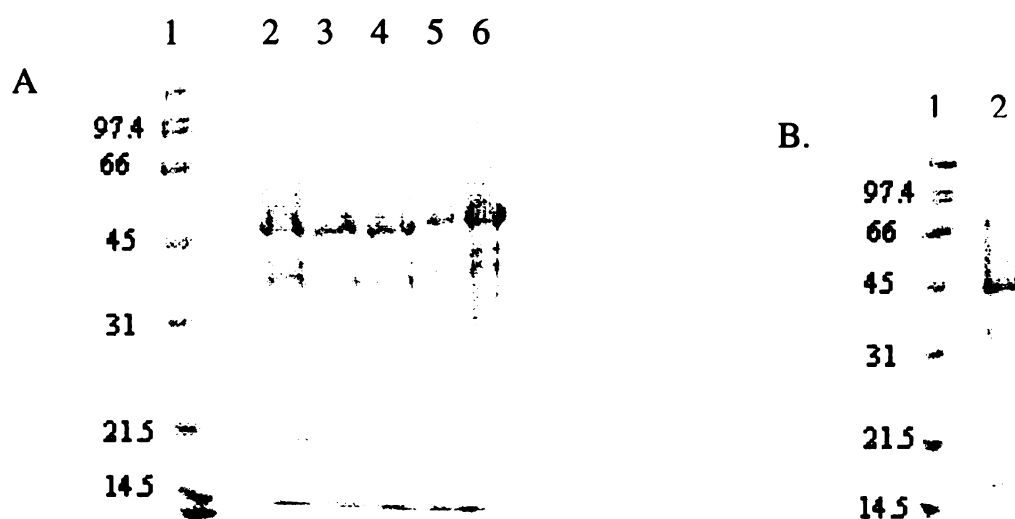


Figure III.1 SDS-PAGE analysis of AdoMet synthetase. **A.** Overexpression of AdoMet synthetase in *E. coli* cells(no induction is required). Lane 1, molecular marker (kDa); lane 2-6, duplicate samples. **B.** AdoMet synthetase crude extract. Lane 1, molecular marker (kDa); lane 2, crude extract.

AdoMet synthetase was further purified from the crude extract by ammonium sulfate fractionation and Phenyl-Sepharose chromatography. Purified protein was > 99 %

pure as judged by SDS-PAGE on a 12 % gel (Figure III.2). Yield was 16.7 mg of purified protein from 23 g cells.

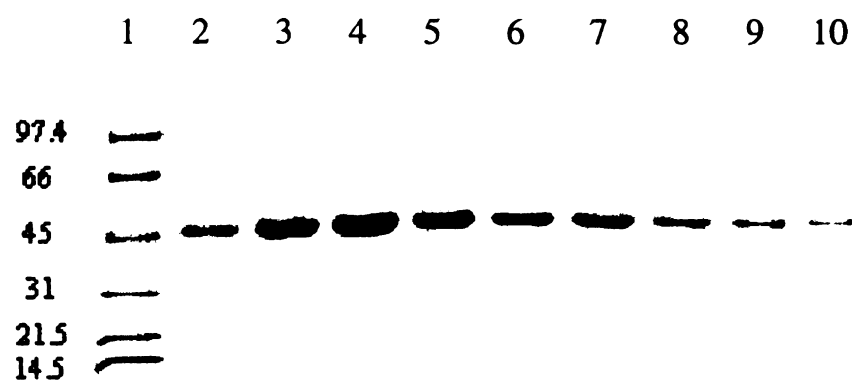


Figure III.2 SDS-PAGE analysis of AdoMet synthetase fractions off the Phenyl-Sepharose column. Lane 1, molecular marker (kDa); lane 2-10, fractions 32-40. Fractions 33-38 were pooled.

III.3.3 Syntheses and purification of isotopically labeled AdoMets and Se-AdoMet

Initial AdoMet synthesis reactions were carried out with purified AdoMet synthetase, using natural abundance methionine and ATP as substrates, but pyrophosphatase was not added in the reaction mixture. The reaction was run for 5 h at ambient temperature according to the literature procedure(96), and the reaction progress was monitored by TLC on cellulose developed in butanol /acetic acid /water (25:4:10) (92). The R_f value of ATP is 0 under these condition, and due to its high polarity, AdoMet also has a very small R_f value, reportedly being 0.04 by descending TLC developed in butanol /acetic acid /water (5:4:1) (82). The reaction did not proceed to the formation of AdoMet as indicated by TLC. It was then found, in some cases, that the crude extract of AdoMet synthetase worked better than the purified enzyme, as a low R_f value spot was observed only on the TLC of the reaction system containing crude extract of AdoMet synthetase. Though the reason for the crude extract of AdoMet synthetase

performing better than the purified enzyme is not clear, it was speculated that the pyrophosphate inhibition was partially overcome by the endogenous pyrophosphatase present in the cell lysate. Some other unknown component in the cell lysate might as well be beneficial to the performance of the enzyme. Therefore, crude extract of AdoMet synthetase was used for the reaction. Not only does it save the labor and time to purify the enzyme, which gives a rather low yield of purified enzyme, but it works very well in terms of yield and purity of the AdoMets synthesized. In addition to using crude extract, a small amount of inorganic pyrophosphatase was introduced into the reaction system to facilitate the hydrolyzation of pyrophosphate to orthophosphate, which is a weaker non-competitive inhibitor of AdoMet synthetase.

The TLC for monitoring the reaction progress was improved by using butanol /acetic acid /water (4:4:1) as the mobile phase and silica plates as the stationary phase to get a better development of AdoMet and a clearer observation of the spots under ultraviolet light. The R_f value of AdoMet, both isotopically labeled and Se substituted AdoMet, was 0.12. Unreacted ATP didn't develop on the plates ($R_f = 0$), and several faint spots were also observed from the reaction mixture, which were presumably contaminants and decomposed products. Longer reaction time (overnight instead of 5 h) was also found to help allow the reaction to go to completion. The isolation of AdoMet from the reaction mixture by chromatography was achieved on a Source S15 (Pharmacia) cation exchange column, after various other cation exchange columns, including Dowex-50W, Amberlite XE-64 and Mono S (HR 5/5, Pharmacia), had been tried without success.

Taking all the previous experience together, the AdoMet synthesis reaction is currently carried out as described in the Experimental Methods. Isolated AdoMets were lyophilized to yield crystalline colorless solids, presumably in the chloride salt form. The purified AdoMet was analyzed by ^1H NMR to check its diastereoisomeric purity, as the methyl group resonances of (-)- and (+)- forms are well resolved ($\Delta\delta \sim 0.4$ ppm). Mole ratios of approximately 94:6 for (-)- / (+)-AdoMet were obtained based on integrations of the two peaks in ^1H NMR spectra. Since (-)-AdoMet is the only form enzymatically synthesized, the contamination of (+)-AdoMet in the purified product results from the method of isolation and the temperature at which the reaction was done, which could cause epimerization of the natural product. This was previously demonstrated by the observation of only (-)- isomer in the HPLC analysis of the enzymatic reaction mixture before isolation (91). A virtually epimerically pure (-)-AdoMet was obtained in small quantities via rapid enzymatic synthesis followed by HPLC purification.

CD_3 -AdoMet was synthesized overnight under normal conditions as for natural AdoMet, and isolated by chromatography on a SOURCE 15S cation exchange column (Figure III.3). Yield was 38.5 mg (87.9 %) for a 10 mL of 10 mM reaction.

^1H NMR (D_2O): δ 2.18-2.39 (m, $\text{H}\beta$ & $\text{H}\beta'$), 3.32-3.42 (m, $\text{H}\gamma$ & $\text{H}\gamma'$), 3.52-3.62 (m, $\text{H}\alpha$), 3.76-3.98 (m, $\text{H}5'$, $\text{H}5''$ & $\text{H}4'$), 4.38-4.73 (m, $\text{H}3'$ & $\text{H}2'$), 6.01 (d, $J=3.91\text{Hz}$, $\text{H}1'$), 8.32 (s, $\text{H}2$ & $\text{H}8$) ppm. The ^2H labeling was confirmed by the absence of a methyl peak in the ^1H NMR (Figure III.6), as well as the presence of a methyl peak in the ^2H NMR.

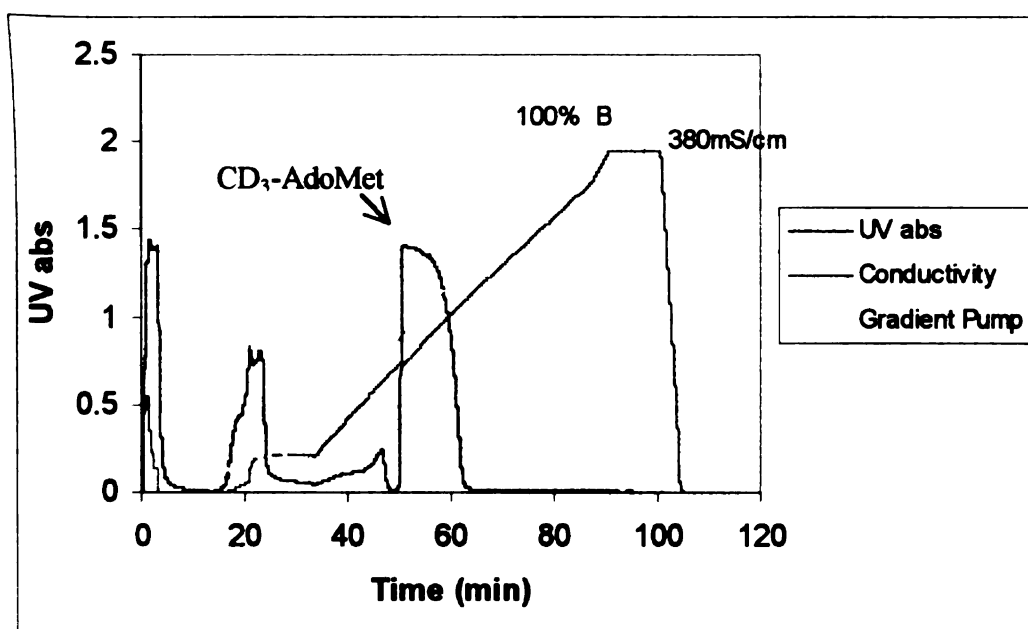


Figure III.3 Chromatogram of isolation of CD₃-AdoMet by SOURCE 15S cation exchange chromatography (Pharmacia, 8 mL), gradient from 0-1 M HCl, flow rate 1 mL/min. CD₃-AdoMet eluted from 38 – 56 % of the gradient as a distinct peak.

¹³CH₃-AdoMet was also synthesized overnight under normal conditions as for natural AdoMet, and isolated by chromatography on a SOURCE 15S cation exchange column (Figure III.4). Yield was 37.5 mg (86.0 %) for a 10 mL of 10 mM reaction.

¹H NMR (D₂O): δ 2.20-2.35 (m, H_β & H_β'), 2.62 & 3.11 (d, J=146.49, (-)-¹³CH₃), 2.59 & 3.08 (d, J=146.49, (+)-¹³CH₃), 3.37-3.43 (m, H_γ & H_γ'), 3.44-3.58 (m, H_α), 3.77-4.01 (m, H₅', H₅'' & H₄'), 4.38-4.71 (m, H₃' & H₂'), 6.01 (d, J=3.91, H₁'), 8.32 (s, H₂ & H₈) ppm. The ¹³C labeling was confirmed by the distinct large splitting of the methyl peak in the ¹H NMR (Figure III.6), as well as the presence of a ¹³C peak in the ¹³C NMR.

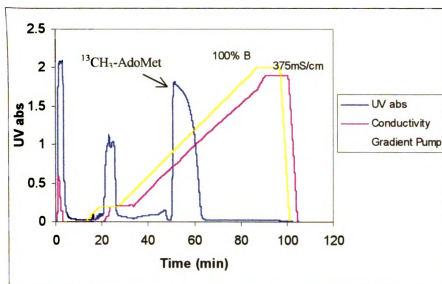
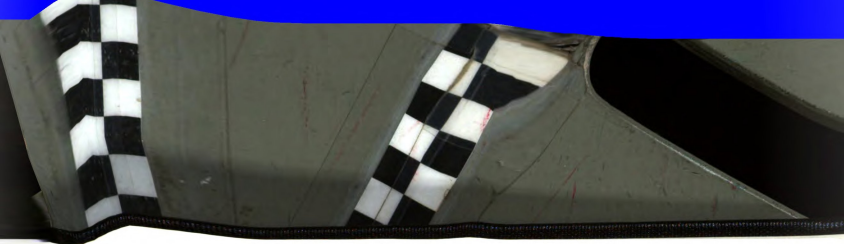


Figure III.4 Chromatogram of isolation of $^{13}\text{CH}_3\text{-AdoMet}$ by SOURCE 15S cation exchange chromatography (Pharmacia, 8 mL), gradient from 0-1 M HCl, flow rate 1 mL/min. $^{13}\text{CH}_3\text{-AdoMet}$ eluted from 38 – 56 % of the gradient as a distinct peak.

In contrast to the isotopically labeled methionines, which behave identically to the natural substrate methionine, selenomethionine has much different chemical properties than its sulfur counterpart. Selenomethionine reacts more rapidly than methionine in the synthesis reaction, as has been reported for AdoMet synthetase from both yeast and *E. coli* (93, 100, 101). The higher reactivity of selenomethionine can be explained as due to the better nucleophilicity of selenium relative to sulfur (102, 103). In addition, more decomposed products and contaminants were found in the reaction mixture as more spots were observed on TLC plates, and the contaminant peaks were of higher intensity in the chromatogram (Figure III.5). Therefore, the Se-AdoMet synthesis reaction was carried out either at room temperature for 2-3 h or at 4 °C for 6-7 h. Yields were 10.2 mg (42.3 %) for a 5 mL of 10 mM reaction run at room temperature and 14.0 mg (58.1 %) for a 5 mL of 10 mM reaction run at 4 °C respectively.



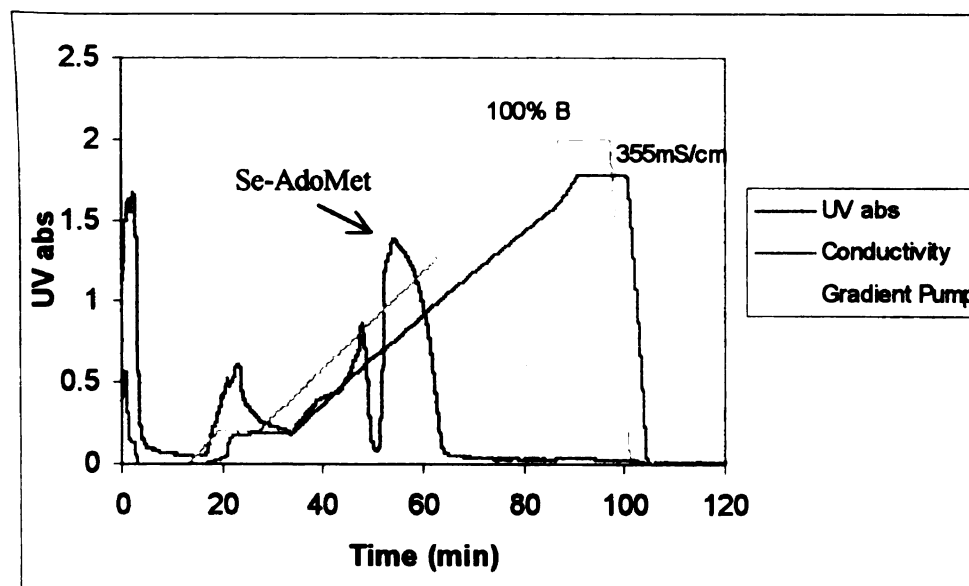


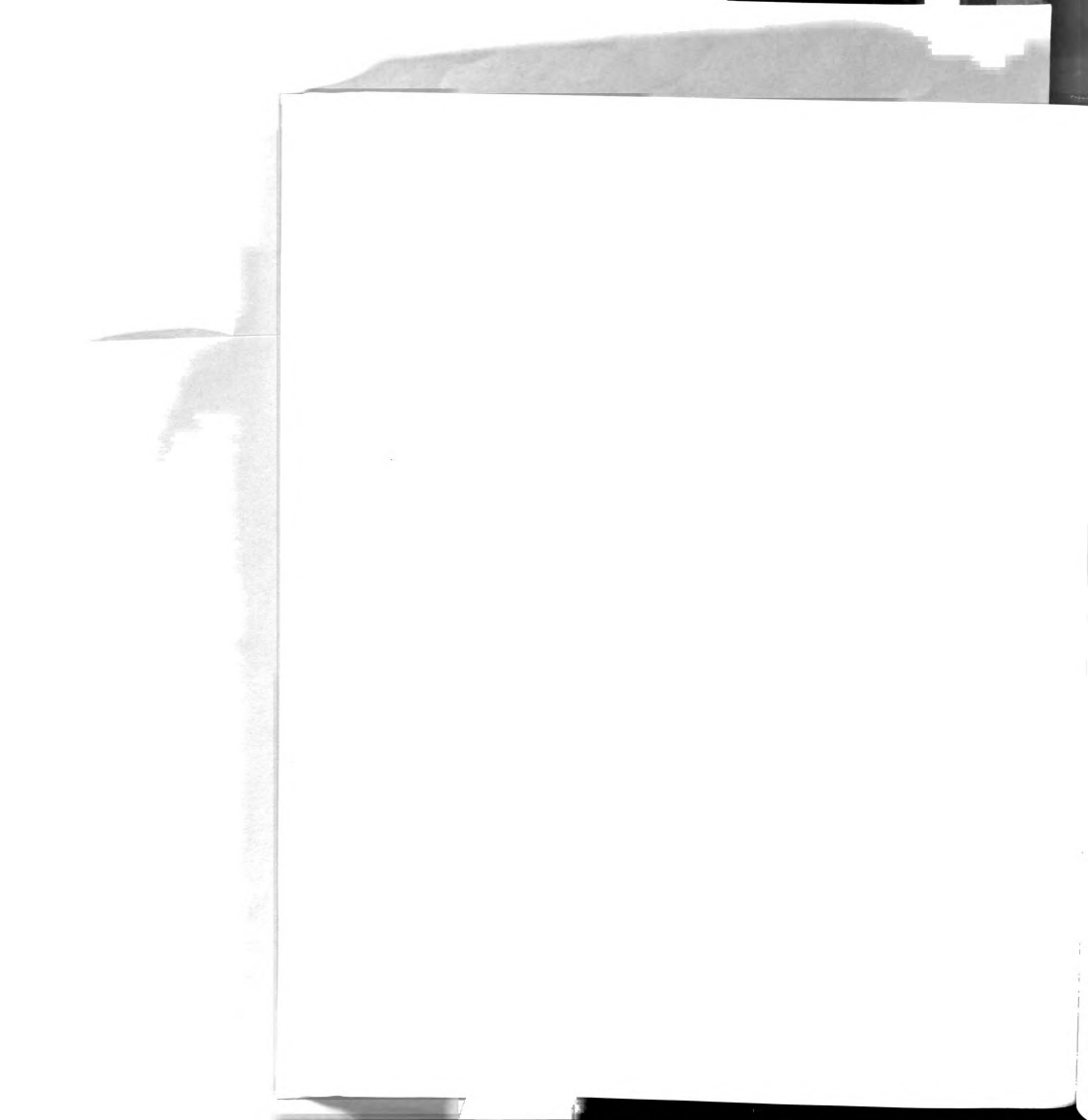
Figure III.5 Chromatogram of isolation of Se-AdoMet by SOURCE 15S cation exchange chromatography (Pharmacia, 8 mL), gradient from 0-1 M HCl, flow rate 1 mL/min. Se-AdoMet eluted from 38 – 56 % of the gradient as a distinct peak. This reaction was run at room temperature for 2 h.

^1H NMR (D_2O): δ 2.21-2.33 (m, $\text{H}\beta$ & $\text{H}\beta'$), 2.72 (s, (-)- CH_3), 2.68 (s, (+)- CH_3), 3.24-3.34 (m, $\text{H}\gamma$ & $\text{H}\gamma'$), 3.40-3.50 (m, $\text{H}\alpha$), 3.69-3.92 (m, $\text{H}5'$, $\text{H}5''$ & $\text{H}4'$), 4.37-4.73 (m, $\text{H}3'$ & $\text{H}2'$), 6.01 (d, $J=3.91$, $\text{H}1'$), 8.32 (d, $J=1.5$, $\text{H}2$ & $\text{H}8$) ppm. The methyl peak of Se-AdoMet shifted upfield relative to the one in the natural abundance AdoMet, which is consistent with the higher electron density of Se relative to S (Figure III.6).

MS (NBA, +FAB): m/z 447 ($\text{C}_{15}\text{H}_{23}\text{O}_5\text{N}_6\text{Se}$).

In conclusion, a fairly simple procedure for enzymatic synthesis of AdoMet on a preparative scale has been established. AdoMet synthetase was overexpressed and grown in *E. coli* cells. The enzyme was lysed by a combination of enzymatic and physical procedures, and the crude extract was used for AdoMet synthesis reaction without further purification. Product inhibition was overcome by addition of 8 % of β -ME in the reaction mixture. A 10 mM reaction can afford over 80 % yield of AdoMet. AdoMet isolated by the method described here has high diastereoisomeric purity, and appears to be more stable than AdoMet iodide salt from commercial sources. AdoMet from Sigma shows more than one spot on the TLC plate, while purified homemade AdoMet shows only one spot. In a NMR time course study, the NMR spectrum of a homemade natural AdoMet sample, which was kept in D₂O at room temperature for 6 days, was essentially the same as the one that was taken right after this AdoMet was made, except for a small decrease of the mole ratio of the (-)- and (+)- forms. The enhanced stability of homemade AdoMet is probably due to the increased purity relative to AdoMet from Sigma. In addition, the high acidity of the lyophilized product, which is eluted by HCl of around 0.5 M, may help to stabilize AdoMet.

This method can be easily applied to isotopically labeled substrates, as has been shown on methyl-D₃-methionine, methyl-¹³C-methionine, and ¹⁵N-methionine, which has also been synthesized in our laboratory. With some modifications of the reaction conditions according to the properties of the substrate analogs being used, AdoMet analogs can also be made. In the case here, selenomethionine is a better substrate to AdoMet synthetase in terms of reaction rate, but the product is more prone to degrade during the synthesis, and the reaction time was thus much shortened to enhance the yield.



Combined with other synthetic techniques, more isotopically labeled AdoMets and AdoMet analogs will be synthesized from a variety of isotopically labeled methionine and ATP, or methionine and ATP analogs. These AdoMet analogs will be used as probes to study the interaction of AdoMet with the Fe-S cluster of PFL-AE from different perspectives.



CHAPTER IV

INVESTIGATING THE INTERACTION OF ADOMET WITH PFL-AE USING EPR AND ENDOR SPECTROSCOPY

IV.1 Introduction

PFL catalyzes the conversion of pyruvate and coenzyme A (CoA) to formate and acetyl-CoA (1, 3, 104, 105). The active form of PFL contains a stable glycy radical located at residue 734 (4). This catalytically essential protein radical is generated post-translationally by PFL-AE, under anaerobic conditions in a reaction that is strictly dependent on the presence of AdoMet as a cosubstrate (66-68). During the PFL activation reaction, the glycy radical is formed by abstraction of the pro-S hydrogen atom of Gly734 of PFL, and AdoMet is converted stoichiometrically to methionine and 5'-deoxyadenosine (Scheme I.4) (2, 8). Isotope-labeling experiments have established that the hydrogen atom abstracted from Gly734 is incorporated into the methyl group of the 5'-dAdo product, suggesting that a 5'-deoxyadenosyl radical is the species that abstracts a hydrogen atom from Gly734 (8).

PFL-AE is a representative of a rapidly growing group of enzymes that utilize iron-sulfur clusters and AdoMet as required cofactors in radical generation (106). The functions of these AdoMet-dependent iron-sulfur enzymes are diverse, including the generation of stable protein radicals (4, 33, 34), as well as substrate radical intermediates (35). However, a common key mechanism is proposed to be involved in the chemistry catalyzed by these enzymes: the generation of an intermediate 5'-deoxyadenosyl radical that initiates catalysis by hydrogen atom abstraction (4, 34, 35, 55).



A variety of iron-sulfur clusters, including [2Fe-2S], [3Fe-4S] and [4Fe-4S], have been identified in these AdoMet-dependent enzymes (13, 14, 17, 34-39, 107). Mössbauer data have provided the first clear description of all the forms of the cluster present in anaerobically isolated PFL-AE and in the dithionite-reduced form of the enzyme (15). The anaerobically isolated enzyme in the absence of DTT contains a mixture of Fe-S clusters with the cuboidal [3Fe-4S]¹⁺ clusters as the primary cluster form, accounting for 66 % of the total iron. Other forms present include [2Fe-2S]²⁺ (12 % of total Fe), [4Fe-4S]²⁺ (8% of total iron), and also a linear [3Fe-4S]¹⁺ (~10 % of total iron). Reduction of the as-isolated enzyme by dithionite converts all cluster types into the [4Fe-4S] form with a majority of 2+ (66 % of total iron) and a small amount of 1+ (12 % of total iron) oxidation states. The quantitation of the paramagnetic [4Fe-4S]¹⁺ was also confirmed by parallel EPR studies. Under current reducing purification conditions in the presence of 1 mM DTT, PFL-AE as-isolated is essentially EPR silent, presumably in [4Fe-4S]²⁺ state, with a very small amount of [3Fe-4S]¹⁺ accounting for approximately 2 % of total iron.

The observation that only cuboidal [4Fe-4S] clusters are present upon reduction of the enzyme suggests that the [4Fe-4S] cluster is the catalytically relevant cluster, especially considering that PFL-AE activity is observed *in vitro* only under anaerobic reducing conditions (1). It has been difficult, however, to identify unequivocally the catalytically relevant cluster by which the 5'-dAdo radical intermediate is generated. A [4Fe-4S]¹⁺ has been shown to be the catalytically active for aRNR-AE (34, 108) and LAM (35). A definite assignment of the [4Fe-4S]¹⁺ of PFL-AE as the catalytically active cluster was achieved in an elegantly designed single turnover experiment (16). In the above work, deazariboflavin-mediated photoreduction of PFL-AE followed by addition

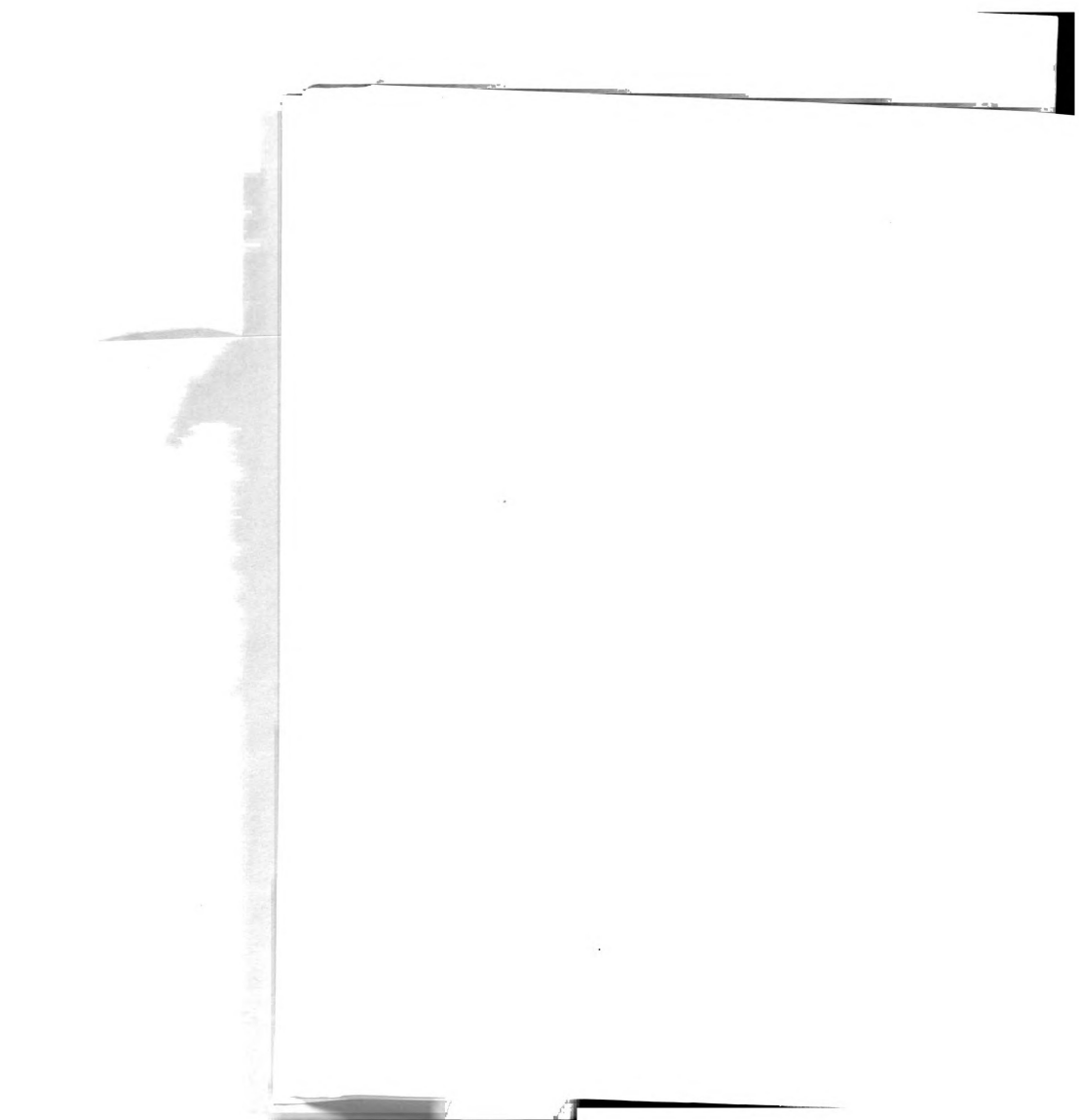
of AdoMet has been shown to afford primarily $[4\text{Fe-4S}]^{1+}$. Saturation of cluster reduction is reached in 1 hour, at which time 85 % of the cluster in PFL-AE is reduced to $[4\text{Fe-4S}]^{1+}$ state. By removing illumination, the exogenous reductant is eliminated and single turnover conditions can be achieved. Equimolar PFL is mixed with the $[4\text{Fe-4S}]^{1+}$ /AdoMet after removing illumination in a time-dependent manner. Spin quantitation of the glycyl radical EPR signals at each time point show a 1:1 correspondence between the amount of glycyl radical observed and the amount of $[4\text{Fe-4S}]^{1+}$ cluster present prior to addition of PFL. No glycyl radical was observed when only the $[4\text{Fe-4S}]^{2+}$ cluster was present prior to the addition of PFL. This is the first direct quantitative spectroscopic evidence that the $[4\text{Fe-4S}]^{1+}$ of PFL-AE is the catalytically relevant cluster, and demonstrates that this cluster provides the electron necessary for AdoMet-dependent glycyl radical generation.

However, a detailed mechanism of this unprecedented reaction still remains elusive. A central mechanistic question is whether the Fe-S cluster plays a simple electron-transfer role in the reductive cleavage of AdoMet, or is more directly involved in the radical generation reaction. In the absence of AdoMet, the $[4\text{Fe-4S}]^{1+}$ of PFL-AE gives rise to a rhombic EPR signal. However, in the presence of AdoMet, the observed EPR signal is nearly axial. The observed effect of AdoMet on the EPR signal of the catalytically relevant $[4\text{Fe-4S}]^{1+}$ could reflect either a close association between AdoMet and the cluster in the enzyme-substrate (ES) complex or allosteric perturbations of the cluster.

In the work described here, the interaction between AdoMet and the $[4\text{Fe-4S}]$ cluster was probed by using electron nuclear double resonance (ENDOR) spectroscopy.



The methyl group on the sulfonium center of AdoMet has been chosen as the initial target of study, because of its proximity to the S-C bond of AdoMet, where the cleavage takes place during radical generation. The methyl group was labeled with ^2H and ^{13}C respectively, both of which have non-zero nuclear spin and can display hyperfine interactions if the atoms coordinate or are in proximity to the paramagnetic Fe-S cluster. Electron-nuclear hyperfine interactions, which are too small to be resolved within the natural width of the EPR line, are generally amenable to study by ENDOR spectroscopy. To characterize the binding of AdoMet to PFL-AE, initial 35 GHz pulsed ^2H and ^{13}C ENDOR studies were performed with labeled AdoMet. Binding of AdoMet to the cluster in the equilibrium geometry associated with the paramagnetic 1+ state of the cluster (denoted [1+/AdoMet]) was examined, as well as binding to the diamagnetic 2+ state (denoted [2+/AdoMet]). In order to probe the binding of AdoMet to the diamagnetic $[\text{4Fe-4S}]^{2+}$ state, as-isolated PFL-AE samples were frozen in the presence of AdoMet and then γ -irradiated at 77 K to produce the 1+ valency cluster trapped in the geometry of the 2+ state (denoted [2+/AdoMet]_{red}). In this cryoreduction technique, γ -irradiation of solutions frozen at cryogenic temperatures (~ 77 K) generates mobile electrons from the matrix that can reduce redox-active sites producing an EPR-visible reduced enzyme form retaining the structure of the parent oxidized species. This technique has been applied to a wide variety of metalloproteins, such as heme proteins (109, 110), diiron oxo proteins (111-114), and iron-sulfur proteins (115-117).



IV.2 Experimental methods

IV.2.1 Synthesis and purification of CD₃-AdoMet and ¹³CH₃-AdoMet

As described in Chapter III, Section III.2.3.

IV.2.2 [1+ / AdoMet] sample preparation

The as-isolated PFL-AE, in 50 mM Hepes, 200 mM NaCl, 1 mM DTT, pH 7.5, was exchanged with 50 mM Tris-HCl, 200 mM NaCl, 1 mM DTT, pH 8.5 buffer, and concentrated in an Amicon pressure cell with an YM-10 membrane in the Coy Chamber. The concentration of the protein was determined by the method of Bradford (77).

The following procedures were carried out anaerobically in an inert atmosphere glove box (Mbraun) with O₂ level \leq 3 ppm. All buffers, solvents and bath water were deoxygenated using a vacuum / inert gas manifold before being taken into the glove box. Solid chemicals were pumped in as solids. Ice was pre-chilled with liquid nitrogen before pumping into the glove box.

PFL-AE was mixed with 20-25 % (v/v) glycerol in an eppendorf to a total volume of 200 μ L for EPR samples, or 300 μ L for parallel EPR and ENDOR samples, and pre-reduced by addition of 1 equivalent of sodium dithionite (freshly made 50 mM solution in 50 mM Tris buffer, pH 8.5). 5-deazariboflavin (10 mM stock solution in DMSO) was added in the dark to a final concentration of 100 μ M for 400 μ M or less concentrated PFL-AE, or 200 μ M for PFL-AE of over 400 μ M, and mixed well. The sample was then transferred to an EPR tube. The EPR tube was capped and inserted in a beaker tightly

packed with ice-water. The sample was illuminated on ice using a 500 W halogen lamp for 1 hour with the lamp situated about 5 cm from the beaker. After illumination, the protein sample was mixed with 2 equivalents of AdoMet on ice by adding the protein to pre-measured AdoMet or isotopically labeled AdoMet solution (10 mM or 30 mM solution in 50 mM Tris buffer, pH 8.5). The sample was transferred back to the EPR tube, or split to EPR and ENDOR tubes, and flash-frozen in liquid nitrogen in the glove box.

IV.2.3 [2+ / AdoMet] sample preparation

As-isolated PFL-AE containing 0.13 % of $[3\text{Fe-4S}]^{1+}$ ($0.73 \mu\text{M}$ spin for $560 \mu\text{M}$ protein, as determined by EPR) was exchanged with 50 mM Tris-HCl, 200 mM NaCl, 1 mM DTT, pH 8.5 buffer, and concentrated as described in IV.2.2. In the inert atmosphere glove box, $574 \mu\text{M}$ PFL-AE, 20 % (v/v) glycerol and 2 equivalents of $\text{CD}_3\text{-AdoMet}$ or $^{13}\text{CH}_3\text{-AdoMet}$ were mixed on ice to make a final volume of $60 \mu\text{L}$. The sample was loaded into an ENDOR tube, and flash-frozen in liquid nitrogen in the glove box.

IV.2.5 $[2+/\text{AdoMet}]_{\text{red}}$ sample preparation

$[2+/\text{AdoMet}]_{\text{red}}$ sample preparation was done in collaboration with Professor Brian M. Hoffman, and Dr. Charles Walsby, Department of Chemistry, Northwestern University.

The $[2+ / \text{AdoMet}]$ sample prepared as described above was γ -irradiated at 77 K to produce the 1+ valency cluster trapped in the geometry of the 2+ state.

IV.2.6 EPR spectroscopy

As described in Chapter II, Section II.2.10.

IV.2.7 ENDOR spectroscopy

ENDOR spectroscopy was done in collaboration with Professor Brian M. Hoffman, and Dr. Charles Walsby, Department of Chemistry, Northwestern University.

35 GHz pulsed ENDOR spectra were recorded on a spectrometer equipped with a helium immersion dewar and all the measurements were carried out at approximately 2 K. Pulsed ENDOR measurements employed the three-pulse Mims ENDOR sequence ($\pi/2$ - τ - $\pi/2$ -T- $\pi/2$ - τ -echo) and its four-pulse 'Remims' variant sequences, where the RF was applied during the interval T. For a nucleus with hyperfine coupling A, the Mims techniques have a response R which depends on the product, $A\tau$, according to the equation,

$$R \sim [1 - \cos(2\pi A\tau)] \quad (\text{Equation 0})$$

This function has zeroes, corresponding to minima in the ENDOR response (hyperfine "suppression holes"), at $A\tau = n$; $n = 0, 1, \dots$, and maxima at $A\tau = (2n+1)/2$; $n = 0, 1, \dots$

The applied radio-frequency was broadened in bandwidth by mixing with a 60 KHz noise to improve the signal-to-noise ratio.

For a nucleus (N), of spin $I = 1/2$ interacting with a paramagnetic center, the first order ENDOR resonance condition for a single molecular orientation can be written as follows:

$$\nu_{\pm} = |\nu_N \pm A/2| \quad (\text{Equation 1})$$

1

1

1

1

where ν_N is the Larmor frequency and A is the orientation dependent hyperfine constant of the coupled nucleus. The equation predicts a doublet with separation A and centered at ν_N when $\nu_N > A/2$, as is true here for both ^1H and ^{13}C nuclei. Similarly, for a nucleus (N) of spin $I=1$, when $\nu_N > A/2$, the first order ENDOR resonance condition can be written as follows:

$$\nu_{\pm} = \nu_N \pm A/2 + P/2(2m_I - 1) \quad (\text{Equation 2})$$

where P is the quadrupolar splitting term. This is the case with ^2H nucleus in the present study. The full hyperfine tensor of a coupled nucleus, both principal values and orientation parameters (Euler angles) with respect to the g -tensor frame, is obtained by simulating the 2-D pattern of orientation-dependent ENDOR spectra recorded across the EPR envelope using the procedures and program described elsewhere. The computer simulation and analysis of the frozen-solution ENDOR spectra used in the present work are described in the same references.

IV.3 Results and Discussion

IV.3.1 Generation of the PFL-AE $[4\text{Fe-4S}]^{1+}$ / isotopically labeled AdoMet complexes by photoreduction

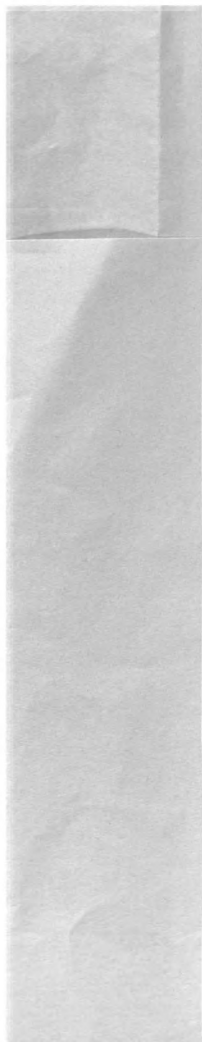
In order for ENDOR spectroscopy to clearly observe possible hyperfine interactions between the isotopes and the $[4\text{Fe-4S}]^{1+}$ cluster of PFL-AE, it is necessary to generate large quantities of PFL-AE $[4\text{Fe-4S}]^{1+}$ in the presence of isotopically labeled AdoMet. Photoreduced 5-deazariboflavin acts as an electron donor, which conveniently replaces the physiological flavodoxin system. Tris buffer is a suitable photo-substrate to generate the effective 5-deazariboflavin radical. Efficient photoreduction of highly





concentrated PFL-AE samples was not as easily achieved as for fairly dilute protein samples. Photoreduction conditions were optimized, including the amount of 5-deazariboflavin and other additives present, the time period of illumination, and the distance of the light source from the samples. The optimal pH for photoreduction was found to be 8.5. Addition of 20-25 % of glycerol to concentrated PFL-AE samples and pre-reduction with 1 equivalent of dithionite also afforded more efficient reduction. In addition, the concentration of 5-deazariboflavin present affects the efficiency of reduction, as a final concentration of 100 μM deazariboflavin works better for 400 μM or less concentrated PFL-AE, and 200 μM deazariboflavin for PFL-AE of over 400 μM . The illumination time was kept at 1 hour, and ice was continuously added to the ice-water bath to keep the samples cool during illumination.

The X-band EPR spectra of the PFL-AE $[\text{4Fe-4S}]^{1+}$ in the presence of $\text{CD}_3\text{-AdoMet}$ and $^{13}\text{CH}_3\text{-AdoMet}$ are essentially indistinguishable from the $[\text{4Fe-4S}]^{1+}/\text{AdoMet}$ spectra. Photoreduced PFL-AE in the presence of $\text{CD}_3\text{-AdoMet}$ generated 38.0 % of $[\text{4Fe-4S}]^{1+}$, based on 324 μM spin for 910 μM protein with 3.75 mol Fe/ mol PFL-AE (Figure IV.1). Photoreduced PFL-AE in the presence of $^{13}\text{CH}_3\text{-AdoMet}$ generated 68.9 % of $[\text{4Fe-4S}]^{1+}$, based on 404 μM spin for 777 μM protein with 3.02 mol Fe/ mol PFL-AE (Figure IV.2).



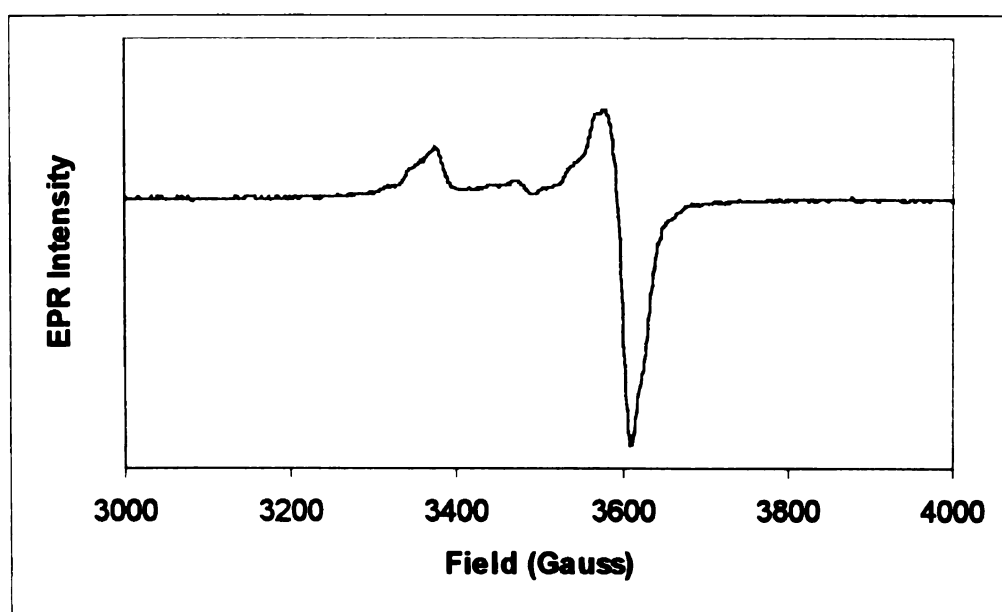


Figure IV.1 X-band EPR spectrum of PFL-AE $[4\text{Fe-4S}]^{1+}$ in the presence of $\text{CD}_3\text{-AdoMet}$. The sample contained $910\ \mu\text{M}$ PFL-AE, 1 equivalent of $\text{Na}_2\text{S}_2\text{O}_4$, $200\ \mu\text{M}$ 5-deazariboflavin, and 2 equivalents of $\text{CD}_3\text{-AdoMet}$; 38.0 % reduction (based on $324\ \mu\text{M}$ spin for $910\ \mu\text{M}$ protein with 3.75 mol Fe/ mol PFL-AE); $g = 2.005, 1.949, 1.883$. Conditions of measurement: $T = 12\ \text{K}$; microwave power, $20\ \mu\text{W}$; microwave frequency, $9.47\ \text{GHz}$; modulation amplitude, $10.053\ \text{G}$; single scan.

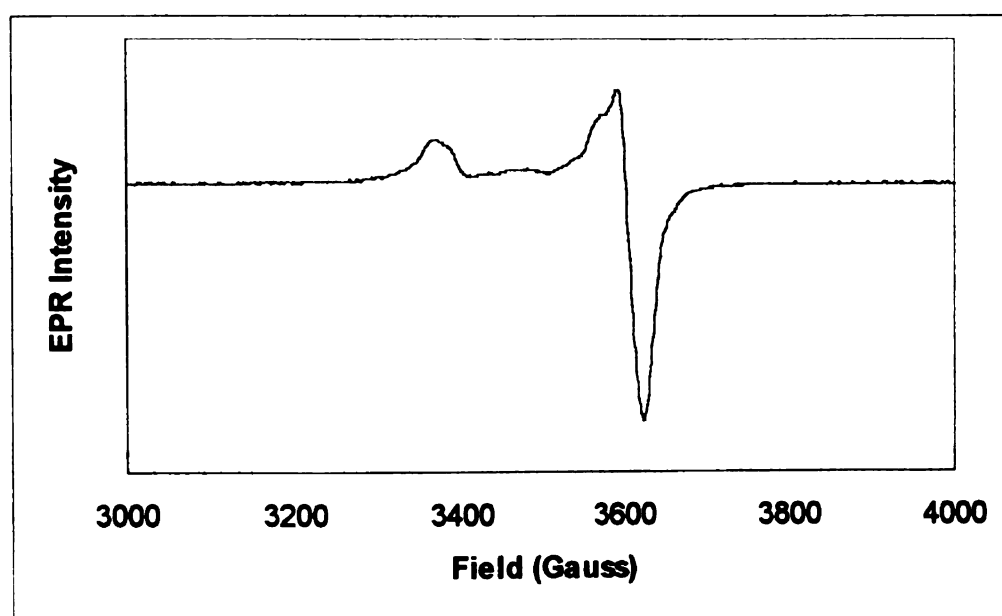


Figure IV.2 X-band EPR spectrum of PFL-AE $[4\text{Fe-4S}]^{1+}$ in the presence of $^{13}\text{CH}_3\text{-AdoMet}$. The sample contained $777\ \mu\text{M}$ PFL-AE, 1 equivalent of $\text{Na}_2\text{S}_2\text{O}_4$, $200\ \mu\text{M}$ 5-deazariboflavin, and 2 equivalents of $^{13}\text{CH}_3\text{-AdoMet}$; 68.9 % reduction (based on $404\ \mu\text{M}$ spin for $777\ \mu\text{M}$ protein with 3.02 mol Fe/ mol PFL-AE); $g = 2.011, 1.948, 1.880$. Conditions of measurement: $T = 12\ \text{K}$; microwave power, $20\ \mu\text{W}$; microwave frequency, $9.49\ \text{GHz}$; modulation amplitude, $9.571\ \text{G}$; single scan.



IV.3.2 ENDOR spectroscopic evidence for a close interaction between AdoMet and the [4Fe-4S] cluster of PFL-AE

^2H and ^{13}C ENDOR

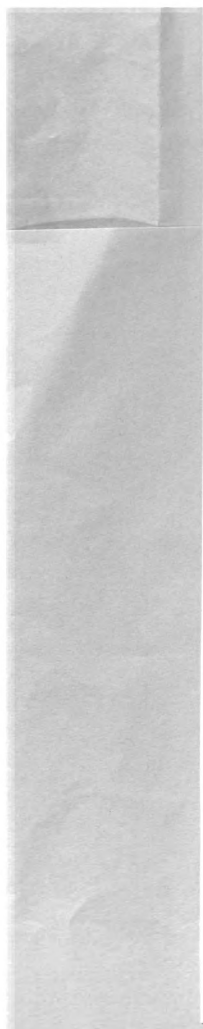
The ^2H ENDOR spectra of [1+/CD₃-AdoMet] and [2+/CD₃-AdoMet]_{red} (Figure IV.3), and the corresponding ^{13}C spectrum of [1+/ $^{13}\text{CH}_3$ -AdoMet] and [2+/ $^{13}\text{CH}_3$ -AdoMet]_{red} (Figure IV.4), immediately demonstrate that the cofactor sits close to the cluster in both the 1+ and 2+ states. The ^2H spectra of [1+/CD₃-AdoMet] taken at g_{\perp} and g_{\parallel} (Figure IV.3) show a well-defined deuteron pattern that overlays a less-intense signal seen in the unlabelled [1+/AdoMet] sample (see supplementary material); this latter is assigned to double-quantum transitions from weakly-coupled ^{14}N , as seen in similar Fe-S clusters. In the ^2H spectrum collected at g_{\perp} , the breadth of the signal is 1.1 MHz which, when corrected for unresolved ^2H quadrupole splitting of ~0.1 MHz (based on the known value for quadrupole coupling for CD₃) corresponds to a ^1H coupling of ~ 6-7 MHz. For comparison, this coupling is ~1/2 that of water bound to a low-spin heme and greater than those to the protons of histidine bound to Fe. Such an interaction could not arise from an AdoMet bound at a remote site and influencing the cluster EPR spectrum by an allosteric process; at minimum it requires the AdoMet lie adjacent to the cluster. The [2+/AdoMet]_{red} state has an EPR signal identical to that of the [1+/AdoMet] state, indicating that AdoMet binds with the same geometry to both the 1+ and 2+ clusters. This inference is confirmed by the ^2H ENDOR spectra of [2+/AdoMet]_{red} as illustrated in Figure IV.3: the spectra of [1+/AdoMet] and [2+/AdoMet]_{red} are indistinguishable.



^{13}C ENDOR spectra collected from $[1+^{13}\text{CH}_3\text{-AdoMet}]$ and $[2+^{13}\text{CH}_3\text{-AdoMet}]_{\text{red}}$ (Figure IV.4) lead to identical conclusions. The two labeled samples exhibit identical hyperfine-split doublets centered at the ^{13}C Larmor frequency and arising from coupling to ^{13}C of the labeled AdoMet lying adjacent to the cluster. The spectra also show ENDOR signals from natural abundance ^{57}Fe . These are assigned to the ν_+ transition of a single iron with a coupling of $A(^{57}\text{Fe}) = 26$ MHz, which is similar to that of the labile Fe site in aconitase ES ($A(^{57}\text{Fe}) = 29$ MHz). The existence of this signal is useful because it allows us to compare spectra from natural-abundance and ^{13}C -enriched samples, by scaling to the signal from the ^{57}Fe . A further use of this ability to scale spectra is described below.

Field dependence of ^{13}C ENDOR

Details of the AdoMet binding have been obtained by analysis of the 2D patterns of 35 GHz Mims-pulsed ^{13}C ENDOR spectra from $[1+^{13}\text{CH}_3\text{-AdoMet}]$ and ^2H spectra from $[1+/\text{CD}_3\text{-AdoMet}]$, each collected across the entire EPR envelope. Figure IV.5 presents the 2D set of Mims pulsed ^{13}C ENDOR spectra; at each field the spectrum is normalized to the 2-pulse electron-spin echo (ESE) signal intensity. We note that with the value, $\tau = 600$ ns employed in the Mims ENDOR pulse sequence, the $n = 1$ 'Mims suppression holes' fall sufficiently far from the ^{13}C Larmor frequency (holes at $\Delta\nu(^{13}\text{C}) = \pm 0.833$ MHz) as not to significantly distort the observed ^{13}C pattern. However the $n = 0$ 'hole' centered at the ^{13}C Larmor frequency ($\Delta\nu(^{13}\text{C}) = 0$ MHz) regardless of τ , has a major impact on the observed signals and as a result it is essential to incorporate Mims suppression into the simulations. This procedure is not completely understood because



the 'simple' application of the Mims suppression formula can be compromised by spin-diffusion effects. However, by the use of the Mims formula in the simulation program and by use of carefully normalized spectra, it is possible to analyze the experiments persuasively. In particular, by reproducing the relative peak intensities from field to field in the 2D pattern, as well as the frequencies, helps to characterize the dipolar part of the hyperfine interaction; this is particularly important at fields and for orientations where the hyperfine coupling approaches zero and may change sign. As shown in Figure IV.5, systematic efforts at simulations yield excellent modeling of the peak positions and intensities, in this case generated with a ^{13}C hyperfine tensor with principal values, $A(^{13}\text{C}) = [-0.6(1), +0.4(1.5), -0.5(1)]$ MHz (NOTE: The relative signs are fixed by experiment. The absolute sign is not, and is chosen to make the dipolar interaction positive. This is consistent with Equation 3 for K positive.) and Euler angles relative to the g-tensor frame of $\theta = 30$, $\psi = 30$. We note that although A_1 and A_3 do not appear to differ, within error, the errors are correlated. To reproduce the curvature of the outer edges of the 2D plot, A_1 must be ~ 0.1 MHz larger than A_3 , and thus $A(^{13}\text{C})$ is constrained to be non-axial.

The ^{13}C tensor can be decomposed into the sum of an isotropic part, $a_{\text{iso}}(^{13}\text{C}) = -0.23\text{MHz}$, and two, mutually perpendicular, purely-dipolar tensors, using $A(^{13}\text{C}) = [-0.6, +0.4, -0.5]$ as an example, $T(^{13}\text{C}) = [-0.33, +0.66, -0.33] = [-T_C, 2 T_C, -T_C]$ MHz, and $(-)\text{t}(^{13}\text{C}) = (+)[-0.03, -0.03, +0.06] = [-t, -t, 2t]$ MHz. The former we assign to the direct through-space dipolar interaction between the ^{13}C and spin of the cluster; the latter we assign to the 'local' interaction with the spin on the ^{13}C itself whose presence is disclosed

by the isotropic term. The hyperfine tensor, thus, can be decomposed into the 'non-local' dipolar term and a 'local' term that arises from spin density on the ^{13}C , $A(^{13}\text{C})_{\text{loc}} = -[\text{laiso}(^{13}\text{C})|I + t(^{13}\text{C})]$. The presence of spin-density at the methyl group of AdoMet, as manifest in this local term, *requires* that AdoMet lie in contact with the cluster, weakly interacting with it through an incipient bond/antibond.

The through-space coupling tensor T , contains information about the geometry of AdoMet binding. The dipole interaction between nucleus j of AdoMet, here the ^{13}C of the labeled methyl, to a cluster can be written as

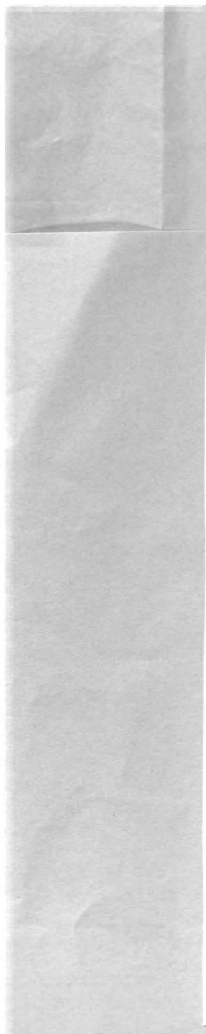
$$H_{\text{HF}} = \hat{S} \cdot \sum_j T_j \cdot \hat{I}_j$$

where:

$$T_j = g_e \beta_e g_j \beta_n \sum_{i=1}^4 \frac{K_i}{r_{ij}^3} \tilde{t}_{ij} \approx \frac{g_e \beta_e g_n \beta_n}{r_{nj}^3} K_n t_{nj} \quad (\text{Equation 3})$$

Here K_i is the spin-projection coefficient for Fe_i of the spin-coupled $S = 1/2$ cluster, the Fe_i -Nuc $_j$ distance is r_{ij} , and t_{kj} is the dimensionless through-space electron-nuclear dipolar matrix. Extensive calculations indicate that only the dipole coupling to the nearest iron ion, k , need be considered to a first approximation, as indicated in Equation 3, and hence the dipole coupling to nucleus j is characterized by the parameter, $T_j \equiv g g_n K_k / r_{jk}^3$.

The modeling process and determination of r_{c-k} itself for the ^{13}C -methyl, requires knowledge of K_n . Mössbauer spectroscopic studies of $[1+(\text{AdoMet})]$ do not yet provide the K_i for the four Fe ions, and therefore we consider the known spin coefficients of the 1+ cluster of substrate-bound aconitase (ES), which also has a labile, non-cysteine cluster ligand; these are $|K| = 0.86, 1.57, 1.60$ and 1.78 (118). When interpreting the ^{13}C dipolar interaction constant, $T_C = 0.33$ MHz, in this way, the point-dipole-calculated distance between the methyl ^{13}C and Fe_k of the cluster then would take one of four approximate



distances, depending on which value of K is associated with Fe_k . The range of possible values for r_{c-k} given the uncertainties in the simulations and K then falls in the range 3.5 - 5.6 Å.

Field dependence of ^2H ENDOR

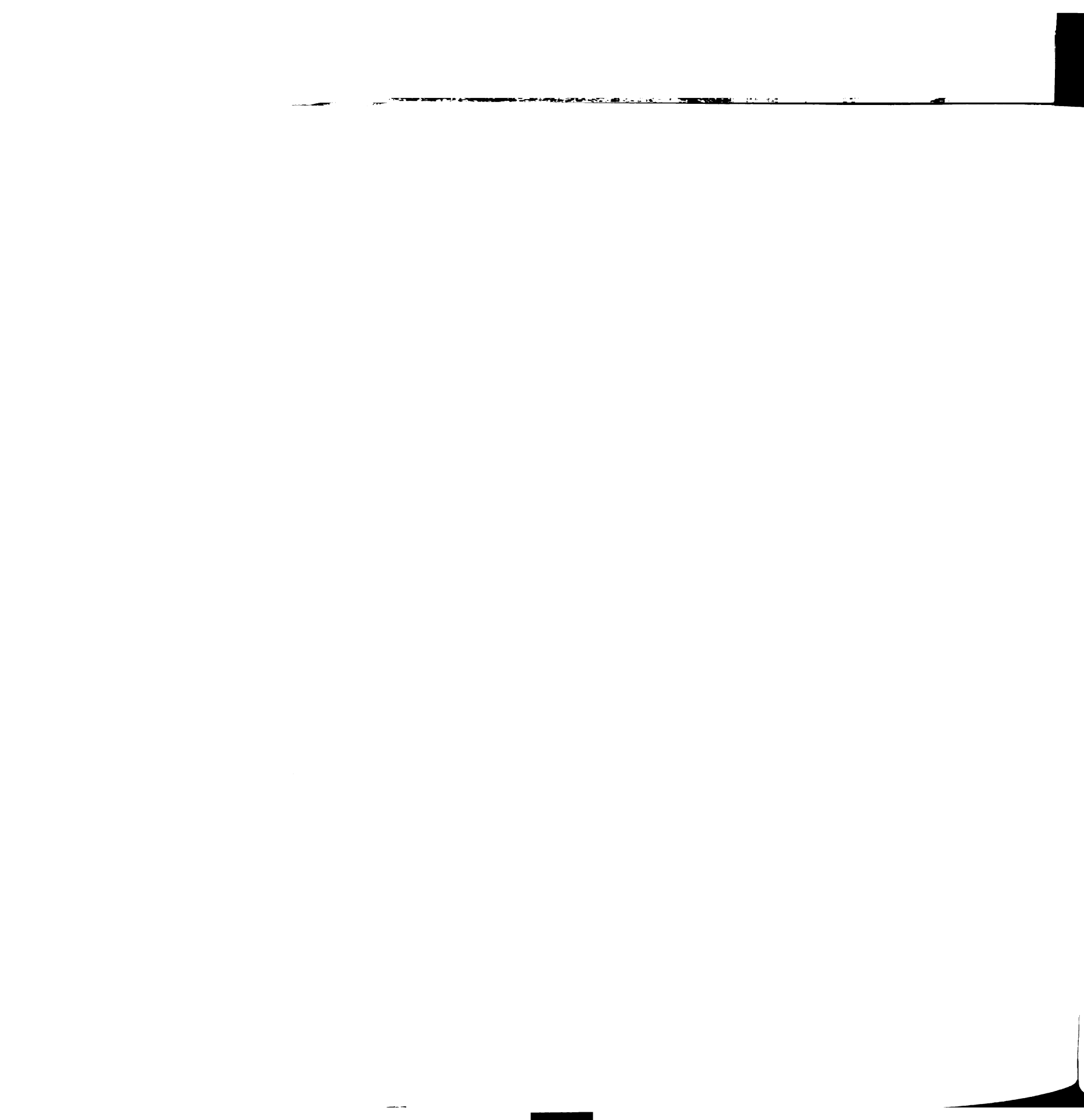
The ^2H and ^{13}C ENDOR data has been tested for self-consistency by analysis of the 2D set of ^2H Mims pulsed ENDOR spectra collected for [1+/CD₃-AdoMet]. Figure IV.3 includes the spectra at both g_{\perp} and g_{\parallel} ; the intervening spectra (not included) show that the breadth of the pattern decreases monotonically from g_{\perp} to g_{\parallel} . The deuteron spectrum is not highly resolved but the hyperfine splitting at g_{\perp} is roughly twice that of the splitting at g_{\parallel} . For a CD₃ moiety, the maximum ^2H quadrupole splitting is only 0.1 MHz and a ^2H spectrum as broad as that shown in Figure IV.3 is dominated by the hyperfine interaction to the three deuterons ($j = 1-3$). The spectra are compatible with a surprisingly simple model in which the AdoMet is bound alongside the cluster and the outer features of the CD₃ ENDOR response are governed by the through-space dipolar interaction between the closest methyl deuteron and the spin density on a single Fe ion of the cluster.

Modeling the outer features of the field-dependent pattern by the interaction of one deuteron with a single iron Fe_n gives the dipole-coupling parameter $T_D \equiv g\beta g_n\beta_n K_n / r_{D-k}^3 = 0.60$ MHz, along with the orientation of the $\text{Fe}_k\text{-D}_1$ vector relative to the g -tensor frame. Contributions from the more remote deuterons were calculated under constraints of the tetrahedral geometry around the methyl carbon and some simple assumptions as to the orientation of the AdoMet. As shown by the calculated spectra in Figure IV.3, the

data can be well represented by the dipolar spin Hamiltonians of Equation 3. The point-dipole-calculated distance between the closest methyl deuteron and Fe_k of the cluster then would take one of four approximate distances, depending on which value of K is associated with Fe_k . These are: $\sim 3.0, 3.6, 3.7$ and 3.8 \AA . Included in the simulations of the perpendicular and parallel spectra in Figure IV.3 are the predicted signals for the other, more distant, deuterons of the labeled methyl group. The distance of these deuterons is dependent on the orientation of the methyl group relative to the cluster and on the value of K used in the calculation; for the simulations in Figure IV.3 a representative value of $K = 1.6$ ($r_{\text{Fe}_k-\text{D}} = 3.7 \text{ \AA}$) was selected.

The above analysis is not unique, however, because the behavior of the D_1 pattern cannot be modeled at small couplings due to uncertainties about the contributions from the D_2, D_3 signals, as well as because of the $n = 0$ 'Mims hole'. Thus, the data do not rule out an alternate model in which an isotropic coupling makes a significant contribution to the ^2H observed pattern. Simulations of the ^2H data with a significant isotropic component are not unique, but a representative simulation that describes the outer spectral features utilized a tensor, $\mathbf{A} = [0.3, 0.3, 1.0] \text{ MHz}$, corresponding to an isotropic coupling $a = 0.53 \text{ MHz}$ and an anisotropic contribution of the form $[-0.23, -0.23, 0.47] \text{ MHz}$. In this model, the lack of resolution in the ^2H spectra again is attributed to the presence of signals from the other two deuterons, which although chemically equivalent, would have different isotropic couplings. The isotropic coupling likely varies as $\cos^2 \theta$, where θ is the dihedral angle between the π orbital on S that requires spin from the cluster and the C-D bonds. For example, if one ^2H has a maximum coupling ($\theta = 0$), the

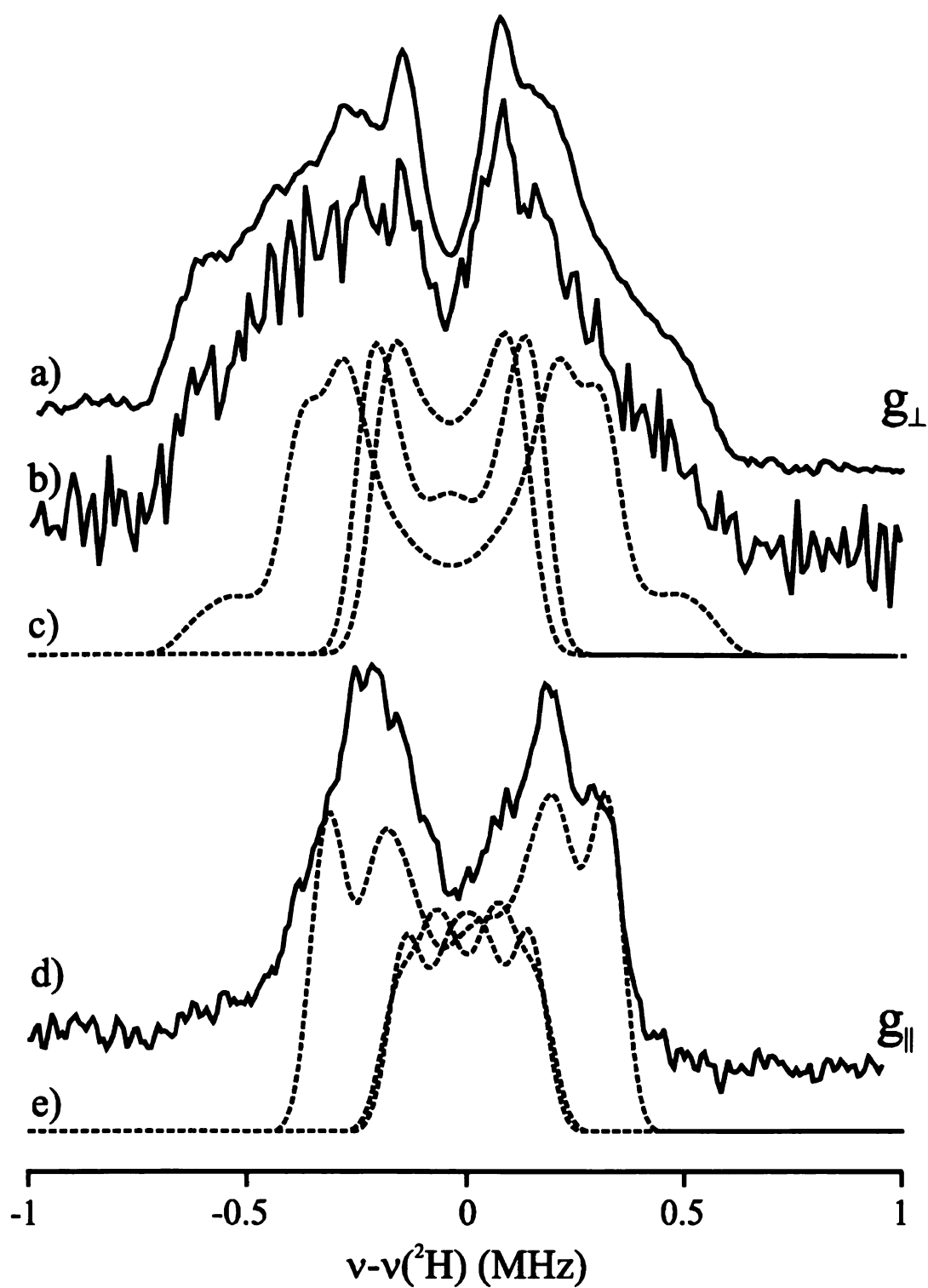
other two will have four-fold smaller values ($\theta = \pm 2\pi/3$, $\cos^2 \theta = 1/4$), thus contributing intensity near the center of the spectrum as required by experiment.





1

Figure IV.3 35 GHz Mims pulsed-ENDOR spectra of PFL-AE with methyl-D₃ AdoMet. a) and d) photoreduced sample, b) cryoreduced sample. The spectra at g₁ have been scaled to the height of the natural abundance ⁵⁷Fe peaks visible to higher frequency of the ¹³C signals. Conditions: $T = 2$ K, $\nu_{\text{MW}} = 34.8$ GHz, MW pulse lengths = 80 nS, $\tau = 456$ ns, RF pulse length = 60 μ s, repetition rate = 30 Hz. Each spectrum consists of 256 points with each point an average of 240-300 transients. c) and e) Simulations with axial, completely anisotropic A tensors. Closest ²H: $T = 0.6$ MHz (corresponding $R = 3.1$ Å for $K = 1.0$), $\alpha = \beta = 30^\circ$, $\gamma = 0^\circ$; $3P = 0.1$ MHz $\alpha = \beta = \gamma = 0^\circ$. More distant methyl deuterons: $R = 4.7$ Å, $K = 1.0$ (corresponding $T = 0.12$ MHz) angles tetrahedraly disposed, quadrupole as above.



- a) photoreduced PFL-AE [4Fe-4S]¹⁺/CD₃-AdoMet at g_{\perp}
- b) cryoreduced PFL-AE [4Fe-4S]²⁺/CD₃-AdoMet at g_{\perp}
- c) simulations of a) and b)
- d) photoreduced PFL-AE [4Fe-4S]¹⁺/CD₃-AdoMet at g_{\parallel}
- e) simulations of c)

Figure IV.3



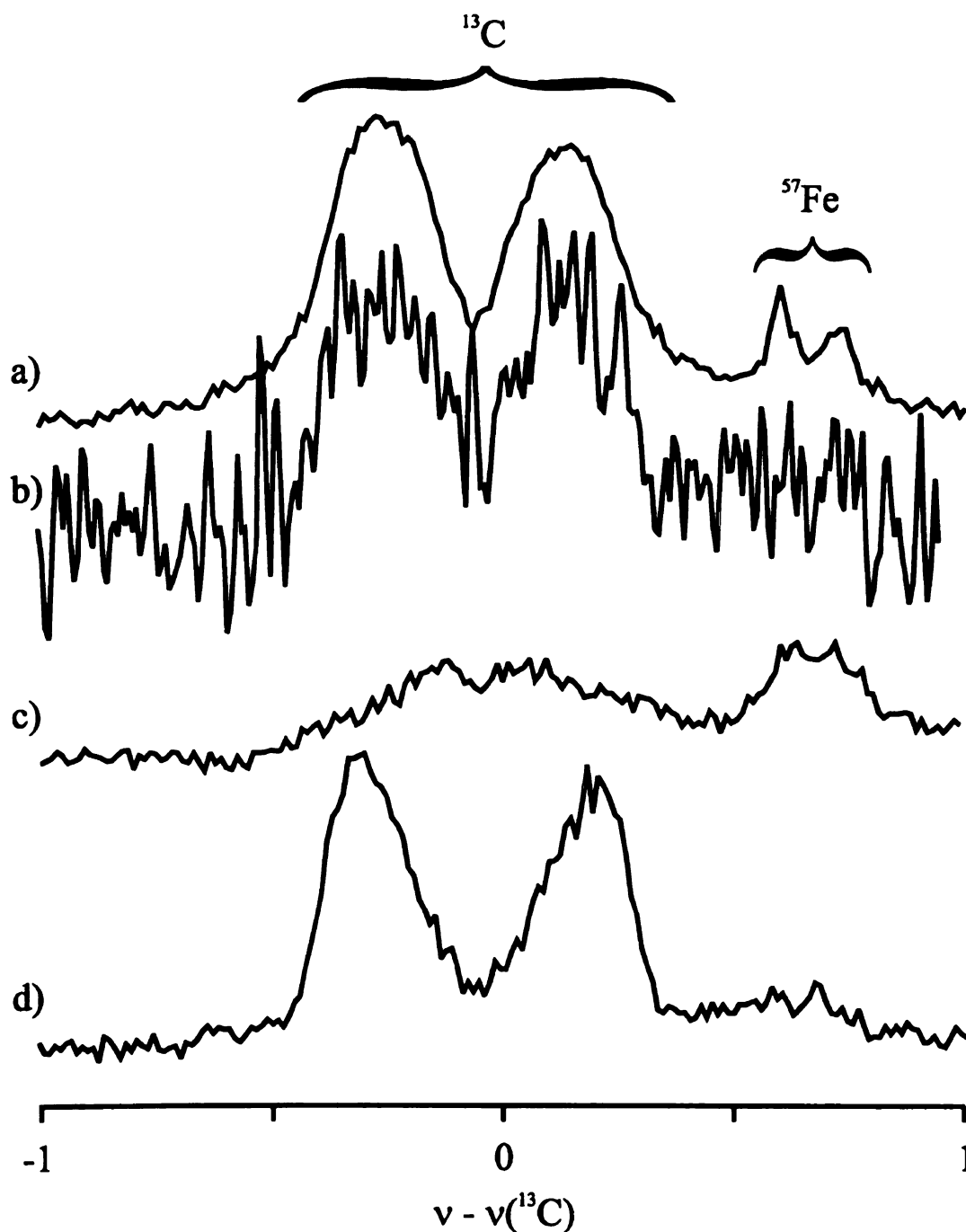


Figure IV.4 35 GHz Mims pulsed-ENDOR spectra of PFL-AE with methyl- ^{13}C AdoMet.

- a) photoreduced PFL-AE $[4\text{Fe-4S}]^{1+}/^{13}\text{CH}_3\text{-AdoMet}$ at g_{\perp}
- b) cryoirradiated PFL-AE $[4\text{Fe-4S}]^{1+}/^{13}\text{CH}_3\text{-AdoMet}$ at g_{\parallel}
- c) photoreduced PFL-AE $[4\text{Fe-4S}]^{1+}/\text{AdoMet}$ (natural abundance ^{13}C) scaled to ^{57}Fe
- d) photoreduced PFL-AE $[4\text{Fe-4S}]^{1+}/^{13}\text{CH}_3\text{-AdoMet}$ at g_{\parallel}

Experimental conditions as for Figure IV.3, except that $\tau = 600$ nS and number of transients = 600.



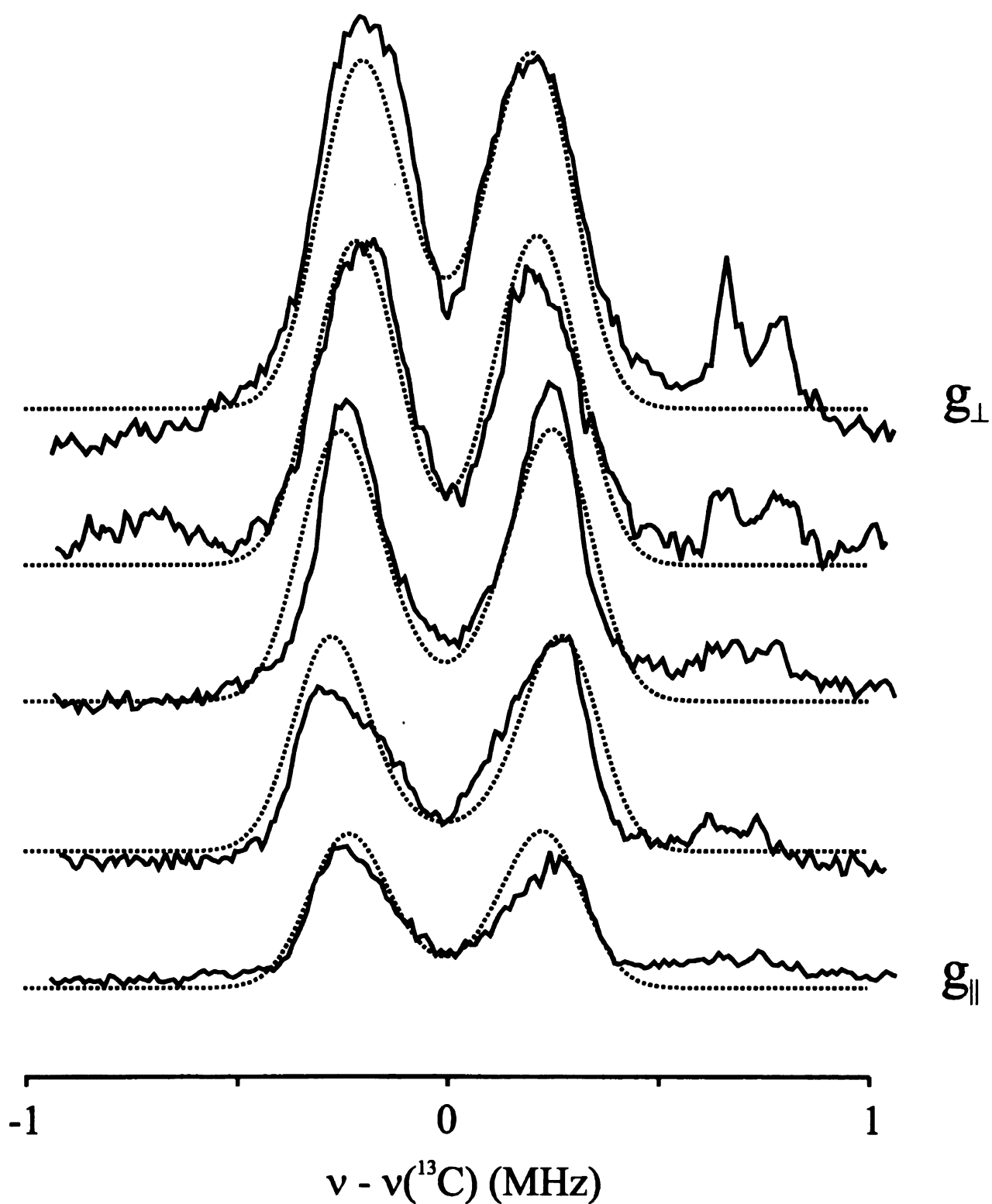
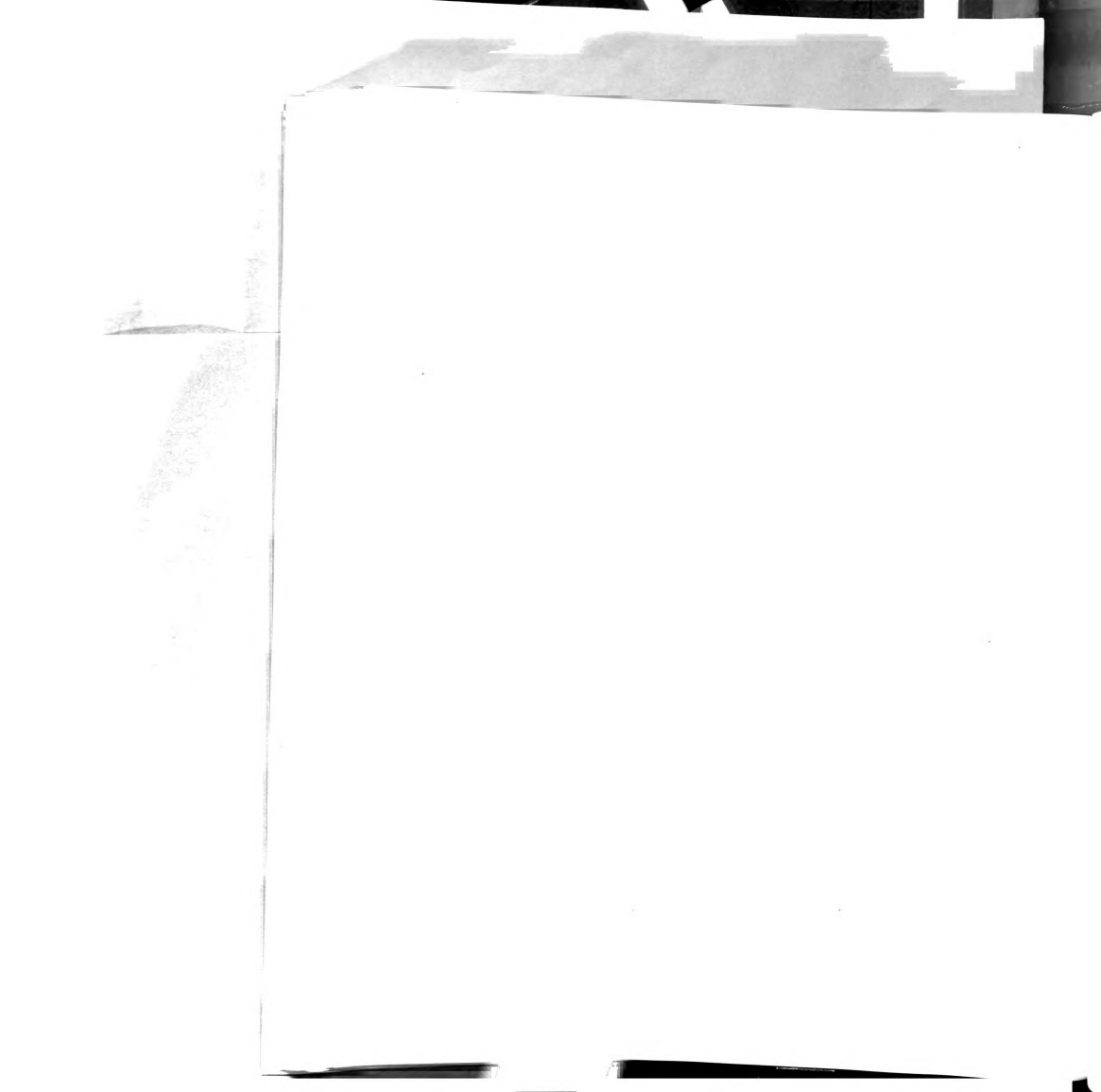


Figure IV.5 ^{13}C field dependence with simulation of line positions and relative intensities. Field dependence data (Full line) conditions as for Figure IV.4. Simulation (dashed line) parameters: $A = [-0.6(\pm 0.1), 0.4(\pm 0.15), -0.5(\pm 0.1)]$ MHz, $\alpha = \beta = 30^\circ$, $\gamma = 0^\circ$; EPR linewidth = 170 MHz, ENDOR linewidth = 0.2 MHz; $\tau = 600$ ns, 100% Mims suppression.



Summary

The observation of substantial ^2H and ^{13}C hyperfine couplings from labeled AdoMet bound to the 1+ cluster of PFL-AE clearly demonstrates that AdoMet binds adjacent to the [4Fe-4S] cluster. The observation of identical spectra from the 1+ and 2+ cryo-reduced enzyme further shows that the position of AdoMet relative to the Fe-S cluster in PFL-AE is identical in the oxidized and reduced states.

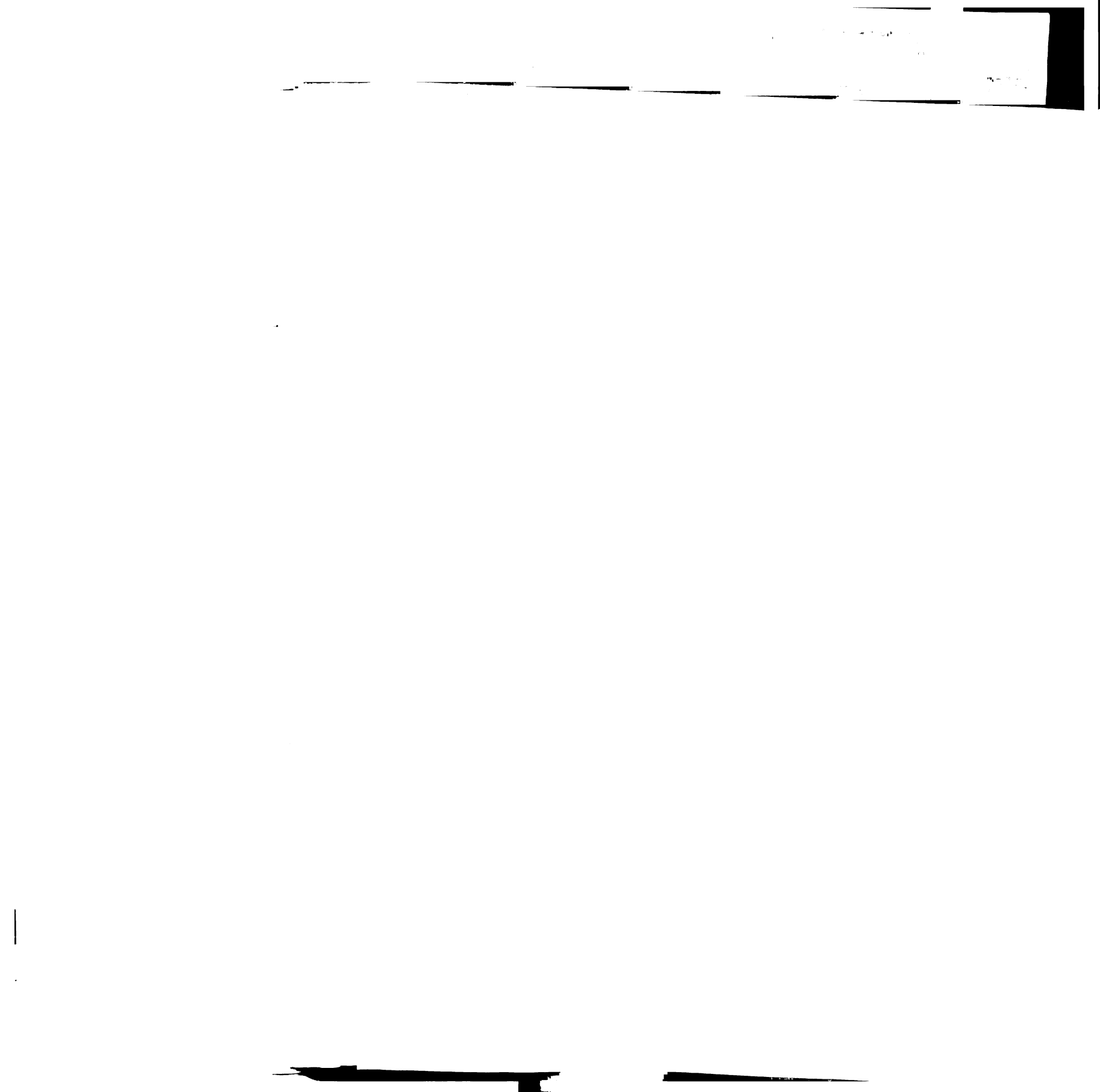
Most intriguingly, the existence of an isotropic contribution to the ^{13}C tensor requires that there be overlap between orbitals on the cluster and on AdoMet, namely that there are incipient covalent interactions between AdoMet and the cluster. The most plausible interpretation is that this interaction is of a dative character, between a negatively-charged sulfide of the cluster and the positively-charged sulfur of AdoMet.

As shown in Table IV.1, the values of r derived from the dipolar interpretation of the ^2H data produce distances to the closest iron ion which are consistent with the C-H single bond separation, with the methyl protons closer than the methyl carbon as required sterically. Any interpretation of the ^2H 2D pattern which includes a significant isotropic component produces a smaller T and thus predicts a larger value of $r(^2\text{H-Fe}_n)$. Given that the 2D pattern always demands a significant dipolar interaction, as evidenced by the 2-fold increase in pattern width between g_{\parallel} and g_{\perp} and that $r(^2\text{H-Fe}_n)$ must not be large enough to place the closest deuterons on the 'other' side of the methyl carbon. We are able to select the purely-dipole model as the better approximation. The distances predicted from T of the model with substantial isotropic ^2H coupling are close to those for $r(^{13}\text{C-Fe}_k)$; for example from the fitting quoted above for the covalent model, choosing the K values in descending order produces distances of 4.5, 4.4, 4.3 and 3.5 Å all of

which are within the range of the distances quoted for $r(^{13}\text{C-Fe}_k)$. We do not, however, believe that the data rules out all isotropic contributions.

K	$r(^2\text{H-Fe}_n)$ - 10% uncertainty in T	$r(^{13}\text{C-Fe}_n)$ - range in T from simulation
1.78	3.8 ± 0.1	5.0 ± 0.6
1.60	3.7 ± 0.1	4.9 ± 0.6
1.57	3.6 ± 0.1	4.9 ± 0.6
0.86	3.0 ± 0.1	4.0 ± 0.6

Table IV.1 r values derived from the dipolar interpretation of the ^2H ENDOR data



The result of these investigations is a structural model of AdoMet bound to both 1+ and 2+ states of PFL-AE in which a cluster sulfide and the AdoMet sulfur are adjacent, with weak dative orbital overlap, while the AdoMet methyl-group carbon lies ~4–5 Å from an Fe ion. This model is illustrated by the structure presented in Figure IV.6.

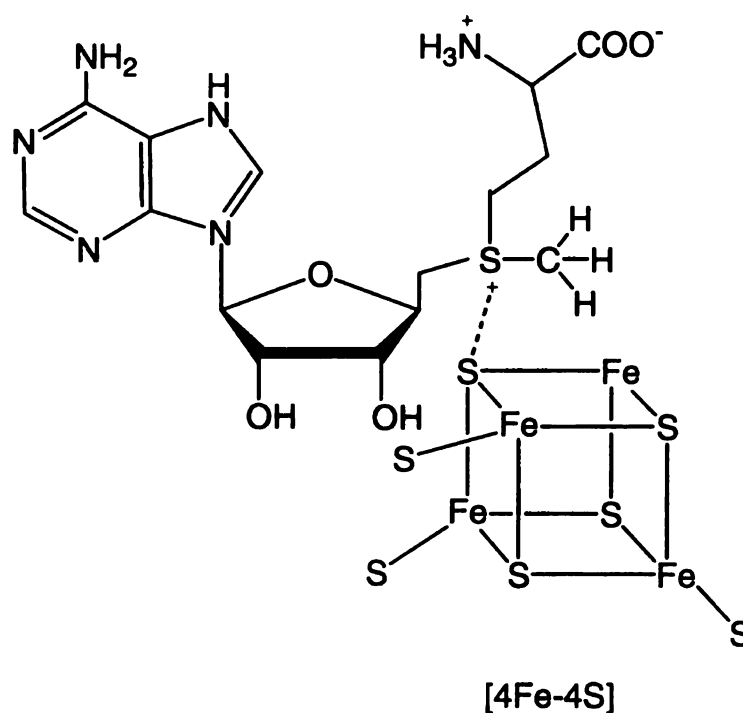


Figure IV.6 Structural model of AdoMet bound to the [4Fe-4S] cluster of PFL-AE

CHAPTER V

Se-ADENOSYL-L-SELENOMETHIONINE AND ITS INTERACTION WITH PYRUVATE FORMATE-LYASE ACTIVATING ENZYME

V.1 Introduction

Selenium is in a bridging position in Group VIA, lying between two nonmetals, oxygen and sulfur, and the increasingly metallic tellurium and polonium. In its period it lies between the metalloid arsenic and the halogen bromine. Selenium has six naturally occurring stable isotopes, ^{74}Se (0.87%), ^{76}Se (9.02%), ^{77}Se (7.58%), ^{78}Se (23.52%), ^{80}Se (49.82%), ^{82}Se (9.19%) and several radioactive isotopes, the most important of which is ^{75}Se , a γ emitter ($t_{1/2} = 120.4$ days), which is widely used as a tracer in biological studies and in certain radiologic diagnostic procedures. Of the naturally occurring isotopes only ^{77}Se has a nuclear spin ($I = 1/2$) and is an increasingly useful probe in some spectroscopic studies (119). Selenium is widely distributed in nature (120-122). It ranks seventieth in order of abundance of the elements and comprises approximately 7×10^{-5} weight per cent of the earth's crust. Selenium has various applications in industry, such as in electronics and metallurgy; in the glass and ceramics industry; in rubber, pigment, and explosive manufacture, and as a catalyst or a constituent in some pharmaceuticals (119).

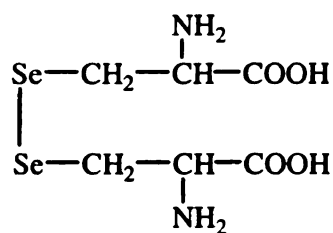
In terms of chemical properties, selenium resembles sulfur more closely than any other element. Both of them occur in the same valence states, -2, 0, +2, +4, and +6, and have similar covalent radii and electronegativities (123). However, the two elements display noteworthy differences in biological systems. Selenium is a paradoxical element



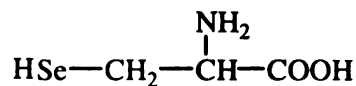
in that it is highly toxic and yet is an essential micronutrient for mammals, birds, several bacteria and probably for fish and many other animal species. "Alkali disease" and "blind stagger", diseases of livestock known for some time, are now attributed to selenium poisoning, resulting from the high toxicity of "selenium accumulator plants" to most animals (121). On the other hand, selenium has been demonstrated to be essential in view of the numerous specific and well-characterized occurrences of selenium in biomolecules (124, 125), and a number of selenium deficiency diseases found in animals as well as human beings (121, 126). Despite its toxicity, selenium compounds have been used as complexing agents to treat heavy metal poisoning, arising from such metals as silver, cadmium, mercury and lead (121, 126). The detoxification is thought to occur because selenium, having a greater affinity than sulfur for heavy metals, can strip the heavy metals from their *in vivo* ligands. In addition, the difference in retention and distribution of sulfur and selenium compounds in the body may facilitate detoxification.

Selenium in plants and animals is found primarily in the form of selenoamino acids (119). Shown in Scheme V.1 are the major selenoamino acids that have been isolated from plants and chemically synthesized. Selenium is also known to be a normal component of several enzymes, proteins and some aminoacyl transfer nucleic acids (tRNAs) (119). Interestingly, most of the selenoamino acids detected in animal and bacterial proteins are selenocysteine, with a number of other selenoamino acids reported (127), including selenomethionine (125). Formate dehydrogenase from *E. coli*, glycine reductase from amino acid-fermenting clostridia, hydrogenases from *Methanococcus vanniellii* and from *Desulfovibrio baculatus*, and mammalian glutathione peroxidase are some examples of the enzymes that have been demonstrated to contain selenium in the

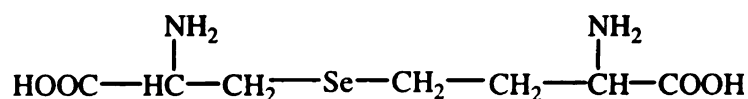




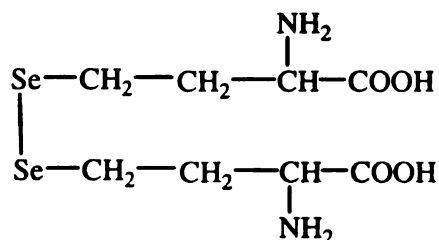
Selenocystine



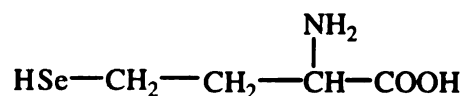
Selenocysteine



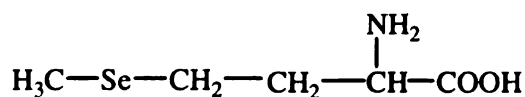
Selenocystathionine



Selenohomocystine



Selenohomocysteine



Selenomethionine

Scheme V.1 Selenoamino acids found in plants

form of selenocysteine (125). Four genes, whose products are required for the incorporation of selenocysteine into proteins, have been identified in *E. coli*. These findings truly establish selenocysteine as the twenty-first naturally occurring amino acid (125).

Following the rationale that selenium substitutes for sulfur in particular functions in various biomolecules, selenium has been artificially incorporated into specific sites of proteins in order to modify their properties and ultimately to understand the targeted sites

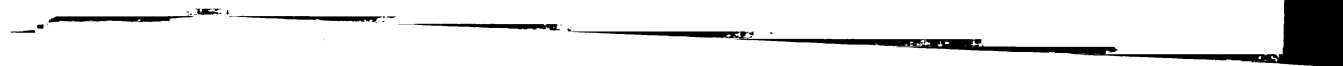
proteins in order to modify their properties and functions in controlling the targeted sites in various physiological systems has been extensively incorporated into specific sites of following the rationale that selected substances for either in particular functions establish specific systems in the body in a naturally occurring amino acid (135).

form of selectivity (136). These amino acids are required for the incorporation of selected amino acids into the body. These amino acids are identified in 3, 4, 5, 6, 7, 8, 9, 10, 11, 12, 13, 14, 15, 16, 17, 18, 19, 20, 21, 22, 23, 24, 25, 26, 27, 28, 29, 30, 31, 32, 33, 34, 35, 36, 37, 38, 39, 40, 41, 42, 43, 44, 45, 46, 47, 48, 49, 50, 51, 52, 53, 54, 55, 56, 57, 58, 59, 60, 61, 62, 63, 64, 65, 66, 67, 68, 69, 70, 71, 72, 73, 74, 75, 76, 77, 78, 79, 80, 81, 82, 83, 84, 85, 86, 87, 88, 89, 90, 91, 92, 93, 94, 95, 96, 97, 98, 99, 100, 101, 102, 103, 104, 105, 106, 107, 108, 109, 110, 111, 112, 113, 114, 115, 116, 117, 118, 119, 120, 121, 122, 123, 124, 125, 126, 127, 128, 129, 130, 131, 132, 133, 134, 135, 136, 137, 138, 139, 140, 141, 142, 143, 144, 145, 146, 147, 148, 149, 150, 151, 152, 153, 154, 155, 156, 157, 158, 159, 160, 161, 162, 163, 164, 165, 166, 167, 168, 169, 170, 171, 172, 173, 174, 175, 176, 177, 178, 179, 180, 181, 182, 183, 184, 185, 186, 187, 188, 189, 190, 191, 192, 193, 194, 195, 196, 197, 198, 199, 200, 201, 202, 203, 204, 205, 206, 207, 208, 209, 210, 211, 212, 213, 214, 215, 216, 217, 218, 219, 220, 221, 222, 223, 224, 225, 226, 227, 228, 229, 230, 231, 232, 233, 234, 235, 236, 237, 238, 239, 240, 241, 242, 243, 244, 245, 246, 247, 248, 249, 250, 251, 252, 253, 254, 255, 256, 257, 258, 259, 260, 261, 262, 263, 264, 265, 266, 267, 268, 269, 270, 271, 272, 273, 274, 275, 276, 277, 278, 279, 280, 281, 282, 283, 284, 285, 286, 287, 288, 289, 290, 291, 292, 293, 294, 295, 296, 297, 298, 299, 300, 301, 302, 303, 304, 305, 306, 307, 308, 309, 310, 311, 312, 313, 314, 315, 316, 317, 318, 319, 320, 321, 322, 323, 324, 325, 326, 327, 328, 329, 330, 331, 332, 333, 334, 335, 336, 337, 338, 339, 340, 341, 342, 343, 344, 345, 346, 347, 348, 349, 350, 351, 352, 353, 354, 355, 356, 357, 358, 359, 360, 361, 362, 363, 364, 365, 366, 367, 368, 369, 370, 371, 372, 373, 374, 375, 376, 377, 378, 379, 380, 381, 382, 383, 384, 385, 386, 387, 388, 389, 390, 391, 392, 393, 394, 395, 396, 397, 398, 399, 400, 401, 402, 403, 404, 405, 406, 407, 408, 409, 410, 411, 412, 413, 414, 415, 416, 417, 418, 419, 420, 421, 422, 423, 424, 425, 426, 427, 428, 429, 430, 431, 432, 433, 434, 435, 436, 437, 438, 439, 440, 441, 442, 443, 444, 445, 446, 447, 448, 449, 450, 451, 452, 453, 454, 455, 456, 457, 458, 459, 460, 461, 462, 463, 464, 465, 466, 467, 468, 469, 470, 471, 472, 473, 474, 475, 476, 477, 478, 479, 480, 481, 482, 483, 484, 485, 486, 487, 488, 489, 490, 491, 492, 493, 494, 495, 496, 497, 498, 499, 500, 501, 502, 503, 504, 505, 506, 507, 508, 509, 510, 511, 512, 513, 514, 515, 516, 517, 518, 519, 520, 521, 522, 523, 524, 525, 526, 527, 528, 529, 530, 531, 532, 533, 534, 535, 536, 537, 538, 539, 540, 541, 542, 543, 544, 545, 546, 547, 548, 549, 550, 551, 552, 553, 554, 555, 556, 557, 558, 559, 560, 561, 562, 563, 564, 565, 566, 567, 568, 569, 570, 571, 572, 573, 574, 575, 576, 577, 578, 579, 580, 581, 582, 583, 584, 585, 586, 587, 588, 589, 590, 591, 592, 593, 594, 595, 596, 597, 598, 599, 600, 601, 602, 603, 604, 605, 606, 607, 608, 609, 610, 611, 612, 613, 614, 615, 616, 617, 618, 619, 620, 621, 622, 623, 624, 625, 626, 627, 628, 629, 630, 631, 632, 633, 634, 635, 636, 637, 638, 639, 640, 641, 642, 643, 644, 645, 646, 647, 648, 649, 650, 651, 652, 653, 654, 655, 656, 657, 658, 659, 660, 661, 662, 663, 664, 665, 666, 667, 668, 669, 670, 671, 672, 673, 674, 675, 676, 677, 678, 679, 680, 681, 682, 683, 684, 685, 686, 687, 688, 689, 690, 691, 692, 693, 694, 695, 696, 697, 698, 699, 700, 701, 702, 703, 704, 705, 706, 707, 708, 709, 710, 711, 712, 713, 714, 715, 716, 717, 718, 719, 720, 721, 722, 723, 724, 725, 726, 727, 728, 729, 730, 731, 732, 733, 734, 735, 736, 737, 738, 739, 740, 741, 742, 743, 744, 745, 746, 747, 748, 749, 750, 751, 752, 753, 754, 755, 756, 757, 758, 759, 760, 761, 762, 763, 764, 765, 766, 767, 768, 769, 770, 771, 772, 773, 774, 775, 776, 777, 778, 779, 780, 781, 782, 783, 784, 785, 786, 787, 788, 789, 790, 791, 792, 793, 794, 795, 796, 797, 798, 799, 800, 801, 802, 803, 804, 805, 806, 807, 808, 809, 810, 811, 812, 813, 814, 815, 816, 817, 818, 819, 820, 821, 822, 823, 824, 825, 826, 827, 828, 829, 830, 831, 832, 833, 834, 835, 836, 837, 838, 839, 840, 841, 842, 843, 844, 845, 846, 847, 848, 849, 850, 851, 852, 853, 854, 855, 856, 857, 858, 859, 860, 861, 862, 863, 864, 865, 866, 867, 868, 869, 870, 871, 872, 873, 874, 875, 876, 877, 878, 879, 880, 881, 882, 883, 884, 885, 886, 887, 888, 889, 890, 891, 892, 893, 894, 895, 896, 897, 898, 899, 900, 901, 902, 903, 904, 905, 906, 907, 908, 909, 910, 911, 912, 913, 914, 915, 916, 917, 918, 919, 920, 921, 922, 923, 924, 925, 926, 927, 928, 929, 930, 931, 932, 933, 934, 935, 936, 937, 938, 939, 940, 941, 942, 943, 944, 945, 946, 947, 948, 949, 950, 951, 952, 953, 954, 955, 956, 957, 958, 959, 960, 961, 962, 963, 964, 965, 966, 967, 968, 969, 970, 971, 972, 973, 974, 975, 976, 977, 978, 979, 980, 981, 982, 983, 984, 985, 986, 987, 988, 989, 990, 991, 992, 993, 994, 995, 996, 997, 998, 999, 1000.

of the proteins. Selenocoenzyme A and selenobiotin have been synthesized and their activities have been studied to compare with their native counterparts (128-130). Many modifications have also been targeted at cysteine or methionine residues (131-137) and inorganic sulfur atoms of iron-sulfur proteins. Substitution of selenium in the active site of ferredoxins has led to interesting findings (Reviewed in Ref.138).

There are also a number of enzymes, which under normal conditions catalyze reactions that result in the transformation of a particular sulfur compound, which have also been found to undergo the same reaction with the analogous selenium compound (139-141). Selenium-containing biomolecules can thus frequently be prepared *in vitro* by enzymatic methods. Some notable enzymes that catalyze reactions in which selenium-containing substrates have been shown to react in place of the corresponding sulfur-containing substrates are tRNA sulfur transferase and cysteinyl-tRNA synthetase (selenocysteine) (140, 142, 143), ATP sulfurylase (adenosine-5'-selenophosphate) (144), AdoMet synthetase (selenomethionine) (100), and AdoMet-dependent methylases and AdoMet decarboxylases (Se-adenosylmethionine) (100, 131, 145, 146).

Selenium compounds are usually more reactive than their sulfur analogues presumably because of the slightly greater polarity and lower bond strength of the C-Se σ bond as well as other σ bonds such as the N-Se and O-Se bonds (119). Selenides are also more nucleophilic than analogous sulfur molecules (102, 103). For example, selenomethionine has been shown to be more reactive than methionine (147), and is much less stable to acid hydrolysis. Selenomethionine completely reacts with cyanogens bromide in 0.1 M HCl to produce homoserine in 15 min while methionine requires 24 h for the same reaction. Selenomethionine also reacts more rapidly than methionine in certain

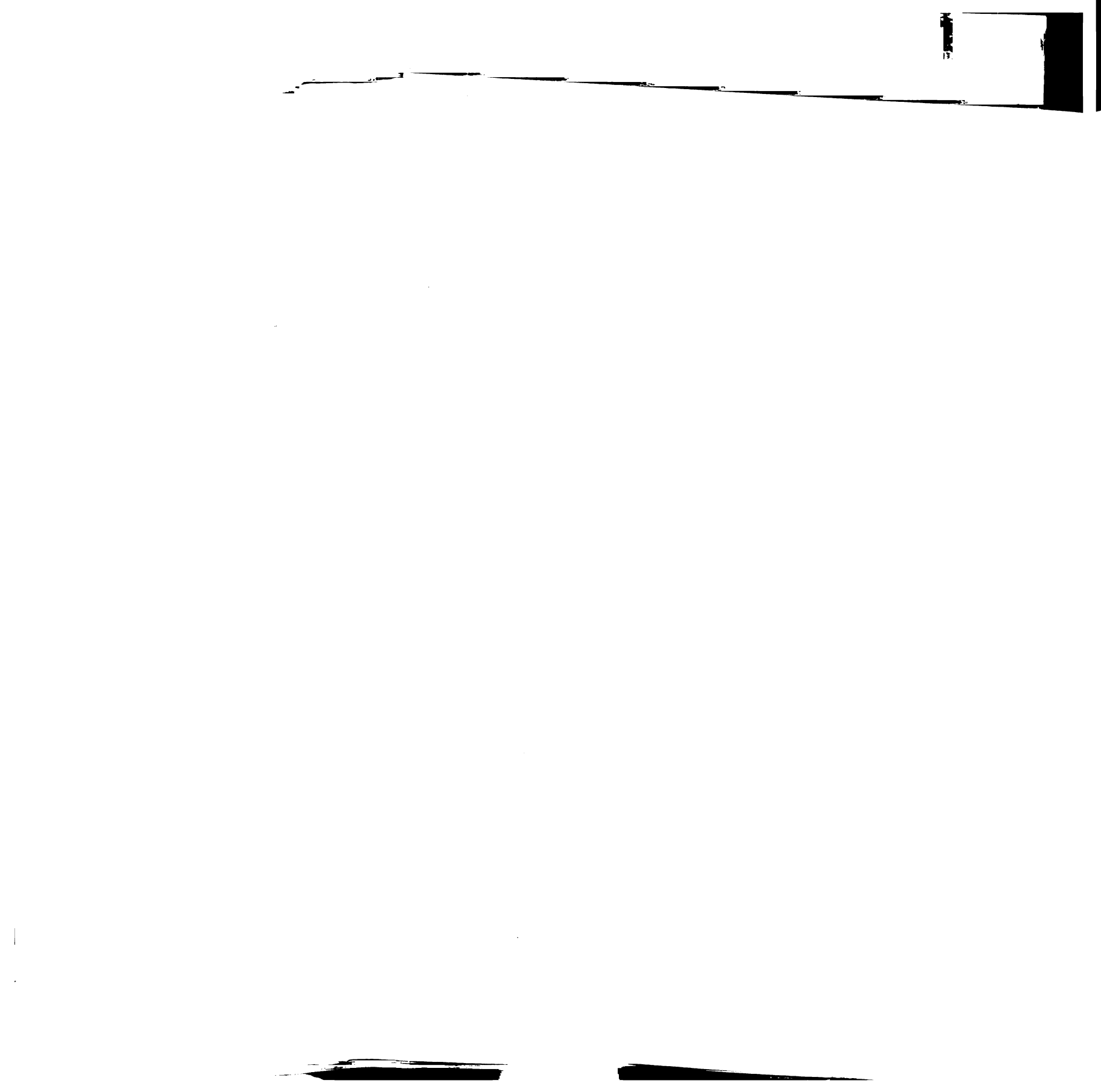


synthesis reactions, as has been reported for AdoMet synthetase from both yeast and *E. coli* (93, 100, 101).

As discussed previously, the chemical properties of selenium are sufficiently similar to those of sulfur to allow replacement of the latter by the former in many biomolecules. However, the two elements differ significantly from each other by some of their physical characteristics, and selenium has proved to be a more efficient probe than sulfur for several spectroscopic methods (119).

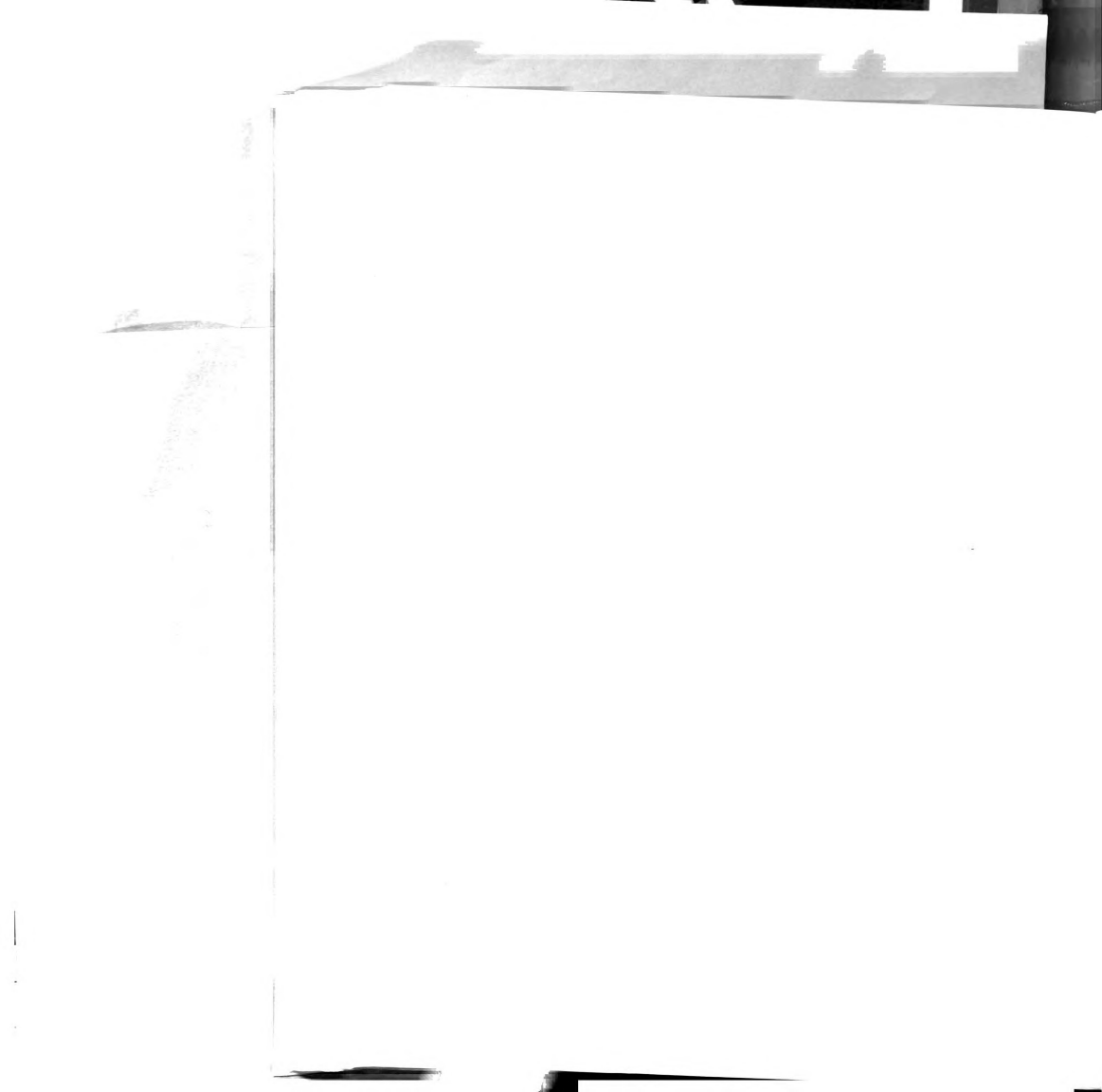
The two chalcogens differ considerably in their atomic mass number A , Se ($A = 79$) being more than twice as heavy as S ($A = 32$). The atomic mass of Se qualifies it as an absorbing atom for X-ray absorption spectroscopy (XAS), which sometimes is difficult to perform with sulfur. For example, S-XAS is not a good method for detecting changes in ligation of an Fe-S cluster, because of the large number of Fe-S bonds present in a typical Fe-S cluster, and since XAS “sees” an average coordination environment for all molecules of a given element in the sample. Measurements on Fe-Se synthetic compounds have demonstrated the feasibility of Se-XAS (148), and it has been used to show that the coordination sphere of Se in a hydrogenase from *D. baculatus* includes nickel and carbon (149). Recently, Frey *et al.* have successfully demonstrated a direct interaction of selenomethionine with the Fe-S cluster of lysine-2,3-aminomutase, a member of the AdoMet dependent Fe-S enzymes, by using Se K-edge XAS in combination with selenium derivatives of methionine and AdoMet (150).

Another advantage of selenium is the presence of an isotope (^{77}Se) with nuclear spin $I = 1/2$. When Se atoms are involved in or near a paramagnetic center, the presence of ^{77}Se may result in EPR spectra displaying hyperfine structures that can provide



detailed information on the environment of the paramagnetic center. This property has been implemented for several Fe-S proteins, where Se was artificially incorporated into the Fe-S clusters or the bacteria which overexpress the proteins were grown in selenium enriched media (138, 151). Moreover, electron nuclear double resonance (ENDOR) and electron spin echo envelope modulation (ESEEM) also have potential in revealing hyperfine interactions of ^{77}Se with a paramagnetic center. ENDOR and ESEEM are two related but complementary techniques that derive from the basic EPR experiment. Broadly speaking, ENDOR is used for investigation of strongly coupled “closer” nuclei having coupling constant A typically in the range of 2 – 40 MHz, while ESEEM is used to study “more distant” weakly coupled nuclei, having A less than about 10 MHz, depending on the nucleus (152). In addition, infrared and resonance Raman spectroscopy, circular dichroism, X-ray diffraction and ^{77}Se NMR also have applications in studies of Se-containing biomolecules (119).

In view of the wide existence of Se in biological systems, its bio-compatibility to several enzymes that catalyze reactions involving sulfur compounds, and its application in certain spectroscopic methods, Se-AdoMet has been proposed to be an effective probe in studying the interaction of the sulfonium center of AdoMet with the Fe-S cluster of PFL-AE. Se-AdoMet, the substrate analog, and selenomethionine (Se-Met), the cleaved product analog, along with the [4Fe-4S] clusters of PFL-AE at different oxidation states were used to mimic the enzyme-substrate (ES) and enzyme-product (EP) complexes, and to follow the course of the cleavage reaction by a variety of spectroscopic methods, including EPR, XAS, ENDOR and ESEEM.



V.2 Experimental methods

V.2.1 Synthesis and purification of Se-AdoMet

As described in Chapter III, Section III.2.3.

V.2.2 Activity assay of PFL-AE with Se-AdoMet

As described in Chapter II, Section II.2.9.

The PFL-AE reaction mix contained in a final volume of 1 mL: 0.1 M Tris-HCl, pH 7.6, 0.1 M KCl, 10 mM DTT, 10 mM oxamate, 9.84 mg PFL, 200 μ M deaza-riboflavin, 0.2 mM Se-AdoMet, and 0.186 μ M PFL-AE.

V.2.3 [1+ / Se-AdoMet] sample preparation

EPR, ENDOR and XAS samples were prepared as described in Chapter IV, Section IV.2.2, except using Se-AdoMet as substrate. [1+/Se-AdoMet] samples for EPR and ENDOR spectroscopy contained 2 equivalents (relative to protein) of Se-AdoMet.

[1+/Se-AdoMet] samples for Se K-edge XAS contained a final volume of 160 μ L: typically approximately 1 mM PFL-AE, 25 % (v/v) glycerol, 1 equivalent of sodium dithionite, 200 μ M deaza-riboflavin and no more than 0.95 equivalents (relative to protein) of Se-AdoMet. A high content of glycerol present in the samples was to prevent formation of ice crystallites, which could result in failure of data collection. A slight excess of protein (relative to seleno-compound) was present in the samples to insure that all metal in the sample was protein-bound, since XAS “sees” an average structure of all selenium sites, including any excess selenium that is coordinated to solvent. The XAS samples were either prepared in parallel with EPR samples, with aliquots transferred to

samples were either prepared in situ or by the following procedures:

1. *Preparation of the 200 nm diameter thin section.* The sample was cut

parallel to the surface of the crystal and then cut perpendicular to the

excess of protein (relative to water) was removed by washing with water.

2. *Preparation of the 200 nm diameter thin section.* The sample was cut

parallel to the surface of the crystal and then cut perpendicular to the

excess of protein (relative to water) was removed by washing with water.

3. *Preparation of the 200 nm diameter thin section.* The sample was cut

parallel to the surface of the crystal and then cut perpendicular to the

excess of protein (relative to water) was removed by washing with water.

4. *Preparation of the 200 nm diameter thin section.* The sample was cut

parallel to the surface of the crystal and then cut perpendicular to the

excess of protein (relative to water) was removed by washing with water.

5. *Preparation of the 200 nm diameter thin section.* The sample was cut

parallel to the surface of the crystal and then cut perpendicular to the

excess of protein (relative to water) was removed by washing with water.

6. *Preparation of the 200 nm diameter thin section.* The sample was cut

parallel to the surface of the crystal and then cut perpendicular to the

excess of protein (relative to water) was removed by washing with water.

7. *Preparation of the 200 nm diameter thin section.* The sample was cut

parallel to the surface of the crystal and then cut perpendicular to the

excess of protein (relative to water) was removed by washing with water.

8. *Preparation of the 200 nm diameter thin section.* The sample was cut

parallel to the surface of the crystal and then cut perpendicular to the

excess of protein (relative to water) was removed by washing with water.

9. *Preparation of the 200 nm diameter thin section.* The sample was cut

parallel to the surface of the crystal and then cut perpendicular to the

excess of protein (relative to water) was removed by washing with water.

both an EPR tube and an XAS cuvet, or the samples were prepared from a previous EPR sample that was thawed and transferred to an XAS cuvet.

V.2.4 [2+ / Se-AdoMet] XAS sample preparation

As described in Chapter IV, Section IV.2.3.

The [2+/Se-AdoMet] mix contained in a final volume of 160 μL : typically approximately 1 mM PFL-AE, 25 % glycerol and 0.95 equivalents of Se-AdoMet.

V.2.5 [2+ / Se-Met / 5'-dAdo] XAS sample preparation

The [2+ / Se-Met / 5'-dAdo] mix contained in a final volume of 160 μL : typically approximately 1 mM PFL-AE, 25 % glycerol, 0.95 equivalents of Se-Met, and 4 mM 5'-deoxyadenosine. The sample was mixed well, loaded into an XAS cuvet, and flash-frozen in liquid nitrogen in the glove box.

V.2.6 [2+ / Se-Met / 5'-dAdo / PFL] XAS sample preparation

The [2+ / Se-Met / 5'-dAdo / PFL] mix contained in a final volume of 160 μL : typically approximately 0.4 mM PFL-AE, 25 % glycerol, 0.95 equivalents of Se-Met, 4 mM 5'-deoxyadenosine, and 1.1 equivalents of PFL. The sample was mixed well, loaded into an XAS cuvet, and flash-frozen in liquid nitrogen in the glove box.

V.2.7 [2+ / Se-AdoMet / PFL] sample preparation

[2+ / Se-AdoMet / PFL] samples were prepared under single turnover conditions (16). The "PFL mix" contained approximately 0.9 mM PFL, 25 % glycerol, 250 mM

dithionite, 10 mM DTT, and 200 μ M 5-deazariboflavin, and was pre-reduced by illumination on ice using a 500 W halogen lamp for 30 min. The “PFL-AE mix” was prepared as described in V.2.3, and an aliquot of the mix was saved to determine the amount of $[4\text{Fe-4S}]^{1+}$ by EPR spectroscopy. The “PFL mix” was then mixed with equimolar “PFL-AE mix”. The final protein concentration was thus diluted by a factor of 2, and was approximately 0.4 mM. The sample was split into an EPR tube and an XAS cuvet, and flash-frozen in liquid nitrogen in the glove box. The amount of glycyl radical generated was determined by EPR spectroscopy.

V.2.8 EPR spectroscopy

As described in Chapter II, Section II.2.10.

V.2.9 ENDOR spectroscopy

ENDOR spectroscopy was done in collaboration with Professor Brian M. Hoffman, and Dr. Charles Walsby, Department of Chemistry, Northwestern University.

V.2.10 Se K-edge X-ray absorption spectroscopy

XAS was done by collaboration with Professor Robert R. Scott, and Nathaniel Cosper, Department of Chemistry, University of Georgia. XAS data were collected at Stanford Synchrotron Radiation Laboratory (SSRL), beamline 7-3.

deposited, 10 mM DTT, and 10 mM EDTA. The reaction was initiated by the addition of 10 mM DTT. The reaction was stopped by the addition of 10 mM EDTA. The reaction mixture was then subjected to SDS-PAGE and transferred to a nitrocellulose membrane. The membrane was probed with anti-PPL-AT antibody (1:1000) and then with a secondary antibody (1:1000). The reaction was then developed using a diaminobenzidine tetrahydrochloride (DAB) substrate. The reaction was then developed using a diaminobenzidine tetrahydrochloride (DAB) substrate. The reaction was then developed using a diaminobenzidine tetrahydrochloride (DAB) substrate.

V.3.8. EPR spectra were recorded on a Bruker EPR spectrometer. The reaction mixture was prepared as described in V.3.7. The reaction mixture was then subjected to EPR spectroscopy.

V.3.9. ENDOR spectra were recorded on a Bruker EPR spectrometer. The reaction mixture was prepared as described in V.3.7. The reaction mixture was then subjected to ENDOR spectroscopy.

V.3.10. X-ray diffraction (XRD) was performed on a Bruker D8 Advance X-ray diffractometer. The reaction mixture was prepared as described in V.3.7. The reaction mixture was then subjected to XRD.

V.3.11. X-ray diffraction (XRD) was performed on a Bruker D8 Advance X-ray diffractometer. The reaction mixture was prepared as described in V.3.7. The reaction mixture was then subjected to XRD.

V.3 Results and Discussion

V.3.1 PFL-AE activity with Se-AdoMet

The activity of PFL-AE in the presence of Se-AdoMet was assayed using a direct enzyme assay in which the amount of glycyl radical on PFL generated by PFL-AE as a function of time was quantified by EPR spectroscopy (Figure V.1). The specific activity of PFL-AE in the presence of Se-AdoMet was estimated to be at least 300 U/mg. This activity is only a lower limit because the time points taken were beyond the linear region of activity. The specific activity determined for PFL-AE with Se-AdoMet is approximately 3 times higher than that with regular AdoMet, which was found to be 95 U/mg.

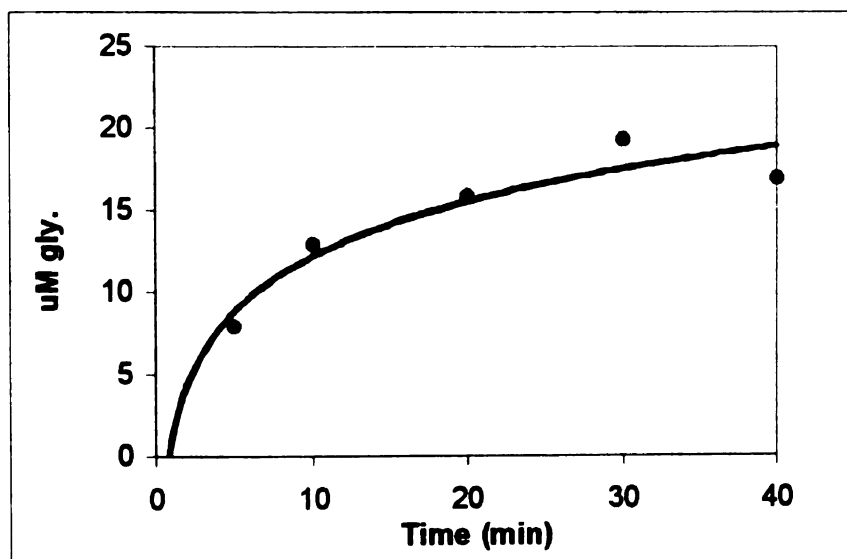


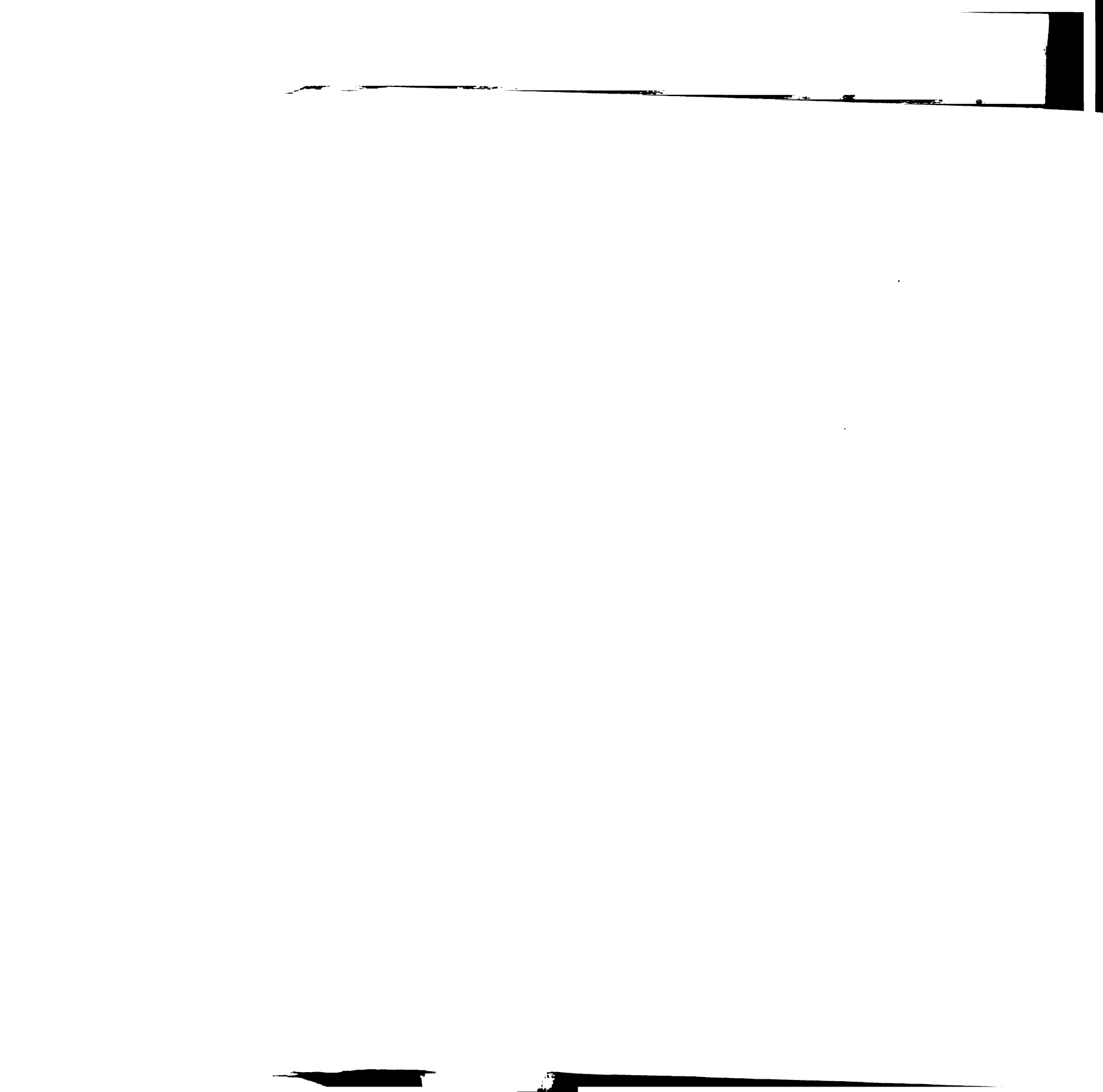
Figure V.1 Activity assay of PFL-AE in the presence of Se-AdoMet. The assay mix (1 mL) contained 9.84 mg/ mL (57.9 mM) PFL, 0.1 M Tris-HCl, pH 7.6, 0.1 M KCl, 10 mM DTT, 10 mM oxamate, 0.2 mM 5-deazariboflavin, 0.2 mM Se-AdoMet, and 0.186 μ M PFL-AE (3.8 mol Fe/ mol PFL-AE, 4.0 mol S/ mol PFL-AE). The assay mix was illuminated for 5, 10, 20, 30, and 40 min, and the amount of glycyl radical generated was determined by X-band EPR spectroscopy.



V.3.2 Generation of $[4\text{Fe-4S}]^{1+}$ of PFL-AE in the presence of Se-AdoMet

Deazariboflavin-mediated photoreduction of PFL-AE followed by addition of Se-AdoMet afforded a high percentage reduction of the $[4\text{Fe-4S}]$ cluster of PFL-AE. In initial experiments, precipitation of protein upon addition of Se-AdoMet solution was observed, which was thought to result from residue acid from the Se-AdoMet purification. The problem was solved by dissolving Se-AdoMet in 50 mM Tris buffer, pH 8.5.

Photoreduction of PFL-AE followed by addition of Se-AdoMet generated a $[4\text{Fe-4S}]^{1+}$ EPR signal accounting for 77.5 % of the iron, based on 512 μM spin for 775 μM protein with 3.41 mol Fe/ mol PFL-AE. A $[1+/\text{AdoMet}]$ sample prepared at the same time generated 63.0 % $[4\text{Fe-4S}]^{1+}$, based on 416 μM spin for 775 μM protein with 3.41 mol Fe/ mol PFL-AE. (Figure V.2). The EPR spectrum of $[1+/\text{Se-AdoMet}]$ was similar to that of $[1+/\text{AdoMet}]$, suggesting that the complexes formed with AdoMet and Se-AdoMet were similar. However, the Se-AdoMet signal was considerably broader than that of the AdoMet. In order to investigate whether the effects of Se-AdoMet on the EPR signal were due to hyperfine interactions of the 7.5 % abundant ^{77}Se , ^{77}Se -ESEEM and ^{77}Se -ENDOR experiments have been carried out with the $[1+/\text{Se-AdoMet}]$ samples. To date, however, ^{77}Se -ESEEM and ^{77}Se -ENDOR spectroscopy have not shown evidence for hyperfine interactions between ^{77}Se and the Fe-S cluster of PFL-AE.



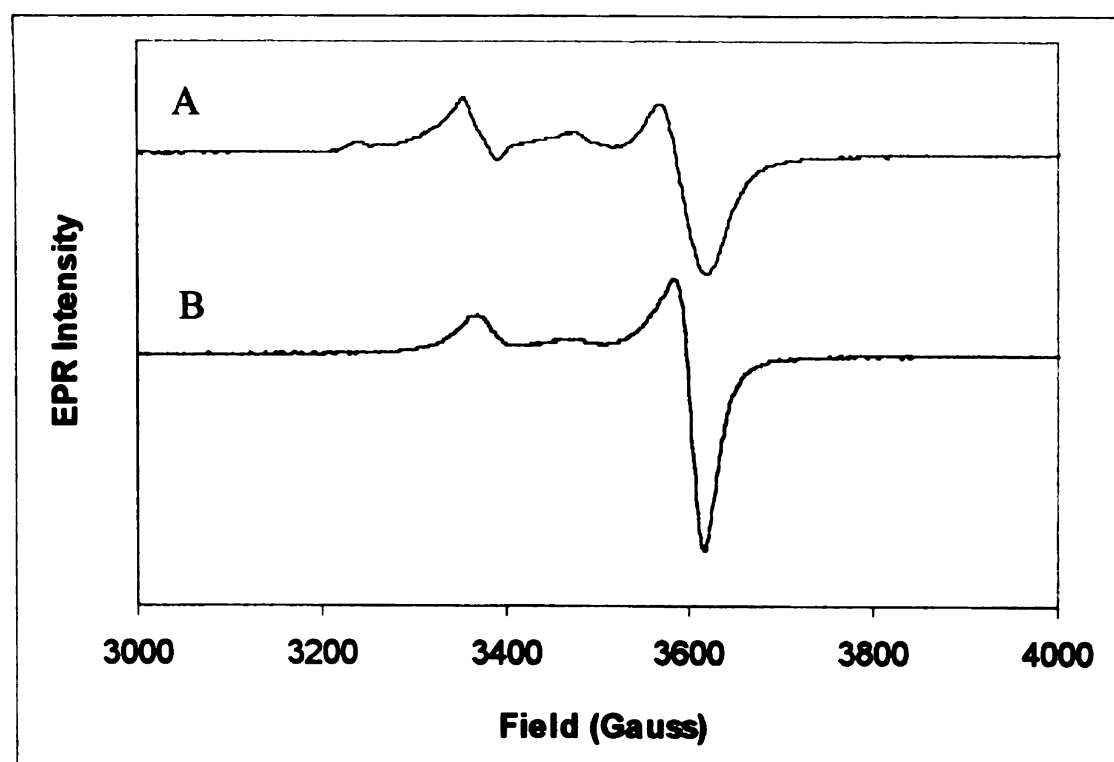


Figure V.2 X-band EPR spectra of photoreduced PFL-AE (**A**) in the presence of Se-AdoMet; the sample contained 775 μM PFL-AE, 1 equivalent of $\text{Na}_2\text{S}_2\text{O}_4$, 200 μM 5-deazariboflavin, and 2 equivalents of Se-AdoMet; 77.5 % reduction (based on 512 μM spin for 775 μM protein with 3.41 mol Fe/ mol PFL-AE); and (**B**) in the presence of AdoMet; the sample contained 775 μM PFL-AE, 1 equivalent of $\text{Na}_2\text{S}_2\text{O}_4$, 200 μM 5-deazariboflavin, and 2 equivalents of AdoMet; 63.0 % reduction (based on 416 μM spin for 775 μM protein with 3.41 mol Fe/ mol PFL-AE). Conditions of measurement: $T = 12$ K; microwave power, 20 μW ; microwave frequency, 9.48 GHz; modulation amplitude, 9.57 G; single scan.

V.3.3 XAS investigation of Se-Fe interaction between the [4Fe-4S] cluster of PFL-AE and Se-AdoMet

Se K-edge XAS spectra of Se-Met and Se-AdoMet displays the expected change in edge position and a significant change in edge shape (Figure V.3). The shift in absorption edge position between Se-Met (12659.6 eV) and Se-AdoMet (12661.2 eV) is indicative of a change in the Se oxidation state of the sample (153). Fourier transform (FT) spectra are characterized by the reduction in FT peak intensity for Se-Met, which is consistent with the coordination number for Se-Met being lower than that for Se-AdoMet. The above features make Se edges a diagnostic fingerprint for distinguishing between samples that resemble these two compounds.

Moreover, a Se-Fe interaction was observed in lysine-2,3-aminomutase after the enzyme turned over (150). The Se-Fe interaction was characterized by a distinct peak at *ca.* 2.7 Å in the FT spectra. This result provides a precedence of observation of Se-Fe interaction in Fe-S enzymes by XAS.

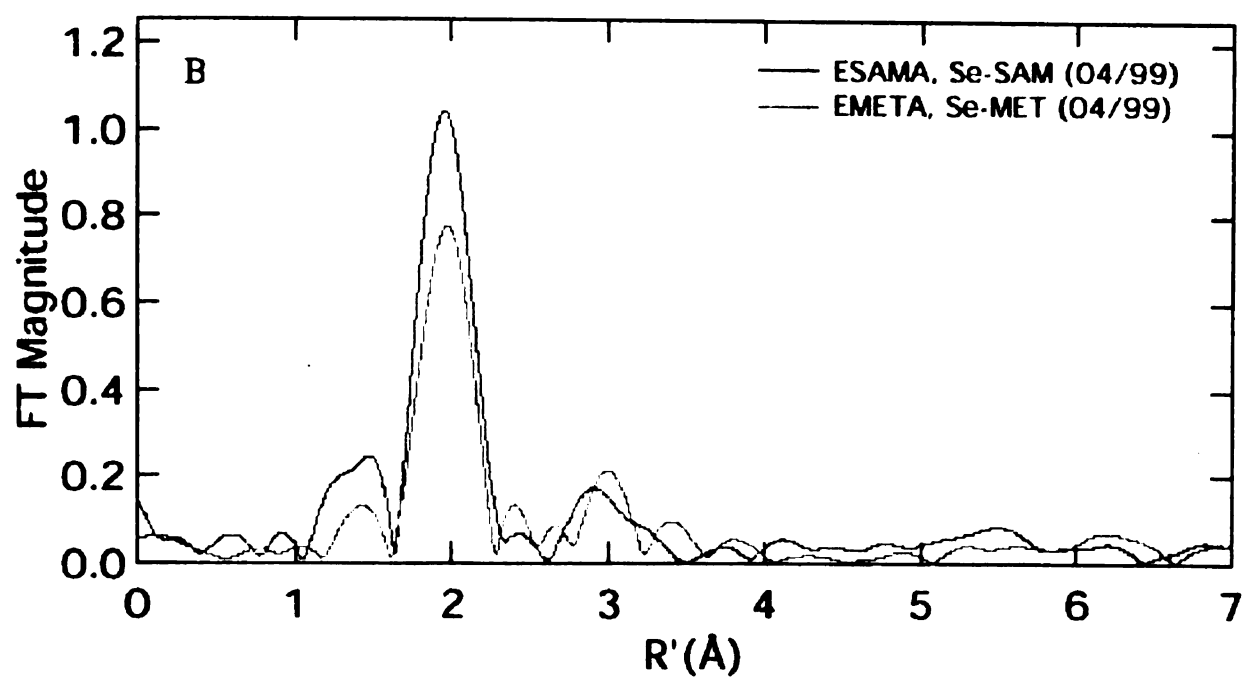
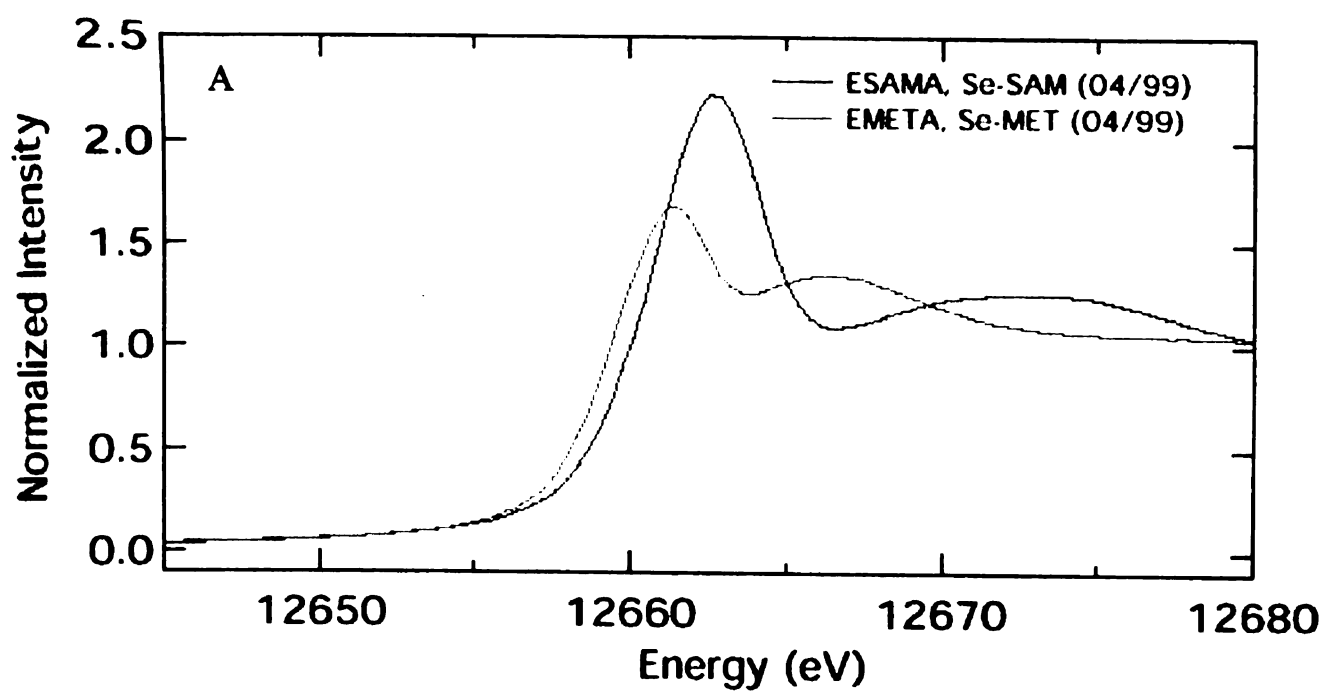


Figure V.3 Se K-edge X-ray absorption spectra (A) and Fourier transforms (B) of Se-AdoMet (ESAMA) and Se-Met (EMETA).



A series of enzyme-substrate (ES) and enzyme-product (EP) complexes were prepared with Se-AdoMet, Se-Met, and the [4Fe-4S] clusters of PFL-AE in different oxidation states, and the course of the AdoMet cleavage reaction was followed by Se K-edge XAS.

Incubating [4Fe-4S]²⁺ of PFL-AE with Se-Met, Se-Met / 5'-dAdo, and Se-Met / 5'-dAdo / PFL yielded Se-edge and FT spectra that were similar to that of Se-Met alone. The spectrum of [4Fe-4S]²⁺ of PFL-AE with Se-AdoMet was similar to that of Se-AdoMet alone (Figure V.4). The observation that the selenium compounds maintained their initial structures was expected, since the [4Fe-4S]²⁺ cluster is not the catalytically relevant cluster, and therefore should not react with AdoMet. In addition, no Se-Fe interaction was observed in the FT spectra of any of the above samples, unlike what was observed in LAM incubated with Se-Met, 5'-dAdo and its substrates (150). The [2+ / Se-AdoMet / PFL] sample was prepared under single turnover conditions. The "PFL-AE mix" was photoreduced to generate 319 μM [4Fe-4S]¹⁺ (out of 927 μM protein) after addition of Se-AdoMet, and 11.2 μM glycyl radical was generated upon mixing equimolar of the pre-reduced "PFL-AE mix" and the "PFL mix". The glycyl radical accounted for 2.8 % of PFL, as the final protein concentration was 395 μM . Although little glycyl radical was produced, it seems that the PFL-AE turned over the Se-AdoMet, since the XAS edge of the [2+ / Se-AdoMet / PFL] sample was more reminiscent of that of Se-Met (Figure V.4). However, the edge of this species was slightly more intense and shifted to higher energy relative to that of Se-Met, indicating that some Se-AdoMet remained. The low percentage of enzymatic turnover could be attributed to reaction of the PFL-AE [4Fe-4S]¹⁺ with Se-AdoMet prior to mixing with PFL. No Se-Fe



interaction was observed in this sample, indicating that Se-Met does not coordinate to the cluster after turnover, in contrast to the results for LAM (150).

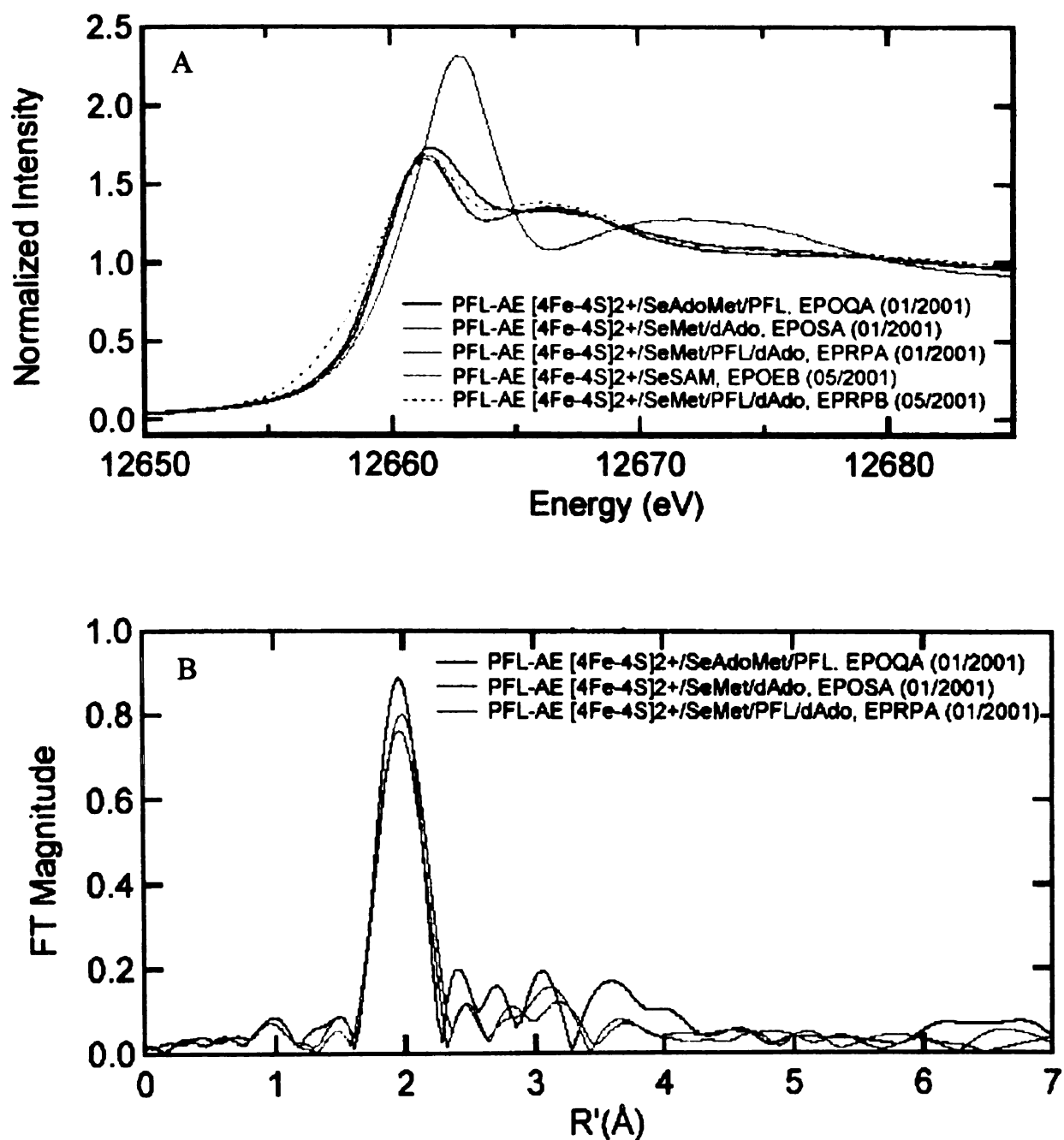


Figure V.4 Se K-edge X-ray absorption spectra (A) and Fourier transforms (B) of PFL-AE [4Fe-4S]²⁺ incubated with Se-Met / 5'-dAdo (EPOSA), Se-Met / 5'-dAdo / PFL (EPRPA and EPRPB), Se-AdoMet (EPOEB), and Se-AdoMet / PFL (EPOQA).

intersection was observed at the 13680 eV position, which is characteristic of the
clusters after turnover, and the 13680 eV position is characteristic of the

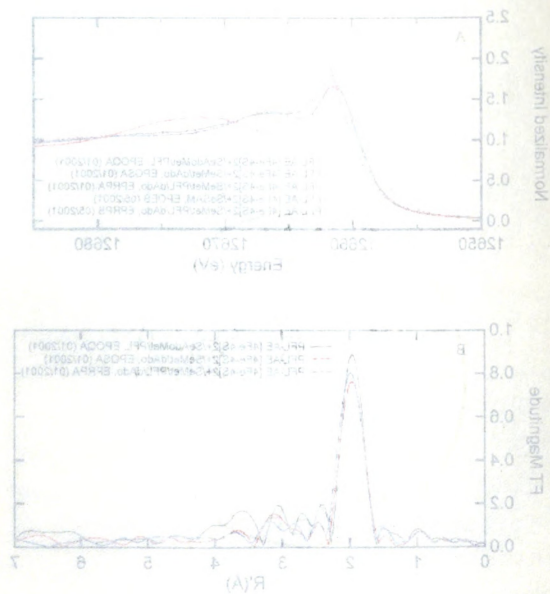


Figure V.4. (A) XPS spectra and (B) Raman spectra of the epoxy resins: PPT (EPOXY) (013001), PPT-4E (EPOXY) (013001), PPT-4E (EPOXY) (013001), and PPT-4E (EPOXY) (013001).

Interestingly, the edge for the three samples of PFL-AE [4Fe-4S]¹⁺ in the presence of Se-AdoMet but in the absence of PFL indicated varying levels of turnover (Figure V.5).

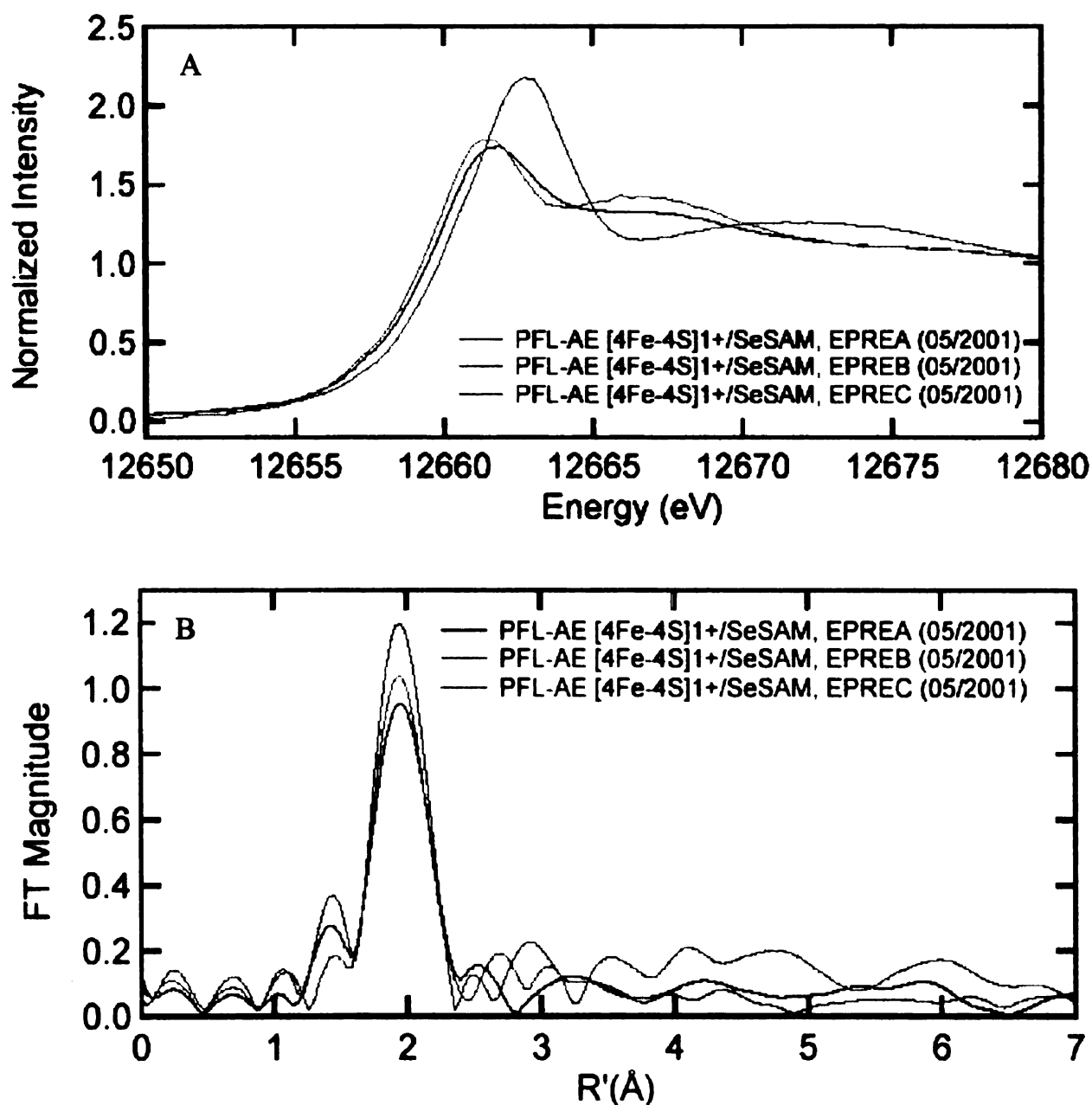


Figure V.5 Se K-edge X-ray absorption spectra (A) and Fourier transforms (B) of PFL-AE [4Fe-4S]¹⁺ in the presence of Se-AdoMet. Sample EPREA: 910 μ M PFL-AE, 590 μ M Se-AdoMet, and 538 μ M [4Fe-4S]¹⁺ generated; EPREB: 600 μ M PFL-AE, 575 μ M Se-AdoMet; EPREC: 1098 μ M PFL-AE, 633 μ M Se-AdoMet, and 214 μ M [4Fe-4S]¹⁺ generated.



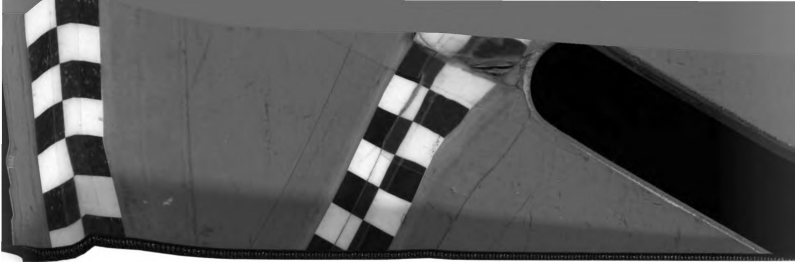
The difference in the amounts of Se-AdoMet being cleaved in the three samples may result from the fast degradation of Se-AdoMet that took place between the time of sample preparation and freezing, which varied from one preparation to another due to the difficulties in loading the XAS cuvettes. Regardless of the amount of Se-AdoMet being cleaved in each sample, the observation of the cleavage of Se-AdoMet in the absence of PFL suggests that PFL might not be required to initiate formation of the adenosyl radical. Thus, the cleavage of Se-AdoMet may be less strictly controlled than in LAM, where no cleavage of Se-AdoMet was observed unless the substrate analog *trans*-4,5-dehydrolysine was present (150).

None of the PFL-AE samples in the presence of Se-AdoMet displayed a Se-Fe interaction in Se K-edge XAS, in contrast to the observations in LAM. LAM is distinct in the class of AdoMet-dependent Fe-S enzymes in that the cleavage of AdoMet is freely reversible. Once the adenosyl radical is generated in LAM, it becomes catalytic, and the enzyme can complete multiple turnovers with only one equivalent of AdoMet. Frey *et al.* postulated that the interaction of methionine with the Fe-S cluster might aid not only in cleaving the cofactor, but also in maintaining methionine in the active site of the enzyme for the back reaction to regenerate AdoMet, which in turn makes it easier to trap the “enzyme-product” complex and observe the Se-Fe interaction (150). However, in PFL-AE, adenosyl radical generation is required for each turnover, which means one mole of AdoMet is expended per mole of glycyl radical. Thus, the AdoMet binding pocket in PFL-AE would have to be emptied after the adenosyl radical is generated, requiring that any Se-Met and Fe-S cluster interaction be short lived. In addition to the fundamental nature of the radical generation in PFL-AE, simply the heterogeneity of the species

1

resulting from the different levels of Se-AdoMet cleavage makes it beyond the capability of the current XAS experiments to observe any putative Se-Fe interaction.



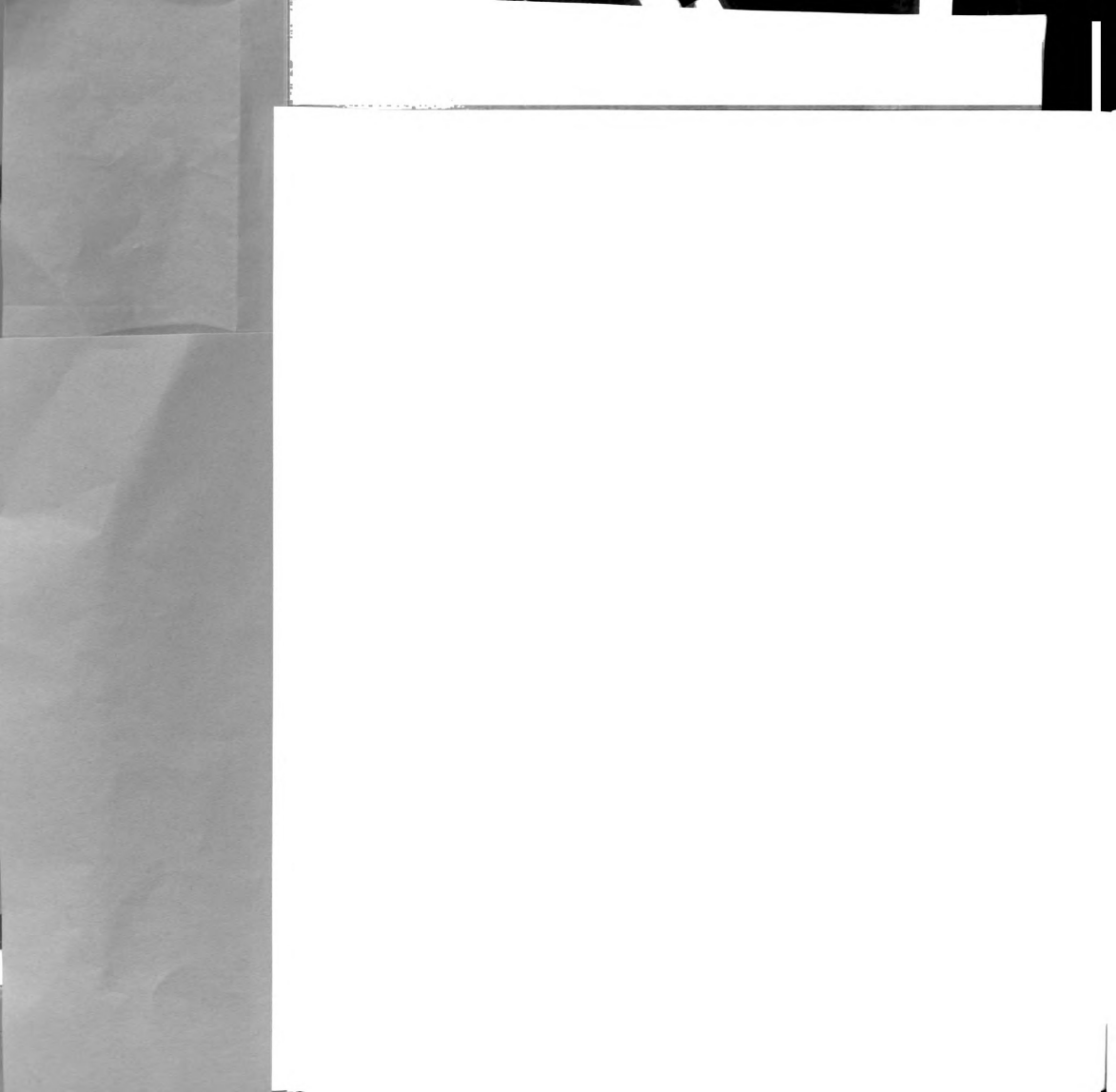


CHAPTER VI

CONCLUSIONS

Since the first isolation of PFL-AE in its native state under strictly anaerobic conditions and identification of the presence of an iron-sulfur cluster in PFL-AE (13, 14), PFL-AE growth and purification conditions have been modified, and the yield of purified protein, as well as the content of intact Fe-S clusters in the as-isolated protein, have been significantly improved. Under current growth conditions, approximately 400 mg of purified PFL-AE was obtained from a 9 L bacteria culture; this represents a 2-3-fold improvement over earlier procedures. In the purification procedures, two passages through the gel filtration column under strictly anaerobic conditions in the presence of 1 mM DTT afforded a higher content of intact Fe-S clusters in the as-isolated PFL-AE. The as-isolated PFL-AE was found to contain 2.5 – 3.8 mol Fe/ mol protein and a stoichiometric amount of acid-labile sulfide. The Fe-S clusters in the as-isolated protein are essentially EPR-silent, presumably in the $[4\text{Fe-4S}]^{2+}$ form, with about 2 % of $[3\text{Fe-4S}]^{1+}$ cluster. A high specific activity of 109 U/ mg enzyme was achieved for PFL-AE containing 3.8 mol Fe/ mol protein.

A fairly simple procedure for enzymatic synthesis of *S*-adenosylmethionine on a preparative scale has been established. AdoMet is synthesized using a crude extract of *E. coli* cells overexpressing AdoMet synthetase. Product inhibition was overcome by addition of 8 % β -mercaptoethanol. The purified AdoMet has high diastereoisomeric purity, and appears to be more stable than AdoMet iodide salt from commercial sources. Methyl- D_3 -AdoMet, methyl- ^{13}C -AdoMet, and Se-AdoMet have been synthesized using

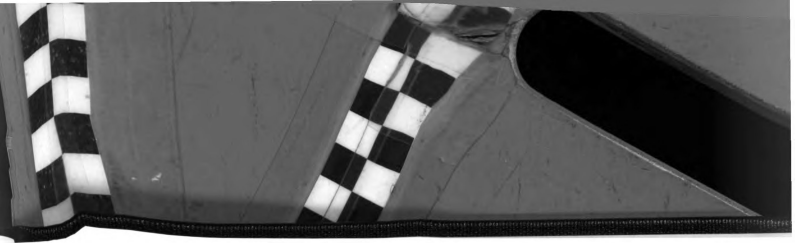




the method described here, with some modifications of the reaction conditions according to the properties of the substrates.

Using isotopically labeled AdoMet and Se-AdoMet, along with ^2H and ^{13}C ENDOR spectroscopy, a close association of PFL-AE [4Fe-4S] cluster with AdoMet has been demonstrated for the first time. These results suggest that the Fe-S cluster of PFL-AE is directly involved in generating the putative adenosyl radical from AdoMet. The ^2H and ^{13}C ENDOR studies have demonstrated that the position of AdoMet relative to the Fe-S cluster of PFL-AE is identical in the oxidized and reduced states, and the sulfonium methyl group lies closely to the Fe-S cluster (Figure IV.6).

EPR spectrum of PFL-AE [4Fe-4S] $^{1+}$ / Se-AdoMet complex displays some different features from the one of PFL-AE [4Fe-4S] $^{1+}$ / natural AdoMet complex, suggesting an effect of selenium on the interaction between AdoMet and the [4Fe-4S] $^{1+}$ cluster of PFL-AE. However, spectroscopic evidence for the Se-Fe interaction has not yet been observed by using Se XAS, and ENDOR spectra of PFL-AE [4Fe-4S] $^{1+}$ / Se-AdoMet complex awaits further analysis.



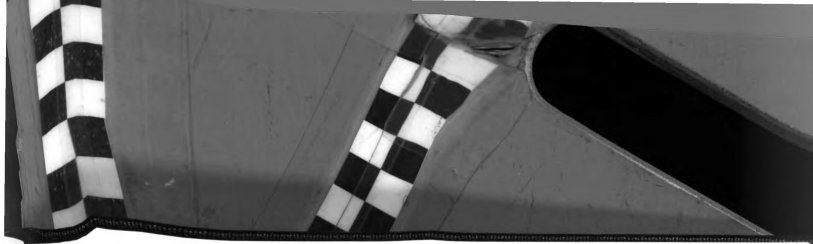
REFERENCES

1. Conradt, H., Hohmann-Berger, M., Hohmann, H. P., Blaschkowski, H. P., and Knappe, J. (1984) *Archives of Biochemistry and Biophysics* **228**, 133-142.
2. Knappe, J., Neugebauer, F. A., Blaschkowski, H. P., and Gänzler, M. (1984) *Proceedings of the National Academy of Science U.S.A.* **81**, 1332-1335.
3. Knappe, J., Elbert, S., Frey, M., and Wagner, A. F. V. (1993) *Biochem. Soc. Trans.* **21**, 731-734.
4. Wagner, A. F. V., Frey, M., Neugebauer, F. A., Schäfer, W., and Knappe, J. (1992) *Proc. Natl. Acad. Sci. U.S.A.* **89**, 996-1000.
5. Reddy, S. G., Wong, K. K., Parast, C. V., Peisach, J., Magliozzo, R. S., and Kozarich, J. W. (1998) *Biochemistry* **37**, 558-563.
6. Parast, C. V., Wong, K. K., Lewisch, S. A., and Kozarich, J. W. (1995) *Biochemistry* **34**, 2393-2399.
7. Becker, A., Fritz-Wolf, K., Kabsch, W., Knappe, J., Schultz, S., and Wagner, A. F. V. (1999) *Nature Structural Biology* **6**, 969-975.
8. Frey, M., Rothe, M., Wagner, A. F. V., and Knappe, J. (1994) *The Journal of Biological Chemistry* **269**, 12432-12437.
9. Kessler, D., Leibrecht, I., and Knappe, J. (1991) *FEBS Letters* **281**, 59-63.
10. Kessler, D., Herth, W., and Knappe, J. (1992) *The Journal of Biological Chemistry* **267**, 18073-18079.
11. Wagner, A. F. V., Demand, J., Schilling, G., Pils, T., and Knappe, J. (1999) *Biochemical and Biophysical Research Communications* **254**, 306-310.
12. Wong, K. K., Murray, B. W., Lewisch, S. A., Baxter, M. K., Ridky, T. W., Ulissi-Demario, L., and Kozarich, J. W. (1993) *Biochemistry* **32**, 14102-14110.
13. Broderick, J. B., Duderstadt, R. E., Fernandez, D. C., Wojtuszewski, K., Henshaw, T. F., and Johnson, M. K. (1997) *Journal of The American Chemical Society* **119**, 7396-7397.
14. Broderick, J. B., Henshaw, T. F., Cheek, J., Wojtuszewski, K., Smith, S. R., Trojan, M. R., McGhan, R. M., Kopf, A., Kibbey, M., and Broderick, W. E. (2000) *Biochemical and Biophysical Research Communications* **269**, 451-456.



15. Krebs, C., Henshaw, T. F., Cheek, J., Huynh, B. H., and Broderick, J. B. (2000) *Journal of The American Chemical Society* **122**, 12497-12506.
16. Henshaw, T. F., Cheek, J., and Broderick, J. B. (2000) *Journal of The American Chemical Society* **122**, 8331-8332.
17. Külzer, R., Pils, T., Kappl, R., Hüttermann, J., and Knappe, J. (1998) *The Journal of Biological Chemistry* **273**, 4897-4903.
18. Rödel, W., Plaga, W., Frank, R., and Knappe, J. (1988) *Eur. J. Biochem* **177**, 153-158.
19. Sun, X., Eliasson, R., Pontis, E., Andersson, J., Buist, G., Sjöberg, R.-M., and Reichard, P. (1995) *The Journal of Biological Chemistry* **270**, 2443-2446.
20. Otsuka, A. J., Buoncristiani, M. R., Howard, P. K., Flamm, J., Johnson, C., Yamamoto, R., Uchida, K., Cook, C., Ruppert, J., and Matsuzaki, J. (1988) *The Journal of Biological Chemistry* **263**, 19577-19585.
21. Hayden, M. A., Huang, I., Bussiere, D. E., and Ashley, G. W. (1992) *The Journal of Biological Chemistry* **267**, 9512-9515.
22. Fajardo-Cavazos, P., Salazar, C., and Nicholson, W. L. (1993) *Journal of Bacteriology* **175**, 1735-1744.
23. Ruzicka, F. J., Lieder, K. W., and Frey, P. A. (2000) *Journal of Bacteriology* **184**, 469-476.
24. Beinert, H. (2000) *Journal of Biological Inorganic Chemistry* **5**, 2-15.
25. Beinert, H., Holm, R. H., and Münck, E. (1997) *Science* **277**, 653-659.
26. Johnson, M. K. (1994) *Encyclopedia of Inorganic Chemistry*, 1896-1915.
27. Howard, J. B., and Rees, D. C. (1996) *Chemical Reviews* **96**, 2965-2982.
28. Flint, D. H., and Allen, R. M. (1996) *Chemical Reviews* **96**, 2315-2334.
29. Beinert, H., Kennedy, M. C., and Stout, C. D. (1996) *Chemical Reviews* **96**, 2335-2374.
30. Harrison, P. M., and Arosio, P. (1996) *Biochim Biophys Acta* **1275**, 161-203.
31. Khoroshilova, N., Popescu, C., Münck, E., Beinert, H., and Kiley, P. J. (1997) *Proc. Natl. acad. Sci. U.S.A.* **94**, 6087-6092.

32. Hidalgo, E., Ding, H. G., and Demple, B. (1997) *Trends Biochem. Sci.* **22**, 207-210.
33. Leuthner, B., Leutwein, C., Schulz, H., Hörth, P., Haehnel, W., Schlitz, E., Schägger, H., and Heider, J. (1998) *Molecular Microbiology* **28**, 615-628.
34. Ollagnier, S., Mulliez, E., Schmidt, P. P., Eliasson, R., Gaillard, J., Deronzier, C., Bergman, T., Gräslund, A., Reichard, P., and Fontecave, M. (1997) *The Journal of Biological Chemistry* **272**, 24216-24223.
35. Lieder, K. W., Booker, S., Ruzicka, F. J., Beinert, H., Reed, G. H., and Frey, P. A. (1998) *Biochemistry* **37**, 2578-2585.
36. Duin, E. C., Lafferty, M. E., Crouse, B. R., Allen, R. M., Sanyal, I., Flint, D. H., and Johnson, M. K. (1997) *Biochemistry* **36**, 11811.
37. Sanyal, I., Cohen, G., and Flint, D. H. (1994) *Biochemistry* **33**, 3625.
38. Busby, R. W., Schelvis, J. P. M., Yu, D. S., Babcock, G. T., and Marletta, M. A. (1999) *Journal of The American Chemical Society* **121**, 4706.
39. Ollagnier-de Choudens, S., and Fontecave, M. (1999) *FEBS Letters* **453**, 25.
40. Rebeil, R., Sun, Y., Chooback, L., Pedraza-Reyes, M., C., K., Begley, T. P., and Nicholson, W. L. (1998) *Journal of Bacteriology* **180**, 4879-4885.
41. Sofia, H. J., Chen, G., Hetzler, B. G., Reyes-Spindola, J. F., and Miller, N. E. (2001) *Nucleic Acids Research* **29**, 1097-1106.
42. Reichard, P. (1988) *Annual Review of Biochemistry* **57**, 349-374.
43. Reichard, P. (1993) *Science* **260**, 1773-1777.
44. Reichard, P. (1997) *Trends in Biochemical Science* **22**, 81-85.
45. Stubbe, J., and van der Donk, W. A. (1998) *Chemical Reviews* **98**, 705-762.
46. Eliasson, R., Pontis, E., Fontecave, M., Gerez, C., Harder, J., Jörnvall, H., Krook, M., and Reichard, P. (1992) *The Journal of Biological Chemistry* **267**, 25541-25547.
47. Bianchi, V., Eliasson, R., Fontecave, M., Mulliez, E., Hoover, D. M., Matthews, R. G., and Reichard, P. (1995) *Biochemical and Biophysical Research Communications* **197**, 792-797.



48. Mulliez, E., Fontecave, M., Gaillard, J., and Reichard, P. (1993) *The Journal of Biological Chemistry* **268**, 2296-2299.
49. Tamarit, J., Mulliez, E., Meier, C., Trautwein, A., and Fontecave, M. (1999) *The Journal of Biological Chemistry* **274**, 31291-31296.
50. Coschigano, P. W., Wehrman, T. S., and Young, L. Y. (1998) *Appl. Environ. Microbiology* **64**, 1650-1656.
51. Bell, H. R., and Spornmann, A. M. (1997) *Journal of Bacteriology* **179**, 670-676.
52. Chirpic, T. P., Zappia, V., Costilow, R. N., and Barker, H. (1970) *The Journal of Biological Chemistry* **245**, 1778-1789.
53. Song, K. B., and Frey, P. A. (1991) *The Journal of Biological Chemistry* **266**, 7651-7655.
54. Petrovich, R. M., Ruzicka, F. J., Reed, G. H., and Frey, P. A. (1991) *The Journal of Biological Chemistry* **266**, 7656-7660.
55. Magnusson, O. T., Reed, G. H., and Frey, P. A. (1999) *Journal of The American Chemical Society* **121**, 9764-9765.
56. Magnusson, O. T., Reed, G. H., and Frey, P. A. (2001) *Biochemistry* **40**, 7773-7782.
57. Ifuku, O., Kishimoto, J., Haze, S., Yanagi, M., and Fukushima, S. (1992) *Biosci. Biotechnol. Biochem.* **56**, 1780-1785.
58. Escalettes, F., Florentin, D., Bui, B. T. S., Lesage, D., and Marquet, A. (1999) *Journal of The American Chemical Society* **121**, 3571-3578.
59. Reed, K. J., and Cronan, J. E. J. (1993) *Journal of Bacteriology* **175**, 1325-1336.
60. Vanden Boom, T. J., Reed, K. E., and Cronan, J. E. J. (1991) *Journal of Bacteriology* **173**, 6411-6420.
61. Hayden, M. A., Huang, I. Y., Iliopoulos, G., Orozco, M., and Ashley, G. W. (1993) *Biochemistry* **32**, 3778-3782.
62. Miller, J. R., Busby, r. W., Jordan, S. W., Cheek, J., Henshaw, T. F., Ashley, G. W., Broderick, J. B., Cronan, J. E. J., and Marletta, M. A. (2000) *Biochemistry* **39**, 15166-15178.
63. Nicholson, W. L., Chooback, L., and Fajardo-Cavazos, P. (1997) *Mol. Gen. Genet* **255**, 587-594.





64. Frey, P. A. (1990) *Chemical Reviews* **90**, 1343-1357.
65. Frey, P. A. (2001) *Annual Review of Biochemistry* **70**, 121-148.
66. Knappe, J., Schacht, J., W., M., Hoepner, T., Vetter, H., Jr., and Edenharter, R. (1969) *European Journal of Biochemistry* **11**, 316-327.
67. Knappe, J., Blaschkowski, H. P., Groebner, P., and Schmitt, T. (1974) *European Journal of Biochemistry* **50**, 253-263.
68. Knappe, J., and Schmitt, T. (1976) *Biochemical and Biophysical Research Communications* **71**, 1110-1117.
69. Kennedy, M. C., Emptage, M. H., Dreyer, J.-L., and Beinert, H. (1983) *The Journal of Biological Chemistry* **258**, 11098-11105.
70. Emptage, M. H., Kent, T. A., Kennedy, M. C., Beinert, H., and Münck, E. (1983) *Proc. Natl. Acad. Sci. U.S.A.* **80**, 4674-4678.
71. Werst, M. M., Kennedy, M. C., Houseman, A. L. P., Beinert, H., and Hoffman, B. M. (1990) *Biochemistry* **29**, 10526-10532.
72. Werst, M. M., Kennedy, M. C., Houseman, A. L. P., Beinert, H., and Hoffman, B. M. (1990) *Biochemistry* **29**, 10533-10540.
73. Janda, M., and Hemmerich, P. (1976) *Angewandte Chemie International Edition English* **15**, 7.
74. Ashton, W. T., Brown, R. D., and Tolman, R. L. (1978) *Journal of Heterocyclic Chemistry* **15**, 489-491.
75. Smit, P. (1986) *Recyl. Trav. Chim. Pays-Bays*. **105**, 538-544.
76. Garboczi, D. N., Hullihen, J. H., and Pedersen, P. L. (1988) *The Journal of Biological Chemistry* **263**, 15694-15698.
77. Bradford, M. (1976) *Analytical Biochemistry* **72**, 248.
78. Beinert, H. (1978) *Methods in Enzymology* **54**, 435-445.
79. Beinert, H. (1983) *Analytical Chemistry* **131**, 373-378.
80. Aasa, R., and Vänngård, T. (1975) *J. Magn. Reson.* **19**, 308.
81. Murib, J. H., and Riter, D. M. (1952) *Journal of The American Chemical Society* **74**, 339.



82. Cantoni, G. L. (1953) *The Journal of Biological Chemistry* **204**, 403-416.
83. Tabor, C. W., and Tabor, H. (1984) *Advances in Enzymology* **56**, 251-282.
84. Tabor, C. W., and Tabor, H. (1985) *Microbiology Reviews* **49**, 81.
85. Satoh, S., and Yang, S. F. (1989) *Plant Physiology* **91**, 1036-1039.
86. Slany, R. K., Bösl, M., Crain, P. F., and Kersten, H. (1993) *Biochemistry* **32**, 7811-7817.
87. Pascale, R. M., Marras, V., Simile, M. M., Daino, L., Pinna, G., Bennati, S., Carta, M., Seddaiu, M. A., Massarelli, G., and Feo, F. (1992) *Cancer Research* **52**, 4979-4986.
88. Kagan, B. L., Sultzer, D. L., Rosenlicht, N., and Gerner, R. H. (1990) *American Journal of Psychiatry* **147**, 591-595.
89. Bell, K. M., Plon, L., Bunney, J. W. E., and Potkin, S. G. (1988) *American Journal of Psychiatry* **145**, 1110-1114.
90. Metz, J. (1993) *Nutrition Reviews* **51**, 12-15.
91. Matos, J. R., Raushel, F. M., and Wong, C.-H. (1987) *Biotechnology and Applied Biochemistry* **9**, 39-52.
92. Schalk-Hihi, C., and Markham, G. D. (1999) *Biochemistry* **38**, 2542-2550.
93. Markham, G. D., Hafner, E. W., Tabor, C. W., and Tabor, H. (1980) *The Journal of Biological Chemistry* **255**, 9082-9092.
94. Markham, G. D. (1981) *The Journal of Biological Chemistry* **256**, 1903-1909.
95. Zhang, C., Markham, G. D., and LoBrutto, R. (1993) *Biochemistry* **32**, 9866-9873.
96. Park, J., Tai, J., Roessner, C. A., and Scott, A. I. (1996) *Bioorganic & Medicinal Chemistry* **4**, 2179-2185.
97. Markham, G. D. (1986) *The Journal of Biological Chemistry* **261**, 1507-1509.
98. Markham, G. D., and Leyh, T. S. (1987) *Journal of The American Chemical Society* **109**, 600-602.
99. Gilliland, G. L., Markham, G. D., and Davies, D. R. (1983) *The Journal of Biological Chemistry* **258**, 6963-6964.

82. Cantoni, G. L. (1972) *Ann. Rev. Biochem.* 41: 1-37.
83. Tabac, C. W., and Fagan, J. A. (1972) *Ann. Rev. Biochem.* 41: 583-607.
84. Tabac, C. W., and Fagan, J. A. (1972) *Ann. Rev. Biochem.* 41: 583-607.
85. Zamb, S., and Fagan, J. A. (1972) *Ann. Rev. Biochem.* 41: 583-607.
86. Zamb, S., and Fagan, J. A. (1972) *Ann. Rev. Biochem.* 41: 583-607.
87. Pascale, R. M., and Fagan, J. A. (1972) *Ann. Rev. Biochem.* 41: 583-607.
88. Cantoni, G. L., and Fagan, J. A. (1972) *Ann. Rev. Biochem.* 41: 583-607.
89. Kagan, R. M., and Fagan, J. A. (1972) *Ann. Rev. Biochem.* 41: 583-607.
90. Bell, R. M., and Fagan, J. A. (1972) *Ann. Rev. Biochem.* 41: 583-607.
91. Bell, R. M., and Fagan, J. A. (1972) *Ann. Rev. Biochem.* 41: 583-607.
92. Bell, R. M., and Fagan, J. A. (1972) *Ann. Rev. Biochem.* 41: 583-607.
93. Bell, R. M., and Fagan, J. A. (1972) *Ann. Rev. Biochem.* 41: 583-607.
94. Bell, R. M., and Fagan, J. A. (1972) *Ann. Rev. Biochem.* 41: 583-607.
95. Bell, R. M., and Fagan, J. A. (1972) *Ann. Rev. Biochem.* 41: 583-607.
96. Bell, R. M., and Fagan, J. A. (1972) *Ann. Rev. Biochem.* 41: 583-607.
97. Bell, R. M., and Fagan, J. A. (1972) *Ann. Rev. Biochem.* 41: 583-607.
98. Bell, R. M., and Fagan, J. A. (1972) *Ann. Rev. Biochem.* 41: 583-607.
99. Bell, R. M., and Fagan, J. A. (1972) *Ann. Rev. Biochem.* 41: 583-607.

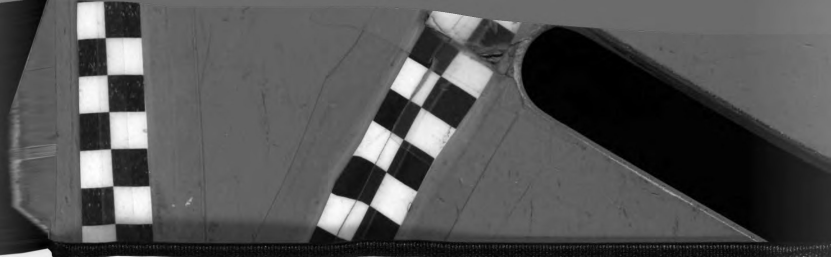
100. Mudd, S. H., and Cantoni, G. L. (1957) *Nature* **180**, 1052.
101. Greene, R. C. (1969) *Biochemistry* **8**, 2255-2265.
102. Barth, H., and Gosselck, J. (1961) *Z. Naturforsch.* **166**, 280.
103. Pearson, R. G., Sobel, H., and Songstad, J. (1968) *Journal of The American Chemical Society* **90**, 319.
104. Knappe, J., and Sawers, G. (1990) *FEMS Microbiology Reviews* **75**, 383-398.
105. Wong, K. K., and Kozarich, J. W. (1994) *Met. Ions Biol. Syst.* **30**, 279-313.
106. Cheek, J., and Broderick, J. B. (2001) *Journal of Biological Inorganic Chemistry* **6**, 209-226.
107. Ollagnier, S., Meier, C., Mulliez, E., Gaillard, J., Schuenemann, V., Trautwein, A., Mattioli, T., Lutz, M., and Fontecave, M. (1999) *Journal of The American Chemical Society* **121**, 6344.
108. Padovani, D., Thomas, F., Trautwein, A. X., Mulliez, E., and Fontecave, M. (2001) *Biochemistry* **40**, 6713-6719.
109. Davydov, R. M., Yoshida, T., Ikeda-Saito, M., and Hoffman, B. M. (1999) *Journal of The American Chemical Society* **121**, 10656-10657.
110. Davydov, R., MacDonald, I. D. G., Makris, T. M., Sligar, S. G., and Hoffman, B. M. (1999) *Journal of The American Chemical Society* **121**, 10654-10655.
111. Davydov, R., Valentine, A. M., Komar-Panicucci, S., Hoffman, B. M., and Lippard, S. (1999) *Biochemistry* **38**, 4188-4197.
112. Davydov, R., Sahlin, M., Kuprin, S., Graslund, A., and Ehrenberg, A. (1996) *Biochemistry* **35**, 5571-5576.
113. Davydov, A., Davydov, R., Graslund, A., Lipscomb, J., and Anderson, K. K. (1997) *The Journal of Biological Chemistry* **272**, 7022-7026.
114. Davydov, R., Kuprin, S., Graslund, A., and Ehrenberg, A. (1994) *Journal of The American Chemical Society* **116**.
115. Dikanov, S. A., Davydov, R. M., Xun, L., and Bowman, M. K. (1996) *Journal of Magnetic Resonance* **112**, 289-294.
116. Telser, J., Davydov, R., Kim, C. H., Adams, M. W. W., and Hoffman, B. M. (1999) *Inorganic Chemistry* **38**, 3550-3553.

100. Mudd, S. H. and L. S. Brown. 1990. The effect of temperature on the growth of *Chlamydomonas reinhardtii* in continuous culture. *Journal of Applied Phycology* 4: 101-106.
101. Greene, R. E. 1990. *Chlamydomonas reinhardtii*. In: *Chlamydomonas reinhardtii*, ed. R. E. Greene, pp. 1-10. Cambridge University Press, Cambridge.
102. Barth, H. and G. H. R. 1990. *Chlamydomonas reinhardtii*. In: *Chlamydomonas reinhardtii*, ed. R. E. Greene, pp. 11-10. Cambridge University Press, Cambridge.
103. Brown, R. E. and L. S. Brown. 1990. The effect of temperature on the growth of *Chlamydomonas reinhardtii* in continuous culture. *Journal of Applied Phycology* 4: 101-106.
104. Brown, R. E. and L. S. Brown. 1990. The effect of temperature on the growth of *Chlamydomonas reinhardtii* in continuous culture. *Journal of Applied Phycology* 4: 101-106.
105. Wong, K. K. and R. E. Brown. 1990. The effect of temperature on the growth of *Chlamydomonas reinhardtii* in continuous culture. *Journal of Applied Phycology* 4: 101-106.
106. Clark, J. and H. R. 1990. *Chlamydomonas reinhardtii*. In: *Chlamydomonas reinhardtii*, ed. R. E. Greene, pp. 1-10. Cambridge University Press, Cambridge.
107. O'Brien, J. and R. E. Brown. 1990. The effect of temperature on the growth of *Chlamydomonas reinhardtii* in continuous culture. *Journal of Applied Phycology* 4: 101-106.
108. Brown, R. E. and L. S. Brown. 1990. The effect of temperature on the growth of *Chlamydomonas reinhardtii* in continuous culture. *Journal of Applied Phycology* 4: 101-106.
109. Brown, R. E. and L. S. Brown. 1990. The effect of temperature on the growth of *Chlamydomonas reinhardtii* in continuous culture. *Journal of Applied Phycology* 4: 101-106.
110. Brown, R. E. and L. S. Brown. 1990. The effect of temperature on the growth of *Chlamydomonas reinhardtii* in continuous culture. *Journal of Applied Phycology* 4: 101-106.
111. Brown, R. E. and L. S. Brown. 1990. The effect of temperature on the growth of *Chlamydomonas reinhardtii* in continuous culture. *Journal of Applied Phycology* 4: 101-106.
112. Brown, R. E. and L. S. Brown. 1990. The effect of temperature on the growth of *Chlamydomonas reinhardtii* in continuous culture. *Journal of Applied Phycology* 4: 101-106.
113. Brown, R. E. and L. S. Brown. 1990. The effect of temperature on the growth of *Chlamydomonas reinhardtii* in continuous culture. *Journal of Applied Phycology* 4: 101-106.
114. Brown, R. E. and L. S. Brown. 1990. The effect of temperature on the growth of *Chlamydomonas reinhardtii* in continuous culture. *Journal of Applied Phycology* 4: 101-106.
115. Brown, R. E. and L. S. Brown. 1990. The effect of temperature on the growth of *Chlamydomonas reinhardtii* in continuous culture. *Journal of Applied Phycology* 4: 101-106.
116. Brown, R. E. and L. S. Brown. 1990. The effect of temperature on the growth of *Chlamydomonas reinhardtii* in continuous culture. *Journal of Applied Phycology* 4: 101-106.

117. Yoo, S., J., Angove, H. C., Burgess, B. K., Münck, E., and Peterson, J. (1998) *Journal of The American Chemical Society* **120**, 9704-9705.
118. Telser, J., Huang, H., Lee, H. I., Adams, M. W. W., and Hoffman, B. M. (1998) *Journal of The American Chemical Society* **120**, 861-870.
119. Odom, J. D. (1983) *Structure and Bonding* **54**, 1-26.
120. Bisbjerg, B. (1972) *Studies on Selenium in Plants and Soils*, Danish Atomic Energy Commission.
121. Rosenfeld, I., and Beath, O. A. (1964) *Selenium Geobotany, Biochemistry, Toxicity and Nutrition*, Academic Press, New York.
122. *Committee on Medical and Biologic Effects of Environmental Pollutants: Selenium* (1976) National Academy of Sciences, Washington, D. C.
123. Pauling, L. (1960) *The Nature of Chemical Bond*, Chaps. 3 and 7, Cornell University Press, Ithaca, N. Y.
124. Spallholz, J. E., Martin, J. L., and Ganther, H. E. (1981) *Selenium in Biology and Medicine*.
125. Stadtman, T. C. (1990) *Annual Review of Biochemistry* **59**, 111.
126. Diplock, A. T. (1981) *Philosophical Transactions of the Royal Society of Londond Series B, Biological Sciences* **294**, 105-117.
127. Sunde, R. A. (1990) *Annual Review of Nutrition* **10**, 451.
128. Günther, W. H. H., and Mautner, H. G. (1965) *Journal of The American Chemical Society* **87**, 2708.
129. Piffeateau, A., Gaudry, M., and Marquet, A. (1976) *Biochemical and Biophysical Research Communications* **73**, 773.
130. Marquet, A. (1977) *Pure and Application Chemistry* **49**, 183.
131. Wu, M., and Wachsman, J. T. (1971) *Journal of Bacteriology* **105**, 1222-1223.
132. Wu, Z.-P., and Hilvert, D. (1989) *Journal of The American Chemical Society* **111**, 4513-4514.
133. Walter, R., and Chan, W. Y. (1967) *Journal of The American Chemical Society* **89**, 3892-3898.

134. Hartrodt, B., Neubert, K., Bierwolf, B., Blech, W., and Jakubke, H.-D. (1980) *Tetrahedron Letters* **21**.
135. Oikawa, T., Esaki, N., Tanaka, H., and Soda, K. (1991) *Proceedings of the National Academy of Science U.S.A.* **88**, 3057-3059.
136. Frank, P., Licht, A., Tullius, T. D., and Hodgson, K. O. (1985) *The Journal of Biological Chemistry* **260**, 5518-5520.
137. Yang, W., Hendrickson, W. A., Kalman, E. T., and Crouch, R. T. (1990) *The Journal of Biological Chemistry* **265**, 13553-13559.
138. Meyer, J., Moulis, J.-M., Gaillard, J., and Lutz, M. (1992) *Advances in Inorganic Chemistry* **38**, 73-115.
139. Stadtman, T. C. (1974) *Science* **183**, 915.
140. Stadtman, T. C. (1979) *Advances in Enzymology* **48**, 1.
141. Klayman, D. L., and Günther, W. H. H. e. (1973) *Organic Selenium Compounds: Their Chemistry and Biology*, Wiley, New York, Chap. XIII.
142. Lipsett, M. N. (1965) *The Journal of Biological Chemistry* **240**, 3975.
143. Abrell, J. W., Kaufman, E. F., and Lipsett, M. N. (1971) *The Journal of Biological Chemistry* **246**, 294.
144. Dilworth, G. L., and Bandurski, R. S. (1977) *Biochemical Journal* **163**, 521.
145. Bremer, J., and Natori, Y. (1960) *Biochimica et Biophysica Acta. International Journal of Biochemistry and Biophysics* **44**, 367-370.
146. Pegg, A. E. (1969) *Biochimica et Biophysica Acta. International Journal of Biochemistry and Biophysics* **177**, 361-364.
147. Shepherd, L., and Huber, R. E. *Canadian Journal of Biochemistry* **47**, 877-881.
148. Weatherill, T. D., Rauchfuss, T. B., and Scott, R. A. (1986) *Inorganic Chemistry* **25**, 1466-1472.
149. Eidsness, M. K., Scott, R. A., Prickril, B. C., derVartanian, D. V., LeGall, J., Moura, I., Moura, J. J. G., and Peck, H. D., Jr. (1989) *Proceedings of the National Academy of Science U.S.A* **86**, 147.
150. Cospers, N. J., Booker, S. J., Ruzicka, F., Frey, P. A., and Scott, R. A. (2000) *Journal of The American Chemical Society* **39**, 15668-15673.

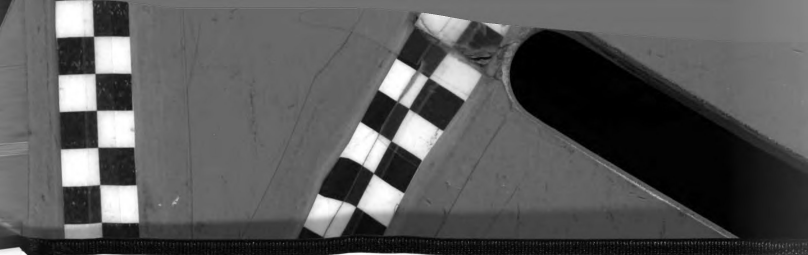
134. Harnett, B. *Journal of the Royal Microscopical Society*, 1938, 58, 1-10.
135. Harnett, B. *Journal of the Royal Microscopical Society*, 1938, 58, 11-12.
136. Harnett, B. *Journal of the Royal Microscopical Society*, 1938, 58, 13-14.
137. Harnett, B. *Journal of the Royal Microscopical Society*, 1938, 58, 15-16.
138. Harnett, B. *Journal of the Royal Microscopical Society*, 1938, 58, 17-18.
139. Harnett, B. *Journal of the Royal Microscopical Society*, 1938, 58, 19-20.
140. Harnett, B. *Journal of the Royal Microscopical Society*, 1938, 58, 21-22.
141. Harnett, B. *Journal of the Royal Microscopical Society*, 1938, 58, 23-24.
142. Harnett, B. *Journal of the Royal Microscopical Society*, 1938, 58, 25-26.
143. Harnett, B. *Journal of the Royal Microscopical Society*, 1938, 58, 27-28.
144. Harnett, B. *Journal of the Royal Microscopical Society*, 1938, 58, 29-30.
145. Harnett, B. *Journal of the Royal Microscopical Society*, 1938, 58, 31-32.
146. Harnett, B. *Journal of the Royal Microscopical Society*, 1938, 58, 33-34.
147. Harnett, B. *Journal of the Royal Microscopical Society*, 1938, 58, 35-36.
148. Harnett, B. *Journal of the Royal Microscopical Society*, 1938, 58, 37-38.
149. Harnett, B. *Journal of the Royal Microscopical Society*, 1938, 58, 39-40.
150. Harnett, B. *Journal of the Royal Microscopical Society*, 1938, 58, 41-42.

- 
151. He, S. H., Teixeira, M., LeGall, J., Patil, D. S., Moura, I., Moura, J. J. G., DerVartanian, D. V., Huynh, B. H., and Peck, H. D., Jr. (1989) *The Journal of Biological Chemistry* **264**, 2678.
 152. Chasteen, N. D., and Snetsinger, P. A. (2000) *Physical Methods in Bioinorganic Chemistry, Spectroscopy and Magnetism*, University Science Books.
 153. Pickering, I. J., George, G. N., Fleet-Stalder, V. V., Chasteen, T. G., and Prince, R. C. (1999) *Journal of Biological Inorganic Chemistry* **4**, 791-794.

131. He, S. H., Tetsuo, M. & ...
 DeVries, D. J. & ...
 Biological Control ...
132. Christen, R. & ...
 Christen, R. & ...
133. Pickering, J. & ...
 R. C. (1999) ...







MICHIGAN STATE LIBRARIES



3 1293 02177 9131